ESTROGEN SIGNALING IN NOCICEPTIVE NEURONS

Dissertation

zur Erlangung des akademischen Grades des
Doktors der Naturwissenschaften (Dr. rer. nat.)

eingereicht im Fachbereich Biologie, Chemie, Pharmazie
der Freien Universität Berlin

vorgelegt von

Julia Annabelle Kuhn

aus Berlin

2010

1. Gutachter: Frau Prof. Dr. Petra Knaus

2. Gutachter: Herr Prof. Dr. Christoph Stein

Disputation am 20. September 2010

Φύσις κρύπτεσθαι φιλεῖ.

Heraklit, Fragmente, B123

Table of contents

1 Summary

Pain is one of the largest health problems, and therapeutic options are still insufficient. More effective treatment of pain requires the understanding of cellular mechanisms underlying pain and sensitization. While electrophysiological properties of nociceptive neurons have been investigated intensively, still little is known about the intracellular mechanisms mediating pain sensitization in nociceptive neurons.

Besides inflammatory mediators, neurotransmitters and growth factors, also the steroid hormone estrogen is known to influence pain. Estrogen-dependent sex differences in pain are well established in humans and in animals, but the underlying signaling mechanisms are so far not described. The aim of this study was to identify the estrogen receptor which mediates estrogen-induced PKCε translocation in nociceptive neurons, to analyze signaling mechanisms downstream of PKCε and to investigate signal integration in primary sensory neurons.

In my thesis estrogen was used as a stimulus to identify new signaling pathways in nociceptive neurons. I found estrogen and agonists of the novel estrogen receptor GPR30 to cause rapid PKCε translocation in a subgroup of primary nociceptive neurons. This PKCε activation was dependent on adenylyl cyclase and was restricted to neurons positive for the subgroup markers IB4 and TRPV1. In contrast, no PKCε translocation was detected in response to agonists of the classical estrogen receptors ERα and ERβ. In behavioral experiments performed in rats and mice, GPR30 agonists as well as estrogen induced robust mechanical sensitization. The observed cellular and behavioral effects mirrored effects induced by G-protein coupled receptor activating inflammatory mediators. This suggests a first physiological function for the novel estrogen receptor GPR30 and indicates a potential role for estrogen as inflammatory modulator of nociception.

The investigation of downstream effects of PKCε activation using computational, biochemical, cell biological as well as behavioral approaches indicated the TRPV1-microtubule complex as a novel target of PKCε signaling towards mechanical sensitization. PKCε-mediated phosphorylation of TRPV1 at serine 800 modulates the interaction between TRPV1 and the microtubule cytoskeleton and thereby controls nociceptive signaling upon PKCε activation. Surprisingly, the observed effect was independent of the ion channel functionality of TRPV1, as it also occurred in presence of the channel blocker 5'I-RTX and in cells expressing only a TRPV1 fragment which does not form a functional channel. Thus, TRPV1 serves as a signaling scaffold in PKCε-dependent mechanical sensitization, a function independent of its ion channel conductivity.

Epinephrine and estrogen signaling converged on PKCε. By analyzing how these convergent signals are computed by the nociceptive neuron, a novel endogenous inhibitory signaling pathway was identified. While estrogen normally induces sensitization, estrogen can also context-dependently abolish sensitization. The switch between these two opposing signaling cascades is set by a Ca^{2+}-dependent mechanism. The inhibition of sensitizing signaling through Ca^{2+} rises is not specific for estrogen alone, as it was also observed for the inflammatory mediator

isoproterenol. The reversal of ongoing and past sensitization through a nociceptive stimulus indicates a new grade of complexity for signaling mechanisms regulating nociception.

Taken together, this thesis demonstrates that estrogen acts as an important regulator of nociceptive signaling. The identification of novel sensitizing as well as desensitizing signaling mechanisms up- and downstream of PKCε opens new prospects for the development of analgesics targeting intracellular signaling mediators and for the improvement of pain therapy, e.g. in gender-dependent pain disorders and cancer therapy-induced pain.

2 Zusammenfassung

Schmerz ist ein zentrales medizinisches Problem. Die therapeutischen Möglichkeiten sind jedoch noch immer sehr begrenzt. Ein Grund dafür ist das unzureichende Verständnis der zellulären Mechanismen, die Schmerz und gesteigerter Sensitivität (Hyperalgesie) zugrunde liegen. Während die elektrophysiologischen Eigenschaften nozizeptiver Neuronen bereits gut charakterisiert sind, sind intrazelluläre Signalwege bisher kaum beschrieben. Neben Entzündungs-mediatoren, Neurotransmittern und Wachstumsfaktoren beeinflussen auch Steroidhormone wie z. B. Östrogen das Schmerzempfinden. Obwohl Geschlechtsunterschiede in der Schmerz-wahrnehmung bei Menschen und in zahlreichen Tiermodellen beschrieben sind, sind die molekularen Ursachen bisher weitgehend unbekannt.

In dieser Arbeit wurde Östrogen verwendet, um neue Signalwege in nozizeptiven Neuronen zu identifizieren. Östrogen führt in sensorischen Neuronen, ebenso wie entzündliche Mediatoren, innerhalb kurzer Zeit zur Translokation der Protein Kinase C epsilon (PKCε) zur Plasma-membran. Während Agonisten des neuartigen Östrogen-Rezeptors GPR30 ebenfalls eine schnelle PKCε-Aktivierung hervorriefen, konnte keine PKCε-Translokation beobachtet werden, wenn die Neuronen mit spezifischen Agonisten für die klassischen Östrogen-Rezeptoren ERα und ERβ behandelt wurden. Die schnelle PKCε-Aktivierung nach der Behandlung mit Östrogen, GPR30 Agonisten bzw. Entzündungsmediatoren war spezifisch für eine Subgruppe sensorischer Neuronen, die das Isolektin B4 binden und den Ionenkanal TRPV1 exprimieren. In Verhaltensexperimenten mit Ratten und Mäusen induzierte die Applikation von Östrogen oder GPR30 Agonisten mechanische Hyperalgesie. Damit deuten die hier vorgestellten Ergebnisse darauf hin, dass Östrogen ähnlich wie entzündliche Mediatoren Schmerzsignalwege moduliert, und legen so eine erste physiologische Funktion für den neuartigen Östrogen-Rezeptor GPR30 nahe.

In weiteren Untersuchungen wurde der TRPV1-Mikrotubuli-Komplex als neues *downstream target* von PKCε in mechanischer Hyperalgesie identifiziert. PKCε-vermittelte Phosphorylierung des Serin 800 von TRPV1 verändert den TRPV1-Mikrotubuli-Komplex, indem es eine Bindung der Mikrotubuli an TRPV1 verhindert und so nozizeptive Signalwege beeinflusst. Der beschriebene Effekt konnte weder durch den Ionenkanal-Inhibitor 5'I-RTX noch durch die Expression eines TRPV1-Fragments anstelle von Wildtyp-TRPV1 blockiert werden. Damit zeigt die hier beschriebene Funktion von TRPV1 als Signalvermittler in mechanischer Sensitivierung eine neue Rolle für TRP Kanäle in Signaltransduktionswegen, zusätzlich zu ihrer Ionenkanal-Funktionalität.

Die sensitivierenden Signalwege von Epinephrin und Östrogen konvergieren in der Aktivierung von PKCε. Die Analyse der Signalverarbeitung solcher konvergenter Signalwege zeigte einen neuen, autoinhibitorischen Signalweg in nozizeptiven Neuronen. Während Östrogen in Abwesenheit anderer Schmerzsignale PKCε-abhängige Sensitivierung hervorruft, kann Östrogen in Verbindung mit anderen nozizpetiven Signalen auch Schmerzsignalwege inhibieren. Die

Regulation dieser entgegengesetzten Signalmechanismen erfolgt über ein Ca^{2+}-Signal. Die Ca^{2+}-abhängige Inhibition nozizeptiver Signale ist nicht spezifisch für Östrogen, sondern kann auch für andere nozizeptive Stimuli beobachtet werden, die ebenfalls PKCɛ-abhängige Sensitivierug hervorrufen. Die Inhibition eines Schmerzsignals durch einen eigentlich Schmerz auslösenden Stimulus deutet auf einen neuen Grad von Komplexität hin, der der Regulation von Schmerzsignalen zugrunde liegt.

Zusammengefasst zeigt diese Arbeit, dass Östrogen bei der Regulation von Schmerzsignalwegen eine wichtige Rolle spielt. Die Identifizierung sowohl sensitivierender als auch inhibitorischer Signalmechanismen deutet auf intrazelluläre Mediatoren hin, die als potentielle Angriffspunkte für die Entwicklung neuer Schmerzmedikamente dienen könnten, und eröffnet dabei neue Perspektiven für eine verbesserte Schmerztherapie, z. B. bei der Behandlung geschlechtsspezifischer Schmerzen oder bei Chemotherapie-induziertem Schmerz.

3 Introduction

Pain is defined by the International Association for the Study of Pain (IASP) as "an unpleasant sensory and emotional experience associated with actual or potential tissue damage" (Loeser and Treede, 2008). The sensation of pain alerts humans and animals to a variety of noxious stimuli and triggers protective responses. Therefore pain sensation is essential for the survival and well being of an organism. While acute pain functions as a warning system, activation of pain signaling pathways often also results in long lasting increased pain sensitivity. In a sensitized state, normally innocuous stimuli like light touch or pleasant warmth are perceived as painful, a phenomenon called allodynia, and normally noxious stimuli induce greater pain responses, a phenomenon referred to as hyperalgesia (Loeser and Treede, 2008). Sensitization is a significant clinical problem, especially in respect of the increasing number of patients suffering from chronic pain syndromes including cancer pain, postherpetic neuralgia or peripheral neuropathies.

The successful treatment of pain requires the identification of exogenous and endogenous substances acting on nociceptive neurons and the knowledge of signaling mechanisms underlying pain sensitization. While pain signaling is mostly investigated by analyzing electrophysiological properties of nociceptive neurons and characterizing ion channels as transducer of nociceptive stimuli, the knowledge of intracellular signaling mechanisms involved in sensitization is only emerging.

3.1 Primary sensory neurons

Primary sensory neurons connect the innervated tissue such as skin, muscles or inner organs with the central nervous system. The peripheral ending of the primary neuron detects stimuli and action potentials are generated. These action potentials are transmitted along the primary neuron to interneurons in the spinal cord. In turn, spinal cord neurons forward the signal to the brain (Fig. 1).

Pain is a complex process, involving the peripheral and the central nervous system. While noxious stimuli are detected by peripheral neurons, also cognitive and emotional aspects contribute to the perception of pain. In contrast to the central nervous system (CNS) phenomenon "pain", the term nociception describes the process by which intense thermal, mechanical or chemical stimuli are detected by the peripheral nervous system (Loeser and Treede, 2008). Already in 1906, Charles Sherrington postulated the existence of "nociceptors", which are distinct from sensory neurons detecting non-nociceptive stimuli such as light touch or pleasant warmth (Sherrington, 1906). Electrophysiological studies indeed identified sensory neurons which are activated only in response to noxious heat, strong pressure and/or by harmful chemicals, but not by innocuous temperatures or light touch (Julius and Basbaum, 2001).

The cell bodies of primary nociceptive neurons are located in the dorsal root ganglia (DRG) and in the trigeminal ganglia (TG). Primary afferent neurons have a unique morphology. They are pseudo-unipolar structures with no distinct biochemical difference between the peripheral and central nerve terminals. Therefore these neurons can send and receive signals from both terminals (Basbaum and Jessell, 2000).

DRG and TG consist of various types of primary sensory neurons which can be assigned to different subgroups based on their anatomical and functional characteristics (Julius and Basbaum, 2001).

According to morphological and functional properties, sensory neurons can be divided into Aβ, Aδ and C fibers. Aβ fibers are myelinated, rapidly conducting fibers which normally detect innocuous stimuli like light touch or pleasant warmth applied to skin, muscles or joints. Aδ fibers are lightly myelinated fibers that built one group of nociceptive neurons. The diameters of Aδ fibers are smaller compared to Aβ fibers and their conduction velocity is slower. C fibers are unmyelinated, small diameter fibers with slow conduction velocities. Most of the C fibers are polymodal and respond to nociceptive mechanical, thermal and chemical stimuli (Perl, 2007).

Neuronal subgroups are also differentiated based on the characteristic expression of ion channels. Heat sensitive neurons express the transient receptor potential vanilloid channel 1 (TRPV1), whereas the detection of cold temperatures is associated with the expression and activation of TRPM8, another ion channel of the transient receptor potential (TRP) family. An acidic environment, like during inflammatory conditions or after tissue injury, is detected by neurons expressing acid sensing ion channels (ASICs), and TRPA1 expressing neurons are activated in response to various chemical irritants (Julius and Basbaum, 2001).

Subpopulations of nociceptive neurons can be further distinguished by their ability to release neuropeptides like Substance P and calcitonin-gene related peptide (CGRP) or to bind the isolectin B4 (IB4) from *Griffonia simplicifolia* (Silverman and Kruger, 1988) which interacts with a splice variant of an extracellular matrix protein versican (Bogen et al., 2005). If a specific subgroup of sensory neurons detects estrogen or other sex steroid hormones leading to an alteration of nociception, is unknown.

Tissue Damage/
Inflammation

Pain

Epithelium   Primary Sensory Neuron   Spinal   Brain
                                                                  Cord
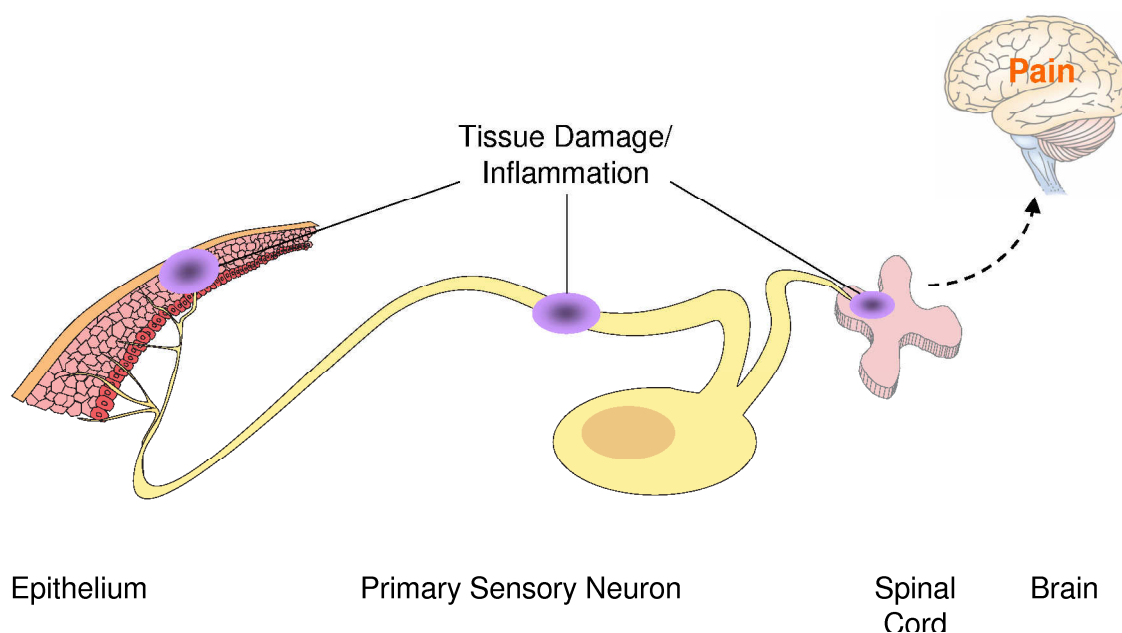
Fig. 1: Sensitization of the primary nociceptive neuron. About 75 % of primary sensory neurons function as detectors for nociceptive stimuli as so called nociceptors. Their peripheral endings innervate skin, muscles or inner organs, where they detect nociceptive signals. The cell bodies of nociceptive neurons are located in the dorsal root ganglia or in the trigeminal ganglia, and the central termini connect the peripheral neuron to the interneuron in the spinal cord. From there, nociceptive signals are forwarded to the brain, where the sensation of pain is generated. Tissue damage and/or inflammation results in the increased responsiveness of nociceptive neurons (adapted from Hucho and Levine, 2007; Sollich, 2008).

3.2 Estrogen in pain and nociception

3.2.1 Sex differences in pain and nociception

A wide variety of endogenous substances influences pain. Inflammatory mediators, growth factors and cytokines, but also gonadal steroid hormones have been shown to modulate nociception (Hucho and Levine, 2007). Gender and sex-hormone related differences in pain and nociception are documented in humans as well as in animal models (Aloisi et al., 2009; Coyle et al., 1996; Fillingim and Ness, 2000; Mogil et al., 1997; Mogil et al., 2000; Unruh, 1996). In humans, pain thresholds and pain tolerance are in general lower in women than in men independent of the modality of the nociceptive stimulus, i.e. heat, pressure or nociceptive chemicals (Chesterton et al., 2003; Craft et al., 2004; Craft, 2007; Frot et al., 2004; Sarlani et al., 2003). Chronic pain conditions such as fibromyalgia, migraine as well as temporomandibular joint disorders are more prevalent in women compared to men and sex hormones play a central role (Berkley, 1997; Unruh, 1996). Accordingly, studies indicate that the female menstrual cycle influences the sensitivity, thresholds and tolerance to pain (Hapidou and Rollman, 1998; Riley et al., 1999). Also

after cross-hormone administration as in transsexual men and woman, changes in pain perception are reported (Aloisi et al., 2007).

In animal models, sex differences are documented in baseline nociceptive thresholds as well as in the response to nociceptive stimuli and in the effect of analgesics. Female rats show lower baseline nociceptive thresholds for mechanical stimulation compared to male animals (Khasar et al., 2005). On the other hand, the inflammatory mediator epinephrine induces stronger sensitization in male than in female rats in an estrogen-dependent manner (Khasar et al., 2005). Dina et al. reported the involvement of different second messengers in male and female rats in epinephrine signaling towards mechanical sensitization (Dina et al., 2001b). While in male rats epinephrine induces PKA-, ERK- and PKCε-dependent mechanical hyperalgesia, in female rats PKA and PKCε do not contribute to epinephrine-induced sensitization. Using gonadectomy and/or estrogen replacement it was shown that estrogen determines the coupling of the inflammatory mediator to the intracellular signaling cascades (Dina et al., 2001b; Hucho et al., 2006).

3.2.2 Pain modulation by estrogen

Estrogen and other sex hormones modulate pain by influencing the central as well as the peripheral nervous system. Direct action on the nociceptive neurons and indirect actions via e.g. the cardiovascular or the immune system have beenn described. In the CNS estrogen alters pain sensitivity by modulating the activity of GABA receptors (Gu et al., 1999; Kelly et al., 1999; McCarthy et al., 2002; Qiu et al., 2003). Estrogen also influences the action of opioid analgesics by controlling the expression of κ and μ opioid receptors in the spinal cord (Aloisi et al., 2005; Liu and Gintzler, 2000).

In the periphery, a number of estrogen effects on nociceptive neurons have been described. Estrogen regulates the mRNA expression of trkA and p75 receptors in DRG neurons which mediate NGF signaling and contribute to NGF-induced sensitization (Sohrabji et al., 1994; Woolf, 1996). Expression levels of the nociceptive second messengers PKA and PKCε are also affected by estrogen (Ansonoff and Etgen, 1998; Kelly et al., 1999). Besides of controlling protein expression, estrogen directly activates nociceptive signaling pathways in primary sensory neurons. Estrogen activates the MAP kinase ERK in TG neurons, resulting in increased facial allodynia (Liverman et al., 2009). In cultured TG neurons, estrogen increased the cAMP production in response to PGE2 and the inositol phosphate accumulation in response to bradykinin (Fehrenbacher et al., 2009). In DRG neurons derived from male rats, estrogen activates PKCε in absence of other nociceptive stimuli, and estrogen application induces PKCε-dependent hyperalgesia in male rats (Hucho et al., 2006). On the other hand, estrogen inhibits the activation of PKCε normally induced by the β-adrenergic agonist isoproterenol (Hucho et al., 2006).

Nevertheless, how estrogen controls signaling pathways in primary nociceptive neurons is so far not known.

3.2.3   The steroid hormone estrogen

Estrogen (17-β-estradiol, E2) is the main estrogenic hormone in non-pregnant woman between menarche and menopause. It belongs to the family of steroid hormones that include progesterone, testosterone, glucocorticoids and mineralcorticoids. Like all steroids, estrogen is derived from cholesterol and finally synthesized by aromatization of testosterone (Bulun, 2000; Prossnitz et al., 2008a).

For a long time, estrogen was considered as a purely female sex hormone, primary synthesized in the ovaries. Today it is known, that estrogen is produced in many other tissues such as brain, bone marrow, adipose tissue and skin in both sexes (Lauber and Lichtensteiger, 1994; Nawata et al., 1995; Sebastian and Bulun, 2001; Shozu et al., 2003). Aromatase expression is described in DRG neurons (Schaeffer et al., 2010) and in the spinal cord, where signals of primary nociceptive neurons are transduced to the CNS (Evrard and Balthazart, 2004). Besides of its function in reproductive organs, estrogen plays an important role in nonreproductive systems such as the cardiovascular, nervous and skeletal system (Prossnitz et al., 2008b; Toran-Allerand et al., 1999; Toran-Allerand, 2004).

3.2.4   Classical estrogen signaling

The classical mechanism of estrogen action is the transcriptional regulation of target genes (Acconica et al., 2006). Like all steroid hormones, estrogen is able to enter the cell, where it binds to intracellular estrogen receptors (ERs) that belong to the steroid hormone family of nuclear receptors (Mangelsdorf and Evans, 1995; Mangelsdorf et al., 1995). Two classical estrogen receptors (ERs) are described: the estrogen receptor alpha (ERα) and the estrogen receptor beta (ERβ). ERα and ERβ are highly homologous in their DNA- and ligand-binding domains, but lack relative homology in their transcriptional activation domains (Kuiper et al., 1997). In absence of a ligand, ERs are localized in the cytoplasm and in the nucleus, where heat-shock proteins and immunophilins keep the receptors in an inactive conformation (Zhang and Trudeau, 2006). Upon estrogen binding, inactivating proteins dissociate from the receptors, ERs dimerize and cytoplasmic receptors translocate into the nucleus, where they bind to specific estrogen response elements (EREs) located in the promoters of target genes. Subsequent, ERs modulate target gene expression by interaction with multiple coactivators and corepressors (Klein-Hitpass et al., 1986; Zhang and Trudeau, 2006). Additionally, ERs influence transcriptional activity by transcriptional crosstalk, e.g. by binding to other transcription factors such as AP-1 or Sp-1 (Castro-Rivera et al., 2001; Gaub et al., 1990; Gottlicher et al., 1998). This genomic action of estrogen is sensitive to transcriptional and translational inhibitors and typically takes several hours until the effect is manifested (O'Lone et al., 2004).

3.2.5 Non-classical estrogen signaling: Rapid effects and signaling via membrane receptors

In addition to classical transcriptional actions, estrogen is known to induce rapid, non-genomic signaling in various cell types. These effects are insensitive towards transcriptional and translational inhibitors and appear within seconds to minutes (Moriarty et al., 2006; Simoncini et al., 2003). Rapid estrogen actions include the activation of protein kinases such as ERK, PKA, PKC, Akt or PI3K, the production of the second messengers cAMP, cGMP and nitric oxide (NO) as well as the modulation of ion channel activity and intracellular Ca^{2+} levels (Edwards, 2005; Gu and Moss, 1996; Ho and Liao, 2002a; Ho and Liao, 2002b). These rapid effects are important in physiological processes such as cardiovascular protection, bone preservation, cell proliferation, neuroprotection and spermatogenesis (Manavathi and Kumar, 2006).

Rapid, non-transcriptional estrogen signaling can be mediated by classical ERs located in the nucleus and in the cytoplasm or by membrane estrogen receptors. The presence of membrane estrogen receptors has been postulated already 1977 by Pietras and Szego, but the precise nature of membrane estrogen receptors is still under debate (Pietras and Szego, 1977). Studies using membrane-impermeable ligands, overexpression systems and various antibodies indicate a plasma membrane localization of the classical estrogen receptors ERα and ERβ (Pappas et al., 1995; Ropero et al., 2002; Watson et al., 2002) and several signaling events are correlated with membrane-associated ERα and ERβ (Razandi et al., 1999; Xu et al., 2008). Other studies suggest the existence of structurally different membrane estrogen receptors as membrane-associated estrogen actions are described in cell types that do not express classical ERs (Zhang and Trudeau, 2006). The discovery of a seven transmembrane receptor, the G-protein coupled receptor 30 (GPR30), as a potential estrogen receptor opened new perspectives for estrogen-initiated signaling mechanisms by linking the steroid hormone estrogen to classical G-protein coupled receptor (GPCR)-induced signaling cascades (Revankar et al., 2005; Thomas et al., 2005).

3.2.6 The novel estrogen receptor GPR30

GPR30 was cloned as an orphan GPCR in the late 1990 by five different groups using cDNA from Burkitt's lymphoblasts (Owman et al., 1996), B cells (Kvingedal and Smeland, 1997), human endothelial cells (Takada et al., 1997), human genomic DNA (Feng and Gregor, 1997) or breast cancer cells lines (Carmeci et al., 1997). G-protein coupled receptors represent the largest class of seven transmembrane receptors that transduce their signals via heterotrimeric G-proteins which dissociate into Gα and Gβγ subunits upon ligand binding (Gether, 2000). Based on several studies indicating the involvement of heterotrimeric G-proteins in rapid estrogen signaling (Gu et al., 1999; Nadal et al., 2000), Filardo et al. provided evidence for a role of GPR30 in estrogen signaling by showing that GPR30 mediates estrogen-induced ERK activation in cells lacking ERα and ERβ (Filardo et al., 2000). Further experiments indicated that GPR30 also mediates estrogen-induced adenylyl cyclase activation observed in ER negative breast cancer cells. Interestingly, this effect was not only observed in response to estrogen, but also after application of the estrogen

receptor antagonists ICI 182,780 and tamoxifen (Filardo, 2002; Filardo et al., 2002). In 2005, two groups reported that estrogen indeed binds to and signals through GPR30 (Revankar et al., 2005; Thomas et al., 2005). Thomas et al. reported the binding of estrogen as well as the classical ER antagonists ICI 182,780 and tamoxifen to the plasma membrane of breast cancer cells expressing GPR30, but lacking classical ERs. Additionally, activation of GPR30 resulted in the activation of a Gαs protein and increased adenylyl cyclase activity, while agents inducing the uncoupling of heterotrimeric G-proteins from GPCRs reduced the membrane binding of estrogen. In a second study, Revankar et al. showed that GPR30 activation by estrogen leads to Ca^{2+} mobilization and phosphatidylinositol-3,4,5-triphosphate production using transfected COS7 and SKBR3 breast cancer cells as model systems. While Thomas et al. reported GPR30 expression at the plasma membrane, Revankar and colleagues showed binding of fluorescent labeled estrogen to GPR30 localized in the endoplasmic reticulum.

Expression of GPR30 mRNA and protein is described in multiple tissues including the reproductive, cardiovascular and nervous system, indicating that GPR30 expression is not restricted to classical estrogen-responsive tissues (Olde and Lee-Lundberg, 2009).

As several G-protein coupled receptors are involved in nociception, GPR30 might also be an interesting candidate to mediate estrogen signaling in nociceptive neurons.

3.2.7 Estrogen receptors in the nervous system

Classical estrogen receptors as well as the novel estrogen receptor GPR30 have been shown to be expressed in different pain-related areas of the central and peripheral nervous system in both, males and females. In the CNS, ERα and ERβ are expressed in the trigeminal brainstem complex (trigeminal subnucleus caudalis) (Bereiter et al., 2005), in the hypothalamus, the amygdala, the periaqueductal gray and the dorsal raphe nucleus with no difference between male and female animals (Chaban and Micevych, 2005). GPR30 expression is reported in the Islands of Calleja and the striatum, in the paraventricular nucleus and the supraoptic nucleus of the hypothalamus and in the hippocampus (Brailoiu et al., 2007). In the peripheral nervous system, ERα and ERβ expression has been shown in DRG and TG neurons of male and female rodents (Liverman et al., 2009; Papka and Storey-Workley, 2002; Taleghany et al., 1999). Thereby it is still controversial if both classical ERs are expressed in the same neurons or in neighboring ones (Papka and Storey-Workley, 2002; Taleghany et al., 1999). GPR30 mRNA and protein expression was detected in rat DRG neurons with no difference between both sexes and in the outer layer of the spinal dorsal horn (Takanami et al.). In TG, GPR30 expression is reported in small diameter neurons that also contained the C-fiber marker peripherin (Liverman et al., 2009).

The expression of classical ERs and GPR30 in different pain-related areas of the nervous system suggests that estrogen can act directly on sensory neurons and thereby influences pain signaling. But detailed descriptions about signaling events mediated by the different ERs and the resulting effects for signaling in nociceptive neurons are still missing.

3.3   Signaling in nociceptive neurons

3.3.1   Signaling towards sensitization

In addition to physical stimuli like temperature and pressure, also a broad variety of chemical substances act on nociceptive neurons. Especially during inflammation or tissue injury, many extracellular mediators are released from activated nociceptors and infiltrating cells. Non-neuronal cells include mast cells, macrophages, basophils, platelets, neutrophils, endothelial cells and fibroblasts (Julius and Basbaum, 2001). All together these cells secrete diverse factors, referred to as "inflammatory soup". The inflammatory soup is composed of neurotransmitters like serotonin and adrenaline, lipid compounds like prostaglandins, leukotrienes and endo-cannabinoids, growth factors such as NGF and GDNF; neuropeptides like CGRP and bradykinin, hormones, cytokines and chemokines, as well as extracellular proteases and protons. Plethora of diverse molecules bind to various cell surface receptors including GPCRs, receptor tyrosine kinases (RTKs) but also ion channels expressed on the peripheral terminals of nociceptive neurons.

So far, research has concentrated on the identification of receptors and ion channels responding to nociceptive stimuli, while not much is known about intracellular signaling molecules involved in sensitization (Fig. 2) (Basbaum et al., 2009; Hucho and Levine, 2007; Meyer et al., 2008). In electrophysiological and pain behavioral experiments, small molecules like cAMP and NO (Aley et al., 1998; Chen and Levine, 1999), the protein kinases PKC, PKA and MAP kinases (Aley and Levine, 1999; Aley et al., 2000; Obata et al., 2003), cytoskeletal components (Dina et al., 2003) as well as the cation Ca^{2+} have been reported to play a role in sensitization. The first second messenger described to be part of sensitizing signaling pathways was cAMP. Application of cAMP analoga induced strong sensitization towards physical stimuli (Ferreira et al., 1990; Kress et al., 1996) and prostaglandin E2 (PGE2)-induced sensitization can be blocked by an inactive cAMP analogon (Taiwo and Levine, 1991). PGE2-induced sensitization not only depends on PKA as a downstream target of cAMP signaling, but also on PKC and ERK (Dina et al., 2001b). In addition to PGE2, PKCs are activated in response to bradykinin, TNFα and adrenaline/epinephrine (Cesare et al., 1999; Khasar et al., 1999a; Parada et al., 2003). Not only cytoplasmic proteins, also structural proteins play a role in nociceptive signaling. In behavioral experiments, PKCε-dependent mechanical hyperalgesia was affected by an alteration of the microtubule cytoskeleton. Interestingly, the microtubule cytoskeleton only plays a role in PKCε-dependent hyperalgesia, while PKA-dependent sensitization is not affected indicating a second messenger-dependent influence (Dina et al., 2003).

Second messenger signaling results in the activation or modification of effector molecules. In sensory neurons, TRP ion channels, ASICs and voltage-gated sodium channels are described as effectors of sensitizing signaling. Activation of PKA and PKC lead to phosphorylation of the TRP ion channels TRPV1 and TRPA1, resulting in changes of their ion channel properties (Bhave et al., 2003; Jeske et al., 2008; Liu et al., 2004; Mandadi et al., 2004; Wang et al., 2008).

Additionally, PKA-/PKC-dependent sensitization is correlated with the sensitization of tetrodotoxin-resistent (TTX-R) sodium channels NaV1.8 (Akopian et al., 1999; Fitzgerald et al., 1999; Gold et al., 1998). The sensitization shifts the voltage-dependence of TTX-R sodium channel activation in the direction of hyperpolarization. Therefore, a reduced extend of membrane depolarization is sufficient to initiate an action potential.

The knowledge about the intracellular signaling machinery underlying mechanical and/or thermal sensitization is still only emerging. While many classical pain-related ligands and their receptors are well characterized, only a few intracellular signaling components are identified yet. To understand the cellular mechanisms underlying sensitization, it will be necessary to characterize nociceptive signaling cascades and identify the mechanisms by which these multiple signals are computed. In addition it is important to concentrate not only on the already established nociceptive stimuli, but also to include further signaling components such as sex steroid hormones that have been shown to modulate nociception.
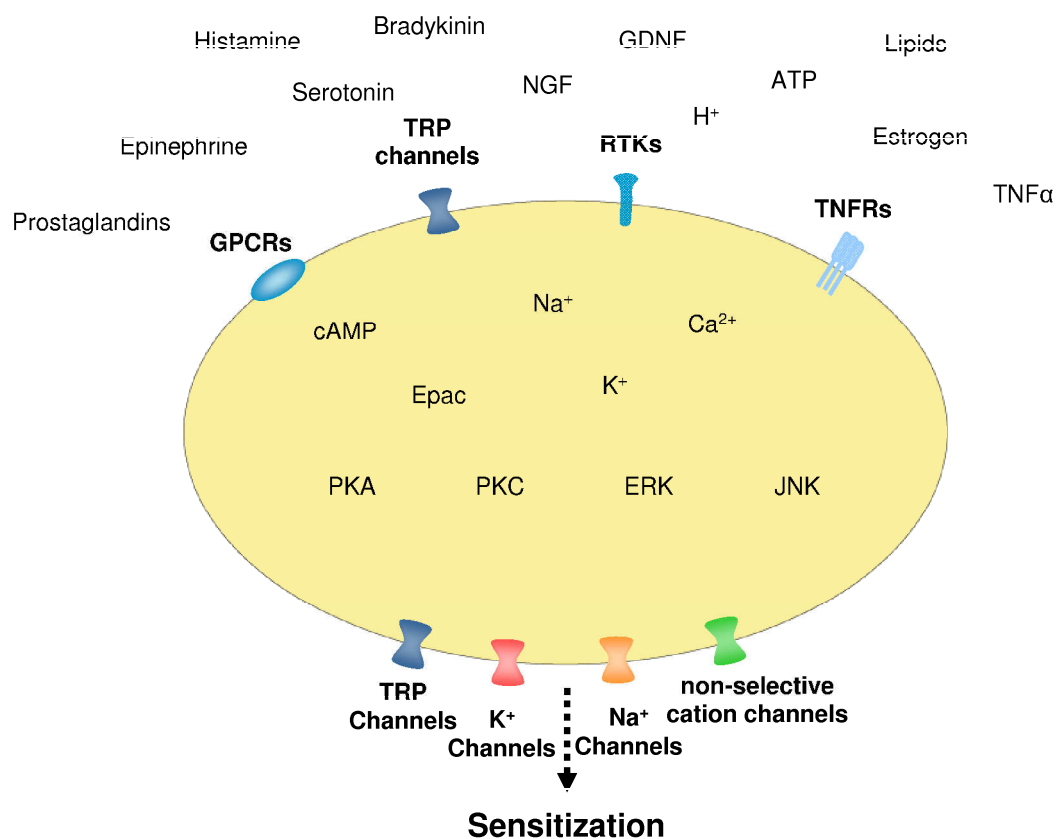
Fig. 2: Diversity of signaling in nociceptive neurons. Especially during inflammation, a broad variety of extracellular mediators acts on primary nociceptive neurons and induces sensitization. Such mediators include neurotransmitters, lipid compounds, growth factors, neuropeptides, cytokines and chemokines, protons and steroid hormones. These diverse stimuli bind to different cell surface receptors including GPCRs, receptor tyrosine kinases or ion channels which in turn lead to the activation of intracellular signaling cascades. While multiple nociceptive stimuli and their receptors have been identified, only a few intracellular signaling mediators such as the protein kinases PKA, PKCε and ERK are described (adapted from Hucho and Levine, 2007). GPCR, G-protein coupled receptor; RTK, receptor tyrosine kinase; TNFR, tumor necrosis factor receptor; TRP channel, transient receptor potential ion channel.

3.3.2 The protein kinase C epsilon: An important second messenger in pain signaling

One of the best characterized intracellular signaling components in sensitization is the epsilon isoform of the protein kinase C (PKCε). PKCs represent a family of ubiquitously expressed phospholipid-dependent serine/threonine kinases that were discovered as Ca^{2+}- and phospholipid-activated kinases (Takai et al., 1979). PKCε belongs to the class of novel PKCs which are activated by DAG, which in contrast to classical PKCs are independent of Ca^{2+}.

PKCε contains four conserved domains (C1-C4) which are typical for PKCs: the cysteine-rich phospholipid binding region (C1), a "C2 like" region that serves as docking site for the intracellular scaffold protein receptor for activated kinases (RACK) and the catalytic domain consisting of the ATP binding site (C3) and the substrate binding site (C4). In an inactive state, an autoinhibitory pseudosubstrate domain adjacent to the C1 region blocks the catalytic domain, while a "pseudo RACK sequence" occupies the RACK binding site (Mochly-Rosen et al., 1991; Schechtman and Mochly-Rosen, 2001). Interaction with an activator leads to the phosphorylation of T566 (activation loop), T710 (turn motif) and S729 (hydrophobic motif). These phosphorylations initiate the activation process, make the kinase fully responsive to its agonists and protect the enzyme against proteolytic cleavage and degradation. Subsequently, PKCε translocates to a target membrane. There, the interaction with DAG and RACK stabilizes the kinase in an open and "active" conformation, resulting in the phosphorylation of target proteins (Fig. 3) (Van Kolen et al., 2007).
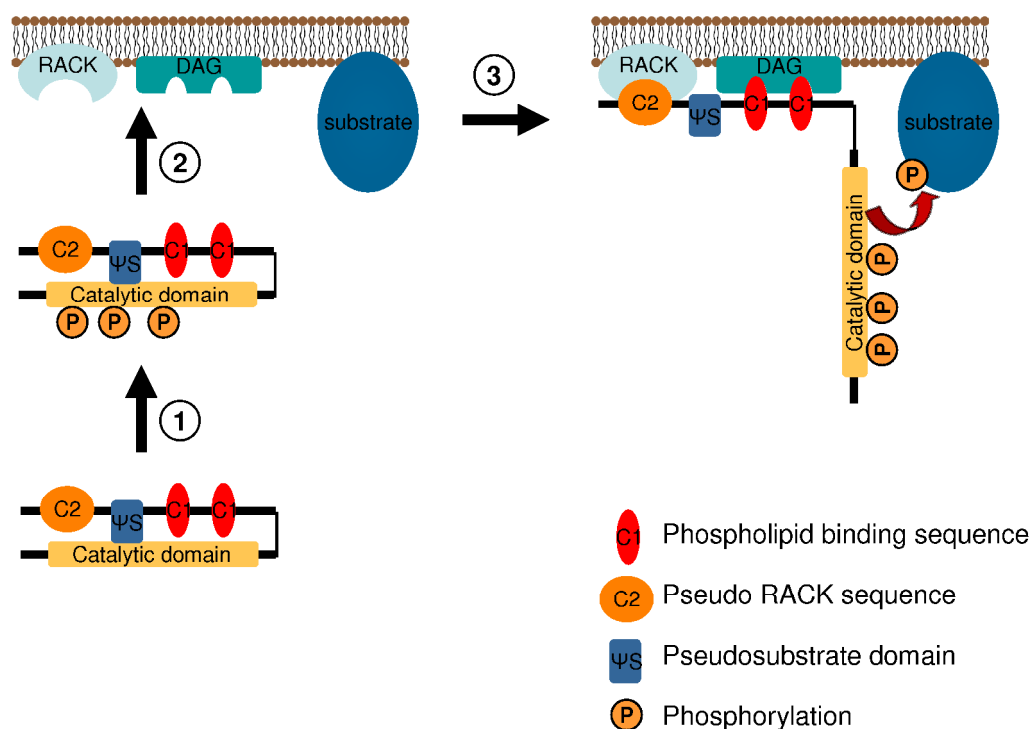
Fig. 3: Schematic representation of the molecular mechanism of PKCε activation. In the inactive state, the autoinhibitory pseudosubstrate domain (ΨS) blocks the catalytic domain and the "pseudo RACK sequence" (C2 domain) occupies the RACK binding site. The first step in the activation process is the phosphorylation of T566, T710 and S729, initiated by the interaction of PKCε with an activator (1). These phosphorylations make the kinase fully responsive to its agonists. Subsequently, PKCε translocates to a target membrane (2). The interaction with DAG and RACK stabilizes the kinase in an open and active conformation, resulting in the phosphorylation of target proteins (3) (modified from Van Kolen et al., 2007).

Several studies using PKCε knock out mice and/or PKCε inhibitor peptides suggest a key role for PKCε in pain signaling pathways. PKCε does not contribute to the baseline nociceptive threshold (Khasar et al., 1999a). Instead, PKCε is described as an important second messenger in models of inflammatory pain (Khasar et al., 1999a; Numazaki et al., 2002; Sweitzer et al., 2004a; Sweitzer et al., 2004b), chronic alcoholism-induced hyperalgesia (Dina et al., 2000), peripheral neuropathies like diabetes (Joseph and Levine, 2003b) and chemotherapy-induced pain (Dina et al., 2001a; Joseph and Levine, 2003a). Recently, Aley et al. showed that also the establishment and persistence of chronic hyperalgesia (hyperalgesic priming) is PKCε-dependent. This form of sensitization occurs after recovery from an inflammation and lasts for several weeks (Aley et al., 2000; Joseph et al., 2003).

PKCε is expressed in more than 90 % of small diameter DRG neurons in the soma as well as in processes and nerve endings, suggesting a function in primary nociceptive neurons (Khasar et al., 1999a). As PKCε is also widely expressed in the central nervous system, centrally as well as peripherally expressed PKCε could contribute to pain phenotypes (Khasar et al., 1999a; Saito et al., 1993).

In DRG neurons, the inflammatory mediator bradykinin has been shown to induce PKCε translocation to the plasma membrane (Cesare et al., 1999) and to activate the protein kinase

(Chuang et al., 2001). This effect is mediated by the G-protein coupled receptor BK2 and phospholipase C (PLC) (Burgess et al., 1989a; Burgess et al., 1989b). Patch-clamp recordings showed that application of bradykinin induces sensitization of DRG neurons in a PKCε-dependent manner (Cesare et al., 1999). Also the inflammatory mediator epinephrine induces PKCε-dependent sensitization in pain behavioral experiments (Khasar et al., 1999a; Parada et al., 2003). In 2005, Hucho et al. described a detailed signaling pathway for epinephrine-induced PKCε activation in DRG neurons: Binding of epinephrine to the β2-adrenergic receptor leads - via an αs coupled mechanism- to activation of the adenylyl cyclase. Surprisingly, activation of PKA is not important for PKCε activation. Instead, the signal is mediated by the cAMP-activated exchange factor Epac that activates the phospholipases C and D which in turn leads to the translocation of PKCε to the plasma membrane. This translocation is restricted to IB4 positive neurons, indicating a first mechanism specific for IB4 positive neurons (Hucho et al., 2005).

One way, by which PKCε modulates nociception, is via the modulation of ion channels. The vanilloid receptor TRPV1 is described as a target of PKCε-phosphorylation in nociceptive neurons (Gold et al., 1998; Khasar et al., 1999a; Mandadi et al., 2006); and the reported interaction of PKCε with the N-type voltage-dependent calcium channel suggests that also calcium channels are targeted by PKCε signaling (Chen et al., 2006). Further investigations have to clarify the role of the identified PKCε targets in nociceptive neurons and demonstrate which other components and signaling cascades are involved in the transduction and maintenance of PKCε signals towards sensitization.

3.3.3 The ion channel TRPV1

The best characterized PKCε target in nociceptive neurons is the ion channel TRPV1. TRPV1 is the first described mammalian TRP channel and was identified by expression cloning in search for receptors that respond with a robust Ca^{2+} influx to the vanilloid capsaicin, the hot compound of red chili peppers. The receptor was initially named capsaicin receptor or vanilloid receptor 1 (VR1) (Caterina et al., 1997). Sequence analysis showed similarities to other members of the TRP channel family, such as six-transmembrane helices, intracellular N- and C-terminal domains and ankyrin repeats in the N-terminal part of the channel (Fig. 4). Therefore, the capsaicin receptor served as the founding member of the vanilloid subfamily of TRP channels (TRPV). TRP channels were first described in *Drosophila melanogaster*, where mutations in *trp* genes lead to a transient voltage response to continuous light (Minke, 1977; Montell et al., 1985). Based on sequence homology to this light-sensitive ion channel in the photoreceptors of *Drosophila*, TRP channels have been identified in almost all eukaryotes and are associated with diverse functions including chemo- and mechanosensation (Damann et al., 2008), taste, temperature sensation and the detection of nociceptive stimuli (Clapham, 2003). Like other TRP channels, TRPV1 forms tetramers that build the functional ion channel. TRPV1 functions as a non-selective cation channel with a high prevalence for Ca^{2+} over other divalent cations, but no differentiation between monovalent cations (Caterina et al., 1997; Hellwig et al., 2005; Venkatachalam and Montell, 2007).

TRPV1   TRPC1   TRPA1   TRPM7

Ankyrin repeats

Kinase domain

TRP domain   Transmembrane helix
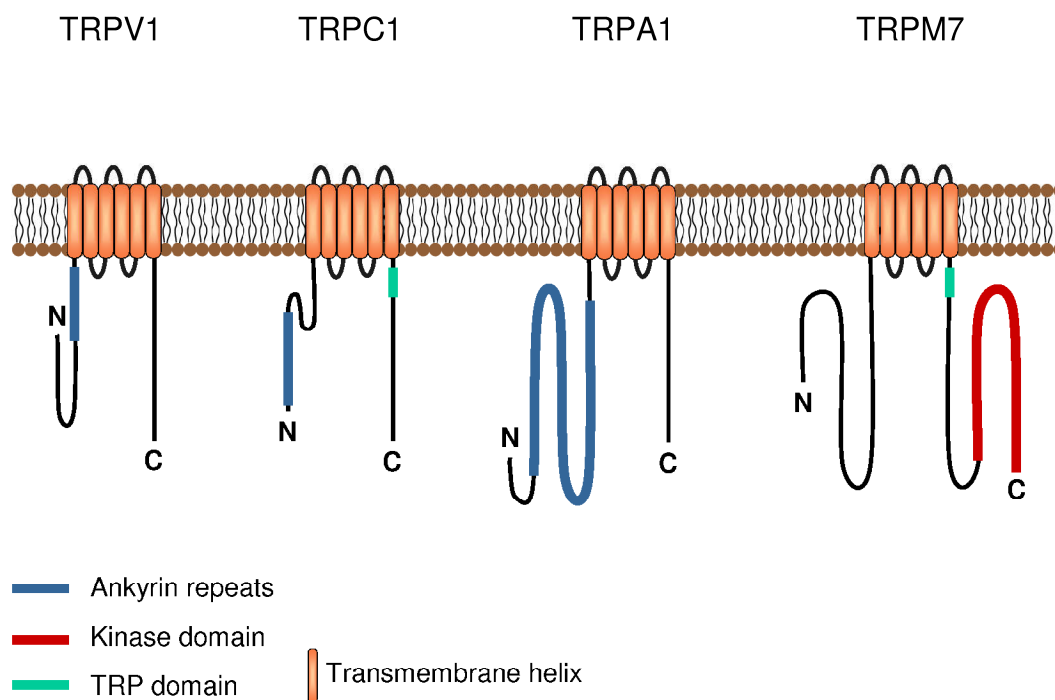
Fig. 4: TRPV1 as a member of the TRP superfamily. TRP ion channels share the common features of six transmembrane helices, cation permeability and a varying degree of sequence homology. Several TRP channels contain ankyrin repeats in the N-terminal region and/or a TRP domain located C-terminal to the transmembrane segments. The mammalian TRP channels TRPM6 and TRPM7 contain an atypical kinase domain in the C-terminal region. Exemplary members of mammalian TRP ion channels are represented; TRPV1, the first member of the vanilloid group; the canonical TRP TRPC1; TRPA1, a member of the ankyrin TRPs; TRPM7, a melastatin TRP family member (adapted from Venkatachalam and Montell, 2007).

In addition to capsaicin, TRPV1 is also activated by high temperatures (>43°C) (Caterina et al., 1997), protons (Jordt et al., 2000) and different endogenous or exogenous chemical ligands. Many of the chemical stimuli are natural compounds including the endocannabinoid anandamide (Zygmunt et al., 1999), the topical analgesic camphor (Xu et al., 2005), the pungent compounds present in black pepper (piperine), garlic (allicin) (McNamara et al., 2005) and ginger (gingerol) (Iwasaki et al., 2006) and the most potent TRPV1 agonist Resinfera toxin (RTX) from the plant *Euphorbia resinfera* (Caterina et al., 1997). Other substances have been shown to sensitize the ion channel, i.e. lowering the activation threshold and potentiate the response to activating stimuli. In fact, low pH >5.9, as observed in injured tissue, induces a shift of the thermal activation threshold of TRPV1 (Caterina et al., 1997). Sensitization of TRPV1 is also observed in response to ethanol (Trevisani et al., 2002), nicotine (Liu et al., 2004) several cytokines (Zhang et al., 2005a) and after PLC-induced cleavage of PIP2 (Chuang et al., 2001).

TRPV1 is expressed in a subgroup of small and medium size DRG neurons that function as nociceptors. There, TRPV1 serves as an acute pain sensor by detecting various noxious stimuli such as noxious heat and inflammatory mediators like protons, bradykinin and NGF. Therefore, TRPV1 can be defined as a polymodal nocitransducer (Patapoutian et al., 2009). In addition to its function as a detector for nociceptive stimuli, TRPV1 is involved in signaling leading to pain

sensitization, where the contribution of TRPV1 to heat hyperalgesia is well established (Amadesi et al., 2004; Pogatzki-Zahn et al., 2005; Zhuang et al., 2004).

Inflammation and tissue injury alter TRPV1 expression and function via multiple signaling mechanism including transcriptional regulation, posttranslational modification and altered trafficking (Ji et al., 2002; Zhang et al., 2005b; Zhu and Oxford, 2007). Especially the processes of phosphorylation, dephosphorylation and rephosphorylation are associated with functional changes of the ion channel (Mandadi et al., 2006). Several kinases that play an important role in nociceptive signaling pathways are reported to phosphorylate TRPV1. PKA has been shown to phosphorylate the serine residue 116 located in the N-terminal region of TRPV1. This phosphorylation blocks capsaicin-induced dephosphorylation, resulting in an inhibition of the normally observed desensitization after capsaicin treatment (Bhave et al., 2002). PKC mediated phosphorylation is associated with the reversal of capsaicin-induced desensitization. Mandadi et al. showed that PKCε-mediated phosphorylation of serine 800 in the C-terminal region of TRPV1 is responsible for the restoration of TRPV1 functionality after desensitization (Mandadi et al., 2006). Interestingly, TRPV1 is so far primarily associated with heat sensitization, but PKCε plays also an important role in the sensitization against mechanical stimuli. The direct regulation of TRPV1 by PKCε therefore points out open questions about the functional relationship of PKCε and TRPV1 in nociception. The involvement of TRPV1 into signaling towards mechanical sensitization is not clear yet. And the signaling mechanism which regulates the contribution of TRPV1 to PKCε signaling is not understood. The fact, that various inflammatory mediators modulate TRPV1 via activation of the same protein kinases, e.g. MAP kinases and PKCε (Mandadi et al., 2006) renders TRPV1 a potential integrator of diverse inflammatory signals.

TRPV1 with its large intracellular C- and N-terminal regions is part of a complex signaling network. Not only protein kinases modify TRPV1, but also other proteins interact with TRPV1 and thereby modulate its function. Direct interaction with TRPV1 has been shown only for a few proteins. One example is the Ca^{2+} binding protein calmodulin, where two binding sites in the N- and C-terminal region of TRPV1 are described. Numazaki et al. reported a calmodulin binding site in the C-terminal region of TRPV1 which is known to be involved in the desensitization of the ion channel (Numazaki et al., 2003). Additionally, Rosenbaum et al. showed a Ca^{2+}-dependent binding of calmodulin to the amino acids 189 to 222 in the N-terminal part of TRPV1. Calmodulin binding to this N-terminal region resulted in a decreased channel-open probability (Rosenbaum et al., 2004).

The anchoring protein 150 (AKAP 150) immunoprecipitates with TRPV1. Functional analysis indicated that AKAP150 is an important mediator for PKA- and PKCε-mediated phosphorylation of TRPV1, acting as a scaffold between activated protein kinases and the ion channel TRPV1 at the plasma membrane (Jeske et al., 2008; Jeske et al., 2009; Schnizler et al., 2008).

Recently, also tubulin, the major compound of the microtubule cytoskeleton, was shown to bind directly to TRPV1 (Goswami et al., 2004). By deletion mapping, two binding sites were identified in the C-terminal region of TRPV1. One binding site is located between amino acid 771 and 797.

This binding region is in close vicinity to other regulatory sites such as the PKCε phosphorylation site at serine 800 (Fig. 5). Activation of TRPV1 resulted in the rapid disassembly of microtubule filaments, suggesting that the microtubule cytoskeleton acts as a downstream effector of TRPV1 activation (Goswami et al., 2006). But the functional role of the microtubule cytoskeleton in TRPV1 signaling towards sensitization is not understood. Interestingly, behavioral experiments showed the involvement of the microtubule cytoskeleton into PKCε-mediated sensitization (Dina et al., 2003). If this microtubule-dependence of PKCε-mediated hyperalgesia is associated with TRPV1, is unknown.

Electrophysiological properties of the ion channel TRPV1 are well characterized, but the knowledge about TRPV1 as a component of signaling pathways in nociceptive neurons is still sparse. The investigation of modifications, interaction partners and signaling cascades concentrated on the effect of the ion channel functionality of TRPV1, while the impact on intracellular signaling processes is still not known.
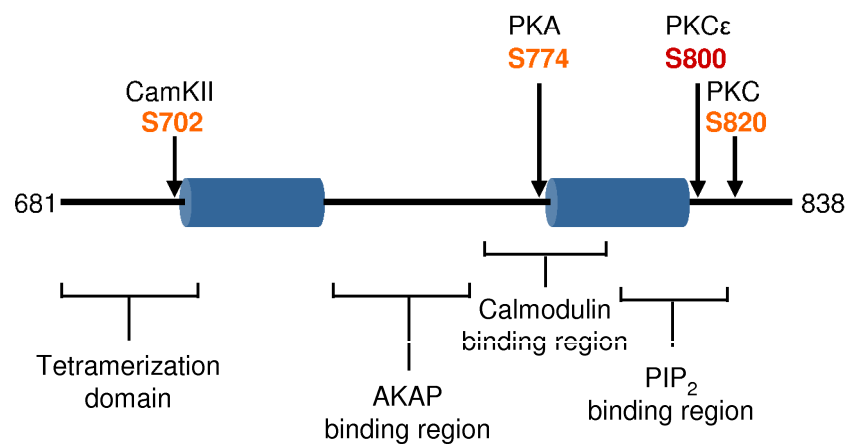
Fig. 5: Schematic representation of the TRPV1-C terminus. The tubulin binding sites (blue cylinders) are in close vicinity to known interaction and regulatory sites of the TRPV1-C terminus. Upper row: phosphorylation sites and responsive kinases. Lower row: tetramerization domain and protein-protein interaction regions.

4 Aim

Pain is a significant health problem. Electrophysiological properties of peripheral "pain" neurons, the nociceptors, have been investigated intensively. Nevertheless, the knowledge about intracellular signaling cascades inducing nociceptor sensitization (hyperalgesia) is only emerging.

Gender differences of pain in humans and in animal models suggest sex steroid hormones to modulate nociception. How they act on nociceptive neurons and if they use similar signaling components as classical sensitizing substances, is not known. Of intense recent interest in estrogen research is the characterization of fast estrogen signaling which is potentially mediated by novel estrogen receptors different from ERα and ERβ.

This thesis aims to characterize the role of the sex steroid hormone estrogen in nociception and its signaling mechanisms in nociceptive neurons. In computational, biochemical, cell biological and behavioral experiments I addressed the following three questions using a model of PKCε-dependent mechanical sensitization:

1. Which receptor and receptor-initiated signaling cascade mediates estrogen signaling toward PKCε activation in nociceptive neurons and in the animal?

2. Is one known PKCε substrate, the ion channel TRPV1, involved in estrogen-induced nociceptor sensitization? And more specifically, does estrogen-induced PKCε activation alter the TRPV1-microtubule complex and thereby contributes to mechanical sensitization?

3. Estrogen signaling converges with other nociceptive stimuli onto PKCε. How are estrogen signals and the multiple physiological signals integrated in the primary nociceptive neuron?

The understanding of pain signaling mechanisms is essential for the development of novel analgesics. It is important to concentrate not only on established nociceptive stimuli, but also to investigate the role of novel substances modulating nociception such as sex steroid hormones. The knowledge of signaling mechanisms underlying estrogen-mediated modulation of nociception might help to explain sex differences in various pain disorders and might open perspectives for novel pain therapies.

5 Materials

5.1   Antibodies and related compounds

5.1.1   Primary antibodies

anti-PKCε	rabbit, polyclonal IgG	The anti-PKCε antibody was a kind gift from R. Messing from the University of California San Francisco (UCSF).
anti-PKCε	goat, polyclonal IgG	Santa Cruz
anti-TRPV1, C-terminal region	rabbit, polyclonal IgG	Alomone
anti-TRPV1, N-terminal region	rabbit, polyclonal IgG	Dianova
anti-tyrosinated tubulin	rat, monoclonal IgG, clone YL1-2	Abcam
anti-alpha-tubulin	mouse, monoclonal IgG, clone DM1A	Sigma
anti-beta-tubulin	mouse, monoclonal IgG, clone D66	Sigma
anti-MBP	mouse, monoclonal IgG2a	NEB

5.1.2   Secondary antibodies

Antibodies for fluorescence microscopy:

FITC-labeled goat anti-rabbit IgG	Dianova
Alexa 488-labeled goat anti-rabbit IgG	Invitrogen
Alexa 488-labeled chicken anti-rabbit IgG	Invitrogen
Alexa 594-labeled goat anti-rat IgG	Invitrogen
Alexa 594-labeled goat anti-mouse IgG	Invitrogen
Alexa 594-labeled chicken anti-mouse IgG	Invitrogen

HRP-coupled antibodies for Western Blot:

HRP-coupled goat anti-rabbit IgG	PIERCE
HRP-coupled goat anti-mouse IgG	PIERCE

5.1.3 Fluorescent dyes and related compounds

FURA-2-AM: The membrane-permeable ratiometric calcium dye FURA-2-AM was purchased from Invitrogen.

TRITC-labeled IB4: TRITC-labeled isolectin from *Bandeiraea simplicifolia* (IB4) was purchased from Sigma.

5.2 Animals and cell lines

5.2.1 Animals

Rats: All animals were housed in a controlled environment under a 12 h light : dark cycle. Food and water were available ad libitum.

Behavioral experiments were preformed on male Sprague-Dawley rats purchased from Charles River Laboratories, Hollister, CA, USA. Care and use of animals conformed to National Institutes of Health guidelines. The UCSF Committee on Animal Research approved the experimental protocols.

For cellular studies adult male Sprague-Dawley rats were purchased from Harlan Winkelmann, Borchen, Germany. Care and use of animals were in accordance with the European Communities Council Directive of 24 November 1986 (86/609/EEC) and were approved by the LaGeSo, Berlin, Germany.

Mice: Mice behavioral experiments were performed with C57BL/6J mice bred at Charité-Universitätsmedizin Berlin, Campus Benjamin Franklin. Animals were housed in a controlled environment with a 12 h light : dark cycle and food and water were available ad libitum. All animal experiments were approved by the local animal care committee LaGeSo, Berlin, Germany.

5.2.2 Cell lines

F-11: Fusion cell line of embryonic rat DRG neurons and the mouse glia blastoma cell line N18TG2 (Plakita et al., 1985).

5.3 Vectors, constructs and proteins

Tubulin-Cherry: the m-cherry fused tubulin construct was a kind gift from R. Y. Tsien from the University of California San Diego (UCSD).

GFP-TRPV1: the construct contains rat TRPV1 cloned into a pcDNA3.1-GFP vector and was a gift from Dr. R. Jahnel from the group of F. Hucho at the FU Berlin.

pcDNA3.1 TRPV1-ΔN: the construct was kindly provided by Dr. R. Jahnel from the group of F. Hucho at the FU Berlin. It contains the transmembrane region of rat TRPV1 as well as the C-terminal cytosplasmic region (amino acid 421 to 838).

GFP-TRPV1 S800A: the GFP-TRPV1 S800A construct was kindly provided by M. Tominaga from the National Institute for Physiological Sciences, Okazaki, Japan.

MBP-TRPV1-C-terminus: the construct containing the cytoplasmic C-terminal region of rat TRPV1 (amino acid 681 to 838) in the pMALc2x vector was cloned by Dr. R. Jahnel from the group of F. Hucho at the FU Berlin.

MBP-lacZ: the construct was purchased from NEB.

pMalc2x: the expression vector was purchased from NEB.

pmCherryC1: the vector was purchased from Clontech.

PKCε: purified PKCε was purchased from Invitrogen.

5.4 Primers and oligonucleotides

Primers

Product	Species	Sequence	Product Size (mRNA)
GPR30	Rat	5'-ATGAATTCGACTACAGTGGCGAGTCGTTTGT-3' 5'-ATGAATTCGACTACAGTGGCGAGTCGTTTGT-3'	172 bp
ERα	Rat	5'-AATTCTGACAATCGACGCCAG-3' 5'-GTGCTTCAACATTCTCCCTCCTC-3'	345 bp
ERβ	Rat	5'-TTCCCGGCAGCACCAGTAACC-3' 5'-TCCCTCTTTGCGTTTGGACTA-3'	262 bp
GAPDH	Rat	5'-CGTTGTGGATCTGACATGC-3' 5'-TCCCTCTTTGCGTTTGGACTA-3'	248 bp

Oligodeoxynucleotides

Target	Species	Sequence
antisense againstTRPV1	Rat	5'-CAT GTC ATG ACG GTT AGG-3'
mismatch*	Rat	5'-CAT G**CT** ATG A**GC** GTT **GA**G-3'

*mismatches are highlighted in bold

5.5 Media, sera and supplements

Neurobasal A: Basal Neurobasal A Medium without Phenol Red was purchased from Invitrogen.

MEM with GlutaMAX: Minimum Essential Medium (MEM) liquid containing GlutaMAX (L-Alanyl-L-Glutamine) was purchased from Invitrogen.

Ham F-12: nutrient mixture was purchased from Sigma.

Opti-MEM: Opti-MEM I reduced-serum medium, Phenol Red free was purchased from Invitrogen.

FBS: fetal bovine serum was purchased from Invitrogen.

NDS: normal donkey serum was purchased from Dianova.

NGS: normal goat serum was purchased from Dianova.

B27: the serum-free supplement B27 for Neurobasal A medium was purchased from Invitrogen.

5.6   Buffers

10 x PCR buffer
100 mM Tris/HCl
500 mM KCl

TAE buffer
40 mM Tris
5 mM Na-acetate
1 mM EDTA

6 x DNA Loading buffer
15 % Ficoll (in H2O)
0.25 % Xylene Cyanol FF

Hank's balanced salt solution with Phenol Red (HBSS)
5.33 mM KCl
0.44 mM KH_2PO_4
4.17 mM Na_2HCO_3
138 mM NaCl
0.34 mM Na_2HPO_4
5.56 mM D-Glucose
10 mM Phenol Red

Hank's balanced salt solution without Phenol Red (HBSS)
5.33 mM KCl
0.44 mM KH_2PO_4
4.17 mM Na_2HCO_3
138 mM NaCl
0.34 mM Na_2HPO_4
5.56 mM D-Glucose

DPBS
200 mg/l KCl
200 mg/l KH_2PO_4
8 g/l NaCl
2.16 g/l Na_2HPO4 x 7 H_2O
1 g/l Glucose
36 mg/l Sodium Pyruvate

Permeabilization buffer

50 mM PIPES, pH 6.8

1 mM EGTA

0.2 mM $MgCl_2$

10 % (v/v) Glycerol

50 µg/ml Digitonin

1 x Complete protease inhibitor cocktail

PEM-S

50 mM PIPES, pH 6.8

1 mM EGTA

0.2 mM $MgCl_2$

100 mM NaCl

Lipid mix

10 mM Hepes, pH 7.4

200 µg/ml phosphatidylserine

20 µg/ml diacylglycerol

6 x Laemmli buffer

65 mM Tris/HCl, pH 6.8

3 % (w/v) SDS

30 % (v/v) Glycin

5 % (v/v) 2-Mercaptoethanol

4 mg/ml Bromphenol blue

4 mg/ml Pyronin G

Electrophoresis buffer

24.8 mM Tris

250 mM Glycin

0.2 % (w/v) SDS

5 x blotting buffer

200 mM Glycin

250 mM Tris

0.2 % (v/v) Tween-20

5.7   Drugs and chemicals

Agarose	Invitrogen
Adenosine 5′-triphosphate disodium salt (APS)	Sigma
Ammonium persulfate (APS)	Biorad
Amylose resin	NEB
Aqua ad iniectabilia	Baxter
Bisindolylmaleimde I hydrochloride (BIM)	Calbiochem
Bovine serum albumin	Sigma
Bromphenol Blue	Serva
Calciumchloride	Merck
Chloroform, p.a.	Merck
Collagenase P	Roche
Destilled water	Bio Whittaker
4',6'-Diamidino-2phenylindole dihydrochloride (DAPI)	Serva
Digitonin	Sigma
DMSO (dimethylsulfoxide)	Sigma
DPN (2,3-bis(4-hydroxyphenyl)-propionitrile)	Tocris
DTT (Dithiothreitol)	Serva
EDTA	Merck
EGTA	Merck
ESCA (8-CPT-2'-O-Me-cAMP)	Calbiochem
Ethanol	Merck
17-β-estradiol, water soluble	Sigma
Ficoll 400	Serva
Fluoromount-G™	Southern Biotech
G-1	Calbiochem
Glutamate	Sigma
L-Glutamine	Sigma
HCl (acidic acid) 32%, p.a.	Merck
HCl (acidic acid) 1N	Merck
ICI 182,780	Tocris

5'-iodine resinfera toxin (5'I-RTX)	Sigma
(-)-Isoproterenol hydrochloride	Sigma
Laminin	Invitrogen
Magnesiumsulfat heptahydrat	Serva
D-(+)-Maltose monohydrate	Sigma
Mangan (II) chlorid tetrahydrat	Sigma
MDL-12,330A hydrochloride	Calbiochem
β-Mercaptoethanol	Sigma
Methanol, p.a.	Merck
$MgSO_4$	Serva
Nocodazole (NDZ)	Sigma
Non-fat milk powder	Sucofin
Paclitaxel (Taxol, TAX)	Sigma
Poly-L-Ornithine hydrochloride	Sigma
Paraformaldehyde (PFA)	Sigma
PEM-S	Sigma
Penicillin/Streptomycin	Cambrex
Phorbol 12-myristate 13-acetate (PMA)	Sigma
PIPES	Sigma
PKCε inhibitory peptide eV1-2	Calbiochem
PPT (4,4',4''-(4-Propyl-[1H]-pyrazole-1,3,5-triyl)trisphenol)	Tocris
Rotiphorese Gel 30 Acrylamid	Roth
Ryanodine	Calbiochem
SDS (sodium dodecyl sulfate)	Sigma
Sigmacote	Sigma
Sucrose	Invitrogen
TEMED (N,N,N',N'-Tetramethylethylenediamin)	Invitrogen
Tris(hydroxymethyl)-aminomethan p.a. (Tris)	Merck
TritonX-100	Sigma
Trypsin/EDTA (cell splitting)	Clonetix

Trypsin (for DRG preparation)	Worthington Biochemical Corporation
Tween 20	Sigma
Xylene Cyanol FF	Sigma

5.8   Kits and markers

Lipofectamine™ 2000 Transfection Reagent	Invitrogen
PLUS™ Reagent	Invitrogen
SuperScript™ III First Strand Synthesis SuperMix	Invitrogen
NucleoSpin® RNA/Protein	Macherey-Nagel
PageRuler™, Prestained Protein Ladder	Fermentas
100 bp DNA Ladder	NEB
Complete™ protease inhibitor cocktail	Roche
ECL™ Western blotting Detection Reagent	Amersham

5.9   Laboratory equipment

Agagel Maxi gel electrophoresis	Biometra
Cell counter CASY® Model DT	Schärfe System
Centrifuge EBA 12	Hettich Centrifuges
Centrifuge ROTANTA T 4402	Hettich Centrifuges
Centrifuge SORVALL® RC-5B, rotors SS-34; GSA	DuPont Instruments
Cleanbench CA/R6E	Clean Air
Cryostar Cryostat HM560	MICROM International
E.A.S.Y WIN 32 gel documentation	Herolab
Forceps, fine (130 mm)	FineScienceTools
Forceps, curved (145 mm)	FineScienceTools
Incubator C24	New Brunswick Scientific
ND-1000 spectrophotometer	NanoDrop Technologies
PCR PTC-250	MJ Research, Inc
pH Meter 766	Knick

PhosphorImager STORM 820	GMI
Power Supplier	BioRad
Rongeur	FineScienceTools
Scale BP2100	Sartorius
Scale BP61	Sartorius
Scalpel	FineScienceTools
Scissors	FineScienceTools
Sonopuls Homogenisator HD 2070	BANDELIN electronics
Steri-Cycle CO_2-Incubator 381	Thermo Forma
Thermo mixer	IKAMAG RC+ IKA Labortechnik
TRANS-Blot® SD semi-dry transfer cell	BioRad
Vortex Genie 1	Scientific industries

5.10   Microscopes

Leica DM IRE2: inverted microscope equipped with a cooled CCD camera from Hamamatsu Photonics

AxioObserver Z1: inverted microscope equipped with the Incubator XL S1, with temperature and CO_2 controller and a Zeiss AxioCam MRm camera

Zeiss Axioplan 2: epifluorescence microscope

Zeiss LSM 510 Meta: inverted laser scanning microscope, equipped with a cooled CCD camera from Hamamatsu Photonics

BD Pathway 855 High-Content Bioimager: equipped with a live temperature and CO_2 controlled live cell chamber, liquid handling and a cooled CCD camera

5.11 Software

Imaging Software

Image J, NIH

Simple PCI, Hamamatsu Photonics, Version 6.4

LSM Image Examiner, Version 4.2, Zeiss

Axiovision, Version 4.6, Zeiss

Attovision, BD

Statistic Software

GraphPad Prism, Version 4.03

Microsoft Excel

6 Methods

6.1   General methods

6.1.1   RNA extraction and purification

RNA extraction and purification from rat DRG as well as F-11 cells was done following the NucleoSpin RNA/Protein Kit Protocol. In short, RNA of disrupted cells was bound to silica gel columns. Bound RNA was washed and eluted from the columns. To minimize DNA contamination, a second DNase digestion was performed. Therefore the eluted RNA was incubated with 1 µl RQ1 DNase for 15 min at 37°C. RNA was precipitated with 0.1 volume of 3 M NaAcetat and 2.5 volume of EtOH for 20 min at -20°C. Samples were centrifuged with 21.000 x g for 10 min at 4°C, the supernatant was removed, samples were washed with 200 µl 70 % EtOH, centrifuged with 21.000 x g for 10 min at 4°C, the supernatant was removed and samples were dried at 42°C. RNA was resuspended in RNase free water and RNA purification was controlled by agarose gel electrophoresis using a 2 % agarose gel. The eluate was shock frozen in liquid nitrogen and stored at -80°C.

For RNA extraction from DRG all 12 DRGs (L1 to L6) were prepared and desheathed as described below. DRG were pooled and the tissue was homogenized in liquid nitrogen with pestle and mortar. For RNA extraction from F-11 cells, at least two 9.2 cm^2 dishes with confluent F-11 cells were used for RNA extraction.

6.1.2   RT-PCR

10 x PCR buffer:	100 mM	Tris/HCl, pH 8.3
	500 mM	KCl

cDNA synthesis

To generate cDNA, 2 µg of total RNA were applied to Superscript III First-Strand Synthesis Super Mix. Negative controls were preformed with dH$_2$O instead of the Superscript III enzyme. Samples were incubated at 25°C for 10 min, followed by incubation at 50°C for 30 min and 85°C for 5 min. Samples were cooled on ice and the RNA template was destroyed by RNase H digestion at 37°C for 20 min. Produced cDNA was stored at -20°C.

PCR

Polymerase chain reaction was preformed to check the expression of GPR30, estrogen receptor α and estrogen receptor β transcripts in RNA preparation from rat DRG as well as F-11 cells using exon spanning primers if possible. To avoid contaminations, all pipetting was done with filter tips under a sterile hood. In control samples, water as well as negative controls of the cDNA synthesis

was used instead of cDNA templates. The following primers were used for the amplification of estrogen receptor transcripts and GAPDH as a control:

Tab. 1: RT-PCR primers.

Product	Species	Sequence	Product Size (mRNA)
GPR30	Rat	5'-ATGAATTCGACTACAGTGGCGAGTCGTTTGT-3' 5'-ATGAATTCGACTACAGTGGCGAGTCGTTTGT-3'	172 bp
ERα	Rat	5'-AATTCTGACAATCGACGCCAG-3' 5'-GTGCTTCAACATTCTCCCTCCTC-3'	345 bp
ERβ	Rat	5'-TTCCCGGCAGCACCAGTAACC-3' 5'-TCCCTCTTTGCGTTTGGACTA-3'	262 bp
GAPDH	Rat	5'-CGTTGTGGATCTGACATGC-3' 5'-TCCCTCTTTGCGTTTGGACTA-3'	248 bp

The PCR reaction mixture was composed as follows:

Template cDNA	2 µl
Primer forward (10 µM)	1 µl
Primer reverse (10 µM)	1 µl
10x PCR Buffer	5 µl
$MgCl_2$ (25 mM)	5 µl
dNTPs (10 mM each)	0.6 µl
Taq polymerase (20 U/µl)	0.4 µl
H_2O ad iniectabilita	35 µl

The reaction was performed with the following protocol:

Initiation	2 min	94°C	
Denaturation	30 sec	94°C	
Annealing	30 sec	58°C	35 cycles
Elongation	60 sec	72°C	
Extension	10 min	72°C	

Expression of estrogen receptor transcripts was analyzed on a 2 % agarose gel performing an agarose gel electrophoresis.

6.1.3 Agarose gel electrophoresis

TAE buffer:	40 mM	Tris
	5 mM	Na-acetate
	1 mM	EDTA

6 x DNA loading buffer:	15 %	Ficoll (in H_2O)
	0.25 %	Xylene cyanol FF

To produce a gel, agarose was weighed and dissolved in TAE buffer by boiling in a microwave. To visualize the DNA, 0.5 µg/ml ethidiumbromide was incorporated into the gel. The sample together with the respective volume of 6 x DNA loading buffer was loaded onto the gel. Electrophoresis was performed with the electric field strength of 10 V/cm for about 1 h and gels were analyzed using a Herolab gel documentation system. The size of DNA fragments was estimated by comparison with the 100 bp DNA Ladder Plus (Gene Ruler).

6.2 Cell biological methods

6.2.1 Primary rat DRG cultures

Neurobasal A medium:	without	Phenol Red
	without	L-Glutamine
complete Neurobasal A medium:	+ 0.25 µM	L-glutamate
	+ 0.5 mM	L-glutamine
	+ 2 % (v/v)	B27 supplement
	+ 1 % (v/v)	Penicillin/Streptomycin
MEM + GlutaMAX ^{TM}		
Hank's balanced salt solution (HBSS):	5.33 mM	KCl
	0.44 mM	KH_2PO_4
	4.17 mM	$NaHCO_3$
	138 mM	NaCl
	0.34 mM	Na_2HPO_4
	5.56 mM	D-Glucose
	10 mM	Phenol Red
DPBS	200 mg/l	KCl
	200 mg/l	KH_2PO_4
	8 g/l	NaCl
	2.16 g/l	Na_2HPO_4 x 7 H_2O
	1 g/l	Glucose
	36 mg/l	Sodium Pyruvate

Preparation of cover slips and coating

For immunofluorescence analysis DRG neurons were seeded on laminin/polyornithine coated glass cover slips or 96-well plates.

Glass cover slips for primary DRG cultures were prepared as follows: Cover slips were immersed in chloroform : methanol (2 : 1, v/v) for 20 min at RT and completely dried by incubation at 50°C. Dried cover slips were incubated in 20 % sulfuric acid for 20 min at RT. Sulfuric acid was removed by thoroughly washing with dH_2O, followed by incubation with 0.1 N sodium hydroxide at RT for 5 min. Sodium hydroxide was again removed by washing with dH_2O and cover slips were stored in pure ethanol.

Before use cover slips were flamed and coated with polyornithine (0.1 mg/ml) and laminin (5 µg/ml) for 2 h at RT. 96-well plates were coated in a similar manner.

DRG dissection

Cellular experiments were preformed on male Sprague-Dawley rats (200–300 g). Animals were killed by CO_2 intoxication. The hair on the back was removed and the skin was cut along the spine using a scalpel. Tissue, muscles and tendons were removed from the lumbar vertebrae L1 to L6 using Rongeur forceps. Starting with L1, the spinal cord and the DRG were exposed by removing articular processes, lamina, pedicles and transverse processes. DRG were carefully separated using curved tweezers, dissected and stored in MEM until the end of the preparation. DRG of L2 to L6 were prepared in the same way.

Desheating

Before dissociation, surrounding tissue, the thin vascular skin layer and free nerve ends of the DRG were removed under a surgical microscope using straight tweezers. Desheathed DRG were pooled and stored in fresh MEM.

Dissociation and culture

Desheathed DRGs were incubated with collagenase (f.c. = 0.1 U/ml) in 5 ml MEM for 1 h at 37°C, transferred into 2.5 ml Hank's BSS with EDTA (f.c. = 0.025 %) and trypsin (f.c. = 470 U/ml) and incubated for 8 min at 37°C. Trypsin digestion was blocked by adding 10 mM $MgSO_4$. The supernatant was discarded and DRGs were triturated in 1.25 ml MEM with a fire polished and silicone coated pasteur pipette by slowly pipetting them 10 times up and down. Undissociated tissue was allowed to sediment. The supernatant was transferred to a separate tube and 1.25 ml of new medium was added to the undissociated tissue. This procedure of separation was repeated 3 times triturating 2 times with a Pasteur pipette with a wider and 2 times with a smaller opening. The collected and pooled supernatant were centrifuged at 100 x g for 5 min at RT. The pellet was washed with 1 ml Neurobasal A medium supplemented with 2 % (v/v) B27, 0.5 mM L-glutamine, 25 µM L-glutamate and penicillin/streptomycin 100 U/ml. Cells were centrifuged again (100 x g, 5 min, RT), the supernatant was discarded and cells resuspended in 1 ml complete Neurobasal A medium by pipetting 10 times up and down with the wide opening

Pasteur pipette. The volume of Neurobasal A medium was adjusted to the experimental conditions and cells were plated onto laminin/polyornithine coated surfaces as follows: 500 µl cell suspension/well in a 24-well plate (0.5 DRG/culture), 50 µl cell suspension/well in a 96-well plate (0.5 DRG/culture). Cells were allowed to adhere by incubation over night at 37 C, 5 % CO_2.

For calcium imaging with the flow through system cells were filtered using a 40 µm nylon cell strainer to remove undissociated cells and nerve endings after dissociation. The strainer was wetted with 0.5 ml complemented Neurobasal A medium, dissociated cells were applied and the strainer was washed 3 times with 0.5 ml complemented Neurobasal A medium. Centrifugation was done as described above and cells were seeded as "drops" containing 25 µl cell suspension on cover slips in 40 mm cell culture dishes. Cells were allowed to adhere by incubation at 37°C, 5 % CO_2 for ~2 h before adding additional 2 ml supplemented Neurobasal A medium.

6.2.2 PKCε translocation assay

Translocation to a target membrane is one essential step in the activation process of PKCs. In DRG neurons, the β-adrenergic agonist isoproterenol as well as the steroid hormone estrogen, two substances known to induce PKCε-dependent mechanical sensitization, have been shown to induce PKCε translocation to the plasma membrane within 30 to 90 sec (Hucho et al., 2005; Hucho et al., 2006). Therefore the translocation to the plasma membrane can be used as a correlate for the activation of PKCε in DRG neurons.

Stimulation of DRG cultures

To investigate the involvement of estrogen receptors in signaling process leading to the activation of PKCε in DRG neurons, overnight cultures of primary DRG neurons in 24-well plates were treated with the specific estrogen receptor α (ERα) agonist PPT (stock solution = 50 mM, f. c. = 1 nM and 10 nM), the estrogen receptor β (ERβ) agonist DPN (stock solution = 50 mM, f. c. = 10 nM and 100 nM), the GPR30 agonist G-1 (stock solution = 10 mM, f. c. = 100 nM) and the mixed ERα/ERβ antagonist, but GPR30 agonist ICI 182,780 (stock solution = 20 mM, f. c. = 1 µM). As control, cells were stimulated with the β-adrenergic receptor agonist isoproterenol in a final concentration of 1 µM (in PBS). To ensure a homogenous dispersion of the stimulants, 250 µl out of 500 µl medium were removed, mixed thoroughly with the respective agonist, and added back to the same culture. Cultures were incubated with the stimulant for the indicated time between 30 sec and 15 min, the medium was removed and cultures were washed once with PBS followed by fixation with 4 % paraformaldehyde (PFA) for 10 min at RT. PFA was removed and cultures were washed once with PBS.

To test the involvement of the adenylyl cyclase in estrogen-induced PKCε translocation overnight DRG cultures were incubated with the adenylyl cyclase inhibitor MDL-12,330A hydrochloride (stock solution = 5 mM in PBS, f. c. = 50 µM) prior to stimulation. Again, 250 µl out of 500 µl medium were removed, mixed with the inhibitor and added back to culture. Cultures were pre-incubated with the inhibitor for 30 min at 37° C, 5 % CO_2. Afterwards cultures were stimulated as

described above. Negative controls were always treated alike but without the addition of any reagent.

Stock solutions of PPT, DPN and G-1 were dissolved in 100 % DMSO (final concentration of DMSO on cells = 0.2 %). 17-β-estradiol, isoproterenol and MDL-12,330A hydrochloride were dissolved in PBS.

Immunocytochemistry of DRG cultures

Paraformaldehyde-fixed cells were permeabilized by incubation for 10 min with 0.1 % Triton X-100 at RT, followed by three washes with 0.1 % BSA in PBS (5 min, RT). For the following incubation steps until mounting onto microscopy slides cultures were transferred into a dark wet chamber. After block of unspecific binding sites by incubation with 5 % BSA/10 % normal goat serum in PBS for 1 h at RT, the cultures were probed with primary antibodies against PKCε (1 : 1000) in 1 % BSA in PBS overnight at 4°C, washed three times (1 % BSA in PBS, 5 min, RT), and incubated with secondary antibodies for 1 h at RT, followed by three washing steps with PBS, again 5 min each at RT. The cultures were mounted with Fluoromount-G containing 0.5 µg/ml DAPI.

For quantification of PKCε translocation FITC-coupled antiserum (goat anti-rabbit) was used in a final concentration of 1 : 500. For confocal imaging Alexa-488-labeled chicken anti-rabbit IgG (1 : 10.000) was used instead of FITC-coupled antiserum.

For detection of IB4-positive neurons, TRITC-coupled isolectin B4 (f. c. = 0.4 µg/ml) was incubated together with the secondary antibody in PBS supplemented with 100 µM CaCl$_2$, 100 µM MgCl$_2$ and 100 µM MnCl$_2$ for 1 h at RT. Afterwards cultures were washed three times with supplemented PBS (5 min, RT) and mounted as described above.

For TRPV1 detection unspecific binding sites were blocked with 5 % BSA/10 % normal donkey serum in PBS for 1 h at RT. Cultures were probed with polyclonal antiserum against the C-terminal region of TRPV1 (1 : 200, in PBS) for 1 h at RT and processed as described above. As a secondary antibody chicken anti-rabbit Alexa 594 was used.

For double staining of PKCε and TRPV1, unspecific binding sites were blocked using 5 % BSA/10 % normal donkey serum in PBS and PKCε was detected using a goat anti-PKCε antibody (1 : 1000). Both primary as well as both secondary antibodies were incubated together.

Evaluation of PKCε translocation

PKCε localization was evaluated with a Zeiss Axioplan 2 microscope, using a 63 x oil-immersion objective. 50 neurons per culture were randomly selected and PKCε localization was determined. Data were plotted as mean percentage of translocating cells per evaluated culture ± standard error of means (SEM) based on the number of evaluated cultures. All counting was done in blind manner. All treatments have been repeated with DRG neurons from different rats on at least two separate days.

Confocal images of representative cells were taken on an inverted Zeiss LSM 510 Meta with a 63 x oil-objective. To analyze the cellular distribution of PKCε, fluorescence intensity profiles were plotted along a line scan through the cell and membrane intensities were compared to overall intensities of the same cell using the NIH imaging software Image J.

6.2.3 Calcium imaging

One way to visualize changes in the intracellular calcium concentration is the use of calcium sensitive dyes, e.g. the polyamino carboxylic acid Fura-2. Fura-2 is a ratiometric fluorescent dye which binds calcium ions with a Kd of 0.14 µM. Fura-2 is excited at 340 nm and 380 nm of light and the ratio of the emission at 510 nm is directly correlated to the amount of free calcium within a cell.

To investigate if treatment of DRG neurons with noxious stimuli including estrogen/G-1 induce changes in the intracellular calcium level, ratiometric calcium imaging was performed with the membrane permeable derivate of Fura-2, the Fura-2-acetoxymethyl ester (Fura-2-AM). In contrast to Fura-2, Fura-2-AM is able to cross the cellular membrane. Within the cell, cellular esterases remove the acetoxymethyl group regenerating Fura-2.

Flow-through system

Overnight cultures of rat DRG neurons were incubated with 1 µM Fura-2-AM for 30 min at 37°C, 5 % CO_2 in Neurobasal A medium. Afterwards Fura-2-AM was removed by washing 3 times 10 min with medium at 37°C, 5 % CO_2. Cultures on cover slips were transferred to a metal-build live cell chamber, covered with medium and placed onto the microscope. A field of view was selected and the flow-through system was adjusted in close vicinity to the cells of interest. Baseline images were taken for 1 min before the response to the application of isoproterenol (1 µM, 1 min) was recorded. Isoproterenol was removed by adding medium for 5 min. Afterwards the viability of the cells was tested by recording the response to 30 mM KCl. Calcium imaging was preformed with an inverted Leica DM IRE2 microscope equipped with a cooled CCD camera and the imaging software Simple PCI version 6.4 (Hamamatsu Photonics). Paired images of 340 nm and 380 nm excitation wavelength were taken every 2 seconds. For evaluation the number of isoproterenol responsive cells was estimated in relationship to all cells showing stable baseline recordings as well as calcium influx in response to KCl application.

Tab. 2: Imaging and pipetting protocol for the flow-through Ca^{2+} imaging system.
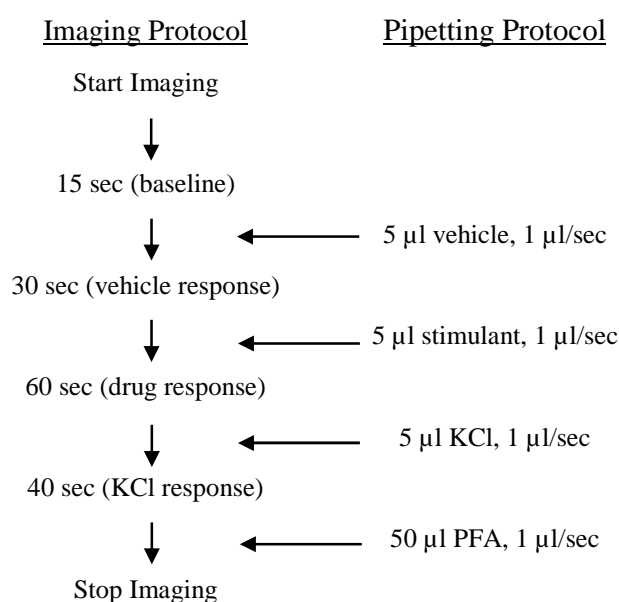
Imaging Protocol	Pipetting Protocol
1 min (baseline)	medium flow
1 min (drug)	drug flow
5 min (wash out)	medium flow
30 sec (KCl)	KCl flow
2,5 min (wash out)	medium flow

High-content Microscope

For the investigation of estrogen/G-1-induced calcium influx in DRG neurons, a high content automated microscope (Bioimager, BD) equipped with a live cell chamber and a liquid handling system was used. Overnight cultures of DRG neurons in 96-well plates were loaded with Fura-2-AM. Therefore, 10 µl out of 50 µl medium were removed, mixed with 1 µl Fura-2-AM (f.c. = 1 µM)) and added back to the same culture. Cultures were incubated with Fura-2-AM for 30 min at 37 C. Fura-2-AM was removed by washing 3 times for 10 min with supplemented Neurobasal A medium. 96-well plates were placed into the live cell chamber of the microscope (37 C, 5 % CO_2) and a field of view was selected in the first well. After the adjustment of the exposure times for both channels, the automated measurement was started. For a detailed description of the imaging and pipetting protocol see Tab. 3. In general, cultures were imaged for 15 sec as baselines measurement, before 5 µl medium or vehicle was added to control the reaction of the cells to mechanical pressure induced by the pipetting itself. This step was followed by ratiometric imaging for about 30 sec. Next, 5 µl of 17-β-estradiol (f. c. = 10 nM) or G-1 (f. c. = 10 nM or 100 nM) was added and images were collected for 60 sec. To control the viability of the cells, 5 µl KCl (f. c. = 30 mM) was added and images were taken for additional about 40 sec. 17-β-estradiol was dissolved in Neurobasal A medium, G-1 in DMSO/Neurobasal A medium with a final concentration of 0.2 % DMSO/culture.

To ensure similar conditions, not more than 8 cultures in a 96-well plate were loaded at the same time and imaged sequentially. The field of view (X-Y-position), the focus (Z-position) and the exposure time for each channel was adjusted manually for all wells.
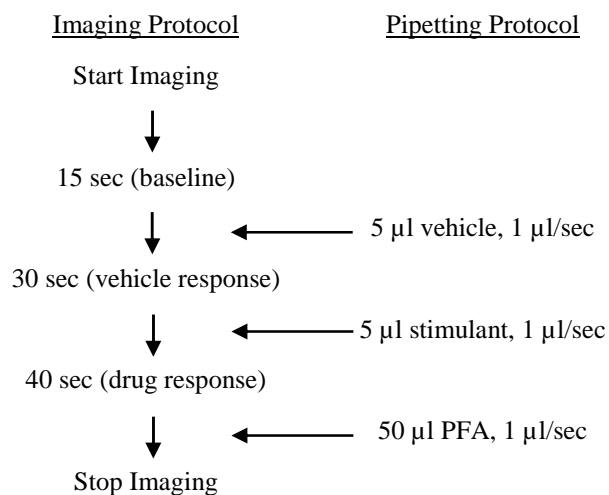
Paired images were taken almost every 2 sec and calcium influx was evaluated using the Bioimager software Attovision and Simple PCI, version 6.4. As described above, the percentage of neurons showing calcium influx in response to 17-β-estradiol or G-1 was calculated based on all neurons showing calcium influx in response to KCl.

Tab. 3: Ca^{2+} imaging protocol for the high content microscope.

Imaging Protocol	Pipetting Protocol
Start Imaging	
↓	
15 sec (baseline)	
↓	← 5 µl vehicle, 1 µl/sec
30 sec (vehicle response)	
↓	← 5 µl stimulant, 1 µl/sec
60 sec (drug response)	
↓	← 5 µl KCl, 1 µl/sec
40 sec (KCl response)	
↓	← 50 µl PFA, 1 µl/sec
Stop Imaging	

6.2.4 Combined assay: Calcium imaging and evaluation of PKCε translocation in the same cell

To investigate if calcium influx and PKCε translocation in response to different stimuli occur in the same neurons, calcium imaging was coupled to the "PKCε translocation Assay" using an automated high content microscope (Bioimager, BD). In the first part of this experiment, calcium imaging was performed as described above (Calcium imaging, high content microscope). After stimulation with 17-β estradiol, G-1 or isoproterenol, cells were imaged for 40 sec. Instead of adding KCl as a second stimulus, cells were fixed by adding 8 % PFA (f. c. = 4 %) directly to the cultures using the liquid handling system of the Bioimager. Cultures were incubated with PFA for 10 min at 37°C. Plates were taken out of the incubation chamber, PFA was removed and cultures were washed with PBS.

In the second part of the experiment, PKCε staining was performed following the protocol described in the corresponding paragraph (Immunocytochemistry). After incubation with the secondary antibody, cultures were washed 3 times with PBS for 10 min at RT and cultures were stored in PBS for imaging. To evaluate the PKCε localization, plates were put back in the Bioimager. Images were taken at the same x-y position selected for the calcium imaging in the first part of the experiment. Actual fluorescent images were compared with the last frame of the calcium imaging series and the x-y-positions were manually corrected if necessary. Images were taken using a 20 x objective at the Bioimager microscope. PKCε localization of cells showing calcium influx after stimulation was evaluated by plotting fluorescence intensity profiles, and membrane intensities were compared to overall intensities of the same cell using the NIH imaging software Image J. For comparison, PKCε localization of cells which did not show an increase of intracellular calcium after stimulation was analyzed alike.

Tab. 4: Ca^{2+} imaging setup for the analysis of Ca^{2+} influx and PKCε translocation.

Imaging Protocol   Pipetting Protocol

Start Imaging

↓

15 sec (baseline)

↓   ← ———— 5 µl vehicle, 1 µl/sec

30 sec (vehicle response)

↓   ← ———— 5 µl stimulant, 1 µl/sec

40 sec (drug response)

↓   ← ———— 50 µl PFA, 1 µl/sec

Stop Imaging

6.2.5   Primary mouse DRG cultures

complete Neurobasal A medium:		
	+ 0.25 µM	L-glutamate
	+ 0.5 mM	L-glutamine
	+ 2 % (v/v)	B27 supplement
	+ 1 % (v/v)	Penicillin/Streptomycin

MEM + GlutaMAX ^{TM}

Hank's balanced salt solution (HBSS):		
	5.33 mM	KCl
	0.44 mM	KH_2PO_4
	4.17 mM	$NaHCO_3$
	138 mM	NaCl
	0.34 mM	Na_2HPO_4
	5.56 mM	D-Glucose
	10 mM	Phenol Red

DPBS:		
	200 mg/l	KCl
	200 mg/l	KH_2PO_4
	8 g/l	NaCl
	2.16 g/l	Na_2HPO_4 x 7 H2O
	1 g/l	Glucose
	36 mg/l	Sodium Pyruvate

Coating

Primary mouse DRG neurons were plated onto polyornithine/laminin coated surfaces. For coating, glass or plastic surfaces were incubated with 0.1 mg/ml polyornithine in PBS over night at 4°C. The polyornithine was completely removed and surfaces were air dried for at least 2 h at RT. Dried surfaces were incubated with 2 µg/ml laminin in PBS for 2-4 h at RT. Laminin was removed, surfaces were washed 2 x with PBS and stored in PBS at RT until cells were plated.

DRG dissection and desheathing

DRG from the lumbar vertebra L1 to L6 of adult male mice were prepared following the preparation protocol for rat DRG neurons. After preparation, surrounding tissue, the thin vascular skin layer and free nerve ends of the DRG were removed under a surgical microscope using straight tweezers.

Dissociation and Culture

Cells were dissociated following the protocol described for rat DRG cultures. Collagenase treatment was done in a volume of 1 ml for 1 h at 37°C (f. c. = 0.1 U/ml collagenase) and trypsin digestion was also performed in a final volume of 1 ml (f. c. = 470 U/ml trypsin). Cells were seeded in a density of 0.5 DRG/culture as a "drop" of 50 µl cell suspension. Cells were allowed to adhere by incubation for 2 h at 37°C, 5 % CO_2. In case of seeding cells on 25 mm glass cover slips, 2 ml completed Neurobasal A medium was added afterwards. Cells were cultured for 3-5 days at 37°C, 5 % CO_2.

6.2.6 Live cell imaging of DRG cultures

DRG cultures with an established neurite network were used to show destabilization of the microtubule cytoskeleton in response to estrogen/G-1. Therefore DRG from adult male rats or mice were prepared as described above, cells were seeded into 24 well-plates (0.5 DRG/well) coated with laminin/polyornithine and cells were cultured for 3-5 days in complemented Neurobasal A medium in absence of additional growth factors. Before imaging culture plates were placed into the incubation chamber of the live cell imaging system (Zeiss observer Z.1 equipped with the incubator XL with temperature and CO_2 controller, 37°C, 5 % CO_2) at least 4 h prior to the experiment. DIC images were taken (1 frame/min) using a 20 x far distance objective and imaging started at least 30 min before the first substance was added to show neurite stability in absence of noxious stimuli. For addition of a stimulus, 50 µl out of 500 µl were removed from the well, mixed with 5 µl of the stimulant and carefully added back into the well. To exclude morphological changes in response to mechanical pressure induced by the addition of the stimulus or in response to the vehicle substance itself, the vehicle (PBS or 0.2 % DMSO) was added and images were taken for at least 1 h (1 image/min). Having a stable system, estrogen (1 nM) or G-1 (10 nM) was added carefully to the culture and imaging was continued for at least 1 h (DIC, 1 frame/min). Alteration of the cytoskeleton was detected by analyzing morphological changes including cell retraction, growth cone retraction and varicosity formation. The system was

equipped with a Zeiss AxioCam MRm camera. Data were analyzed with Zeiss Axiovision version 4.6 and the LSM image examiner software. Experiments were repeated on at least 4 different days with different animals.

6.2.7 F-11 cell culture

F-11 cells were cultured in Ham's F-12 medium (Invitrogen) supplemented with 15 % fetal bovine serum (FBS), 1 % Penicilin/Streptomycin and 1.5 % L-glutamine.

6.2.8 Transfection of F-11 cells

To analyze the estrogen/G-1-induced and TRPV1-dependent alteration of the microtubule cytoskeleton F-11 cells were transiently transfected with different TRPV1 constructs (TRPV1-GFP, TRPV1-S800A-GFP or TRPV1ΔN) or the empty vectors using Lipofectamine 2000 and the Lipofectamine Plus Reagent (Invitrogen) following the provided protocol. For live cell imaging cells were co-transfected with TRPV1-GFP constructs and m-Cherry-tubulin or only with m-Cherry-tubulin for control experiments. All experiments were performed approximately 48 h after transfection.

6.2.9 Analysis of *in situ* cytoskeleton of F-11 cells

Hank's balanced salt solution (HBSS):		
	5.33 mM	KCl
	0.44 mM	KH_2PO_4
	4.17 mM	$NaHCO_3$
	138 mM	NaCl
	0.34 mM	Na_2HPO_4
	5.56 mM	D-Glucose
	without	Phenol Red
Permeabilization buffer:	50 mM	PIPES, pH 6.8
	1 mM	EGTA
	0.2 mM	$MgCl_2$
	10 % (v/v)	glycerol
	50 µg/ml	digitonin
	complete™ protease inhibitor cocktail	

Stimulation of F-11 cells and preparation of *in situ* cytoskeleton

To investigate the integrity of the microtubule cytoskeleton after stimulation with estrogen/G-1, transfected as well as non-transfected F-11 cells were treated with estrogen/G-1 and the *in situ* cytoskeleton was prepared.

For that purpose, cells were seeded on glass cover slips in 24-well plates, transfected with TRPV1-GFP, TRPV1ΔN or TRPV1-S800A-GFP or control vectors and cultured for ~48 h.

Medium was replaced by serum-free medium ~1 h before stimulation. Cells were stimulated for 1 min with either 17-β-estradiol (f. c. = 1 nM) or G-1 (f. c. = 10 nM), or ICI 182,780 (f. c. = 100 nM). To analyze the influence of the ion channel function of TRPV1 on the observed morphological alterations, cells were pre-incubated with the TRPV1 antagonist 5'I-RTX (f. c. = 1 µM) for 10 min at 37°C prior to stimulation with estrogen/G-1. To ensure homogeneous dispersion of the stimulants, 500 µl out of 1 ml medium was removed, mixed thoroughly with the respective stimulant, and added back to the same culture. All stock solutions of the respective reagents were dissolved in 100 % DMSO (final concentration for DMSO on cells = 0.2 %). Buffer-controls were treated alike without adding any stimulus. After treatment cells were washed once with HBSS buffer and a membrane permeabilization buffer was added for 1 min at RT. The buffer contained 50 mM PIPES, pH 6.8, 1 mM EGTA, 0.2 mM $MgCl_2$, 10 % v/v glycerol, complete™ protease inhibitor cocktail and the detergent digitonin 50 µg/ml. Rapid extraction of cells using this buffer permeabilizes the plasma membrane without influencing cellular morphology which allows the analysis of stable cytoskeletal filaments (Lieuvin et al., 1994). The permeabilization buffer was removed and cells were fixed by adding 4 % PFA for 10 min at RT. Cells were washed 3 x with 1 ml PBS and subsequently processed for immunofluorescence analysis.

Immunocytochemistry and analysis of cytoskeletal structures

Paraformaldehyde-fixed cells were permeabilized by incubation for 10 min with 0.1 % Triton X-100 at RT, followed by three washes with 0.1 % BSA in PBS (10 min, RT).

Unspecific binding sites were blocked by incubation with 5 % BSA/10 % normal goat serum for 1 h at RT, blocking solution was removed and cells were probed with primary antibodies against TRPV1 and tubulin for 1 h at RT. The primary antibodies were used in the following dilutions: rabbit polyclonal anti-TRPV1 IgG (1 : 1000, alomone, directed against C-terminal region of TRPV1 or 1 : 1000, Dianova, directed against the N-terminal region of TRPV1), rat monoclonal anti-tyrosinated tubulin IgG (Clone YL1-2, 1 : 1000). Cells were washed three times with PBS (10 min, RT) and incubated with secondary Alexa 488/Alexa 594-coupled antibodies (1 : 1000, 1 h RT). After three final washes (10 min, RT) cells were mounted with Fluoromount-G (Southern Biotech/Biozol) containing DAPI (0.5 µg/ml). Confocal images were taken on an inverted Zeiss LSM 510 Meta with a 63 x objective and analyzed with the Zeiss LSM image examiner software.

6.2.10   Live cell imaging of F-11 cells

Hank's balanced salt solution (HBSS):		
	5.33 mM	KCl
	0.44 mM	KH_2PO_4
	4.17 mM	$NaHCO_3$
	138 mM	NaCl
	0.34 mM	Na_2HPO_4
	5.56 mM	D-Glucose
	without	Phenol Red

To analyze estrogen/G-1-induced morphological changes in presence and absence of TRPV1, live cell imaging of F-11 cells transiently transfected with either only m-Cherry-tubulin or m-Cherry-tubulin together with a TRPV1-GFP construct (wildtype or TRPV1-S800A) was performed. Therefore cells were seeded on 25 mm cover slips, transfected using Lipofectamine as described above and cultured for 36-48 h after transfection. For imaging, cover slips were transferred into a live cell chamber, covered with HBSS buffer and the chamber was placed onto the microscope at least 10 min before imaging started.

For treatment with estrogen/G-1 drugs were pre-diluted in 50 µl HBSS buffer and added onto the culture during imaging with a final concentration between 0.1 and 10 nM 17-β-estradiol and 1 to 100 nM G-1. 17-β-estradiol dilutions were prepared in HBSS from a 10 µM stock solution in HBSS, G-1 dilutions were prepared in 10 % DMSO/HBSS from a 100 µM stock solution in 100 % DMSO. Images of cells expressing TRPV1 as well as of non-TRPV1 expressing cells were taken at least 10 min prior to estrogen/G-1 treatment (1 frame/min) and imaging was continued for at least 15 min after the stimulus was added.

To investigate the involvement of protein kinases C (PKCs) into the observed morphological changes, TRPV1-GFP expressing cells were selected before the PKC inhibitor BIM (f. c. = 5 µM) was applied and cells were incubated for 12 min prior to estrogen/G-1 treatment.

Images were taken with an inverted Zeiss LSM 510 Meta confocal microscope with a 63 x objective in the red as well as the green channel. Additionally bright field images were collected for all time points. In case of cultures pre-treated with BIM, only bright field images are shown due to the high autofluorescence of the inhibitor. Images were analyzed with the Zeiss LSM image examiner software. All experiments were repeated at least 6 times.

6.3 Biochemical and computational methods

6.3.1 Computational modeling

To investigate the possibility of tubulin and/or microtubule binding to the C-terminal region of TRPV1, computational modeling was performed by our cooperation partners G. Fernandez-Ballester and X. Ferrer-Montiel. The tubulin structure used for the docking process was 1TUB.PDB, obtained by X-Ray diffraction at 3.7 Å resolution (Nogales et al., 1998). The TRPV1 C-terminal used for docking was detached from the full human TRPV1 channel previously modeled (Fernandez-Ballester and Ferrer-Montiel, 2008). Structure edition were made with Swiss PDB viewer v3.7 (Guex and Peitsch, 1997) and WHATIF (Vriend, 1990). The protein-protein docking interaction prediction was accomplished with GRAMM-X v.1.2.0 (Tovchigrechko and Vakser, 2006) using default conditions. Refinements in the orientation and optimization of the side chains in protein complexes were carried out in two steps: first, those residues making Van-der-Waals clashes were selected and fitted with "Quick and Dirty" algorithms; second, models were energy minimized (5 x 1000 steps of steepest descent and 5 x 1000 conjugate gradient, cutoff of 10 Å for non-bonded interactions) with Insight II (Biosym/MSI, Accelrys Software Inc., http://www.accelrys.com/). Finally, the protein complexes were evaluated in terms of energy with FoldX (Guerois et al., 2002; Schymkowitz et al., 2005) at the CRG site (http://foldx.crg.es). The molecular graphic representations were created and rendered with PyMOL v0.99rc2 (http://www.pymol.org).

6.3.2   Tubulin binding assay

PEM-S:	50 mM	PIPES, pH 6.8
	1 mM	EGTA
	0.2 mM	$MgCl_2$
	100 mM	NaCl
Lipid mix:	10 mM	Hepes, pH 7.4
	200 µg/ml	Phosphatidylserine
	20 µg/ml	Diacylglycerol
6 x Laemmli buffer:	65 mM	Tris/HCl, pH 6.8
	3 % (w/v)	SDS
	30 % (v/v)	Glycin
	5 % (w/v)	2-Mercaptoethanol
	4 mg/ml	Bromphenol blue
	4 mg/ml	Pyronin G
Electrophoresis buffer:	24.8 mM	Tris
	192 mM	Glycerin
	0.01 % (w/v)	SDS
5 x Blotting buffer:	200 mM	Glycin
	250 mM	Tris
	0.2 % (w/v)	SDS
TBST:	25 mM	Tris
	137 mM	NaCl
	27 mM	KCl
	0.1 % (v/v)	Tween-20
Blocking buffer:	5 %	Non-fat milk in TBST

The tubulin binding assay was performed by C. Goswami.

To characterize the relationship between PKCε-mediated phosphorylation of the TRPV1-C terminus (TRPV1-Ct) and tubulin binding to the TRPV1-Ct, tubulin-binding assays with TRPV1-Ct in its phosphorylated as well as non-phosphorylated form were performed.

Tubulin binding

In the first part of the experiment the influence of tubulin binding to TRPV1-Ct on PKCε-mediated phosphorylation was tested. Therefore purified MBP-TRPV1-Ct and MBP-LacZ was coupled to amylose beads and suspended in PEM-S buffer (50 mM PIPES pH 6.8, 1 mM EGTA, 0.2 mM $MgCl_2$ and 100 mM NaCl). Approximately 100 µl of this suspension were incubated with 20 µg soluble tubulin purified from adult porcine brain (200 µl from 100 µg/ml stock solution) for

1 h at RT. In control samples, 200 µl PEM-S buffer were added instead of tubulin. After incubation, the amylose resin was washed 3 times with PEM-S buffer (600 µl/each) and the PKCε phosphorylation assay was performed.

In vitro phosphorylation

For the in vitro phosphorylation assay a kinase reaction mixture was prepared containing $MgCl_2$ (12 µl from 1 M stock), DTT (12 µl from 1 M stock), lipid mix (phosphatidylserine f. c. = 200 µg/ml, diacylglycerol f. c. = 20 µg/ml in 10 mM HEPES (pH 7.4), 0.03 % Triton X100; 80 µl from a 10 x stock), cold ATP (12 µl from 10 mM stock) and 5 µl of hot ATP (γP32 with 10 µCi/µl). PBS was added to a final volume of 160 µl. 20 µl of the reaction mixture were applied in each tube and samples were complemented with 1 µl purified PKCε (Invitrogen) or buffer in case of negative controls. The kinase reaction was performed for 1 h at RT. Afterwards bound proteins were eluted with 10 mM maltose/PEM-S, mixed with Laemmli buffer and incubated for 5 min at 95°C.

SDS-PAGE

Sodium dodecyl sulfate polyacrylamide gel electrophoresis (SDS-PAGE) was used for the separation of proteins according to their molecular weight. Using the Mini-PROTEAN™ Electrophoresis System (BIO-RAD), 10 % (w/v) acrylamide mini gels and 5 % stacking gels were prepared. Denatured protein samples were loaded onto the gel using a Hamilton syringe and empty lanes were filled with an equal amount of 1 x Laemmli buffer. PAGE was performed at 100 V for approximately 1 h until colored migration front had reached the bottom of the gel.

Tab. 5: Composition of SDS gels.

	Separating gel	Stacking gel
dH_2O	1.9 ml	1.1 ml
30 % Acrylamide	1.7 ml	330 µl
1.5 M Tris, pH 8.8	1.3 ml	—
1.5 M Tris, pH 6.8	—	0.5 ml
10 % SDS	50 µl	20 µl
10 % APS	50 µl	20 µl
Temed	2 µl	2 µl
Total volume	~ 5 ml	~ 2 ml

Western Blot

Separated proteins were transferred from the SDS gel to a PVDF membrane (Millipore) by semidry electro blotting. Therefore membranes were activated by incubation in methanol for 5 min at RT and rinsed with blotting buffer. The blot was assembled as follows: blotting paper (BIO-RAD, dipped into blotting buffer), activated membrane with gel on top, blotting paper (BIO-RAD, dipped into blotting buffer). Proteins were transferred by applying 2.5 mA/cm^2

(~0.12 A/membrane) for 30 min. Membranes were transferred into an incubation chamber, unspecific binding sites were blocked by incubation with 5 % non-fat milk in TBST buffer (25 mM Tris, 137 mM NaCl, 27 mM KCl, 0.1 % Tween-20) for 1 h at RT while shaking. Afterwards membranes were incubated with primary antibodies (anti-MBP, NEB and anti-β-tubulin (Sigma), each 1 : 1000) for 1 h at RT, washed 3 x with TBST at RT (10 min each) and subsequently incubated with horseradish peroxidase-conjugated anti-mouse and anti-rabbit antibodies (Amersham Bioscience) for 1 h at RT while shaking. After three final washes with TBST (10 min each), the ECL detection system (Amersham Biosciences) was used to detect tubulin and TRPV1-Ct.

Detection of phosphorylation

PKCε-mediated phosphorylation of the TRPV1-C terminus was monitored with the PhosphorImager STORM 820.

Reverse Experiment

In the second part of the experiment was investigated if PKCε-mediated phosphorylation of the TRPV1-Ct influences tubulin binding to the C-terminal region of TRPV1. Therefore the *in vitro* phosphorylation step was performed first, followed by the tubulin binding experiment.

For the *in vitro* phosphorylation assay MBP-TRPV1-Ct or MBP-LacZ coupled to amylose resin were used as phosphorylation template. 100 µl of template suspension were incubated with the kinase reaction mixture containing $MgCl_2$ (12 µl from 1 M stock solution), DTT (1.5 µl from 0.1 M stock solution), 1.5 µl Lipid Mix, 15 µl cold ATP (0.01 M), 1.5 µl hot ATP ($\gamma P32$ with 10 µCi/µl) and 4 µl purified PKCε (Invitrogen) or PEM-S in case of controls for 1 h at RT. Samples were washed 3 x with PEM-S (800 µl each) and subsequently incubated with 20 µg tubulin (20 µl from 100 µg/ml solution) for 1 h at RT. Samples were washed again 3 x with PEM-S (600 µl/each), the buffer was completely removed using a Hamilton syringe and bound proteins were eluted with 10 mM maltose/PEM-S. Samples were separated on a SDS gel and phosphorylation of TRPV1-Ct and tubulin binding were analyzed as described above.

6.4   Pain behavioral experiments

6.4.1   Testing of the mechanical nociceptive threshold in the rat

All pain behavioral experiments in rats were performed by Olayinka A. Dina in the lab of Jon D. Levine at the UCSF.

Quantification of the nociceptive flexion reflex

Experiments were performed with adult male Sprague-Dawley rats with a weight between 250 g and 300 g and all experiments were performed at the same time of the day. The nociceptive

flexion reflex was quantified using the Randall-Selitto paw pressure device (Analgesymeter, Stoelting, Wood Dale, IL, USA) which applies a linearly increasing mechanical force to the dorsum of the hindpaw of a rat. During the experiment the paw rests on a Teflon platform. Therefore the paw can easily be withdrawn without injury. The nociceptive mechanical threshold was defined as the force in grams at which the rat withdrew its paw. In the week preceding the experiments, rats were familiarized with the testing procedure at 5 min-intervals for a period of 1 h per day for 3 days. On the day of the experiment, baseline paw withdrawal threshold was defined as the mean of six readings before test agents were injected. Each paw was treated as an independent measure and each experiment was performed on a separate group of rats.

Test substances were injected intradermally into the dorsal surface of the hindpaw in a volume of 2.5 µl. The onset of mechanical hyperalgesia is already statistically significant after 2 min (Khasar et al., 1999b) mirroring the cellular results. Paw-withdrawal thresholds were determined 30 min after application of the test substance as the mean of three independent measurements, a time point where the maximal response reached a plateau. The effect of each drug is expressed as the percentage change of the baseline nociceptive threshold which was calculated as follows:

(threshold in presence of the test agent – baseline threshold)/baseline threshold x 100.

This transformation was done to normalize baseline thresholds of individual rats in one group.

G-1 and ICI 182,780 were dissolved to stock solutions of 10 mg/ml in 100 % DMSO. Further dilutions were done in PBS. For dose-response curves 1, 10, 100 and 1000 ng of G-1 or ICI 182,780 were injected in a final volume of 2.5 µl. For further analysis, G-1 was used in a final concentration of 1 µg/2.5 ml and ICI 182,780 in a final concentration of 100 ng/2.5 µl.

PKCε-dependence of G-1/ICI 182,780-induced mechanical sensitization

To investigate the involvement of PKCε into G-1- and ICI 182,780-induced mechanical hyperalgesia, PKCε was blocked using the PKCε inhibitor peptide εV1-2 (εV1-2) (Johnson et al., 1996). Because it is less membrane-permeable, injections of the PKCε inhibitor were always preceded by administration of 2.5 µl of distilled water in the same syringe, separated by a small air bubble, to produce a hypo-osmotic shock, thereby enhancing cell membrane permeability to the drug (Khasar et al., 1995; Khasar et al., 1999a; Khasar et al., 1999b). The PKCε inhibitor was injected 30 min prior to injection of G-1 or ICI 182,780 and the mechanical nociceptive threshold was measured 30 min after application of G-1/ICI 182,780. The influence of εV1-2 injections itself was tested in control animals treated only with the PKCε inhibitor peptide.

Influence of microtubule alternating drugs on G-1-induced mechanical sensitization

To investigate the influence of the microtubule cytoskeleton on G-1-induced mechanical hyperalgesia, microtubule structure was altered by application of the microtubule disruptor nocodazole or the microtubule stabilizing agent Taxol. Microtubule alternating drugs were injected intradermally into the dorsum of the hindpaw 30 min prior to G-1 injection (1 µg/2.5 µl PBS from a 10 mg/ml stock solution in 100 % DMSO). The mechanical nociceptive threshold was

tested 30 min after the last injection. Nocodazole was dissolved in 10 % DMSO with a final concentration of DMSO <1 %. Injection was done with a final concentration of 1 µg/2.5 µl. Taxol (1 mg/ml) was formulated at a concentration of 1 mg/ml in a vehicle comprising absolute ethanol and Cremophor EL (Dina et al., 2001a). Final Taxol concentration of 1 µg/2.5 µl was made in normal saline-diluted Cremophor vehicle.

To evaluate if an alteration of the microtubule cytoskeleton itself influences the mechanical nociceptive threshold, animals were treated with nocodazole or Taxol and the nociceptive threshold was determined 30 min after injection of microtubule alternating drugs.

Downregulation of TRPV1

One method to down-regulate the expression of proteins in DRG neurons of adult rats is the intrathecally administration of antisense oligodeoxynucleotides (ODNs) daily over three days (Alessandri-Haber et al., 2003; Dina et al., 2004; Dina et al., 2005; Joseph et al., 2007; Malik-Hall et al., 2005).

To reduce the expression of TRPV1 the 18-mer antisense ODN with the sequence 5'-CAT GTC ATG ACG GTT AGG-3' directed against a unique sequence of rat TRPV1 was used which has been shown to down-regulate TRPV1 *in vivo* (Christoph et al., 2006). As a control, an ODN corresponding to the TRPV1 antisense with six bases mismatched was created. The mismatch ODN had the following sequence 5'-CAT **GCT** ATG A**GC** GTT **GA**G-3' (Christoph et al., 2006) mismatches are denoted in bold).

Lyophilized ODNs were reconstituted in nuclease-free 0.9 % NaCl to a concentration of 10 µg/µl and stored at −20 °C. A dose of 40 µg TRPV1 antisense or mismatch ODN was intrathecally administered in a volume of 20 µl once daily over 3 days. Prior to each injection rats were anaesthetized with 2.5 % isoflurane containing oxygen. ODNs were injected by using a 30-gauge needle inserted intrathecally on the midline between the fifth and sixth lumbar vertebrae.

The nociceptive flexion reflex was quantified in animals treated with TRPV1 as well as mismatch ODNs to control the effect of the ODN treatment itself and of the down-regulation of TRPV1 on the mechanical nociceptive threshold. Injection of microtubule alternating agents and G-1 was done as described above and the nociceptive flexion reflex was measured 30 min after the last injection. In all experiments involving rats treated with TRPV1 antisense ODNs, mismatch ODN treated animals as well as wild type animals were used as a control.

Sequential stimulation

To check the effect of two independent drugs both inducing PKCε-dependent mechanical hyperalgesia, G-1 and the Epac activator ESCA (8-(4-chlorophenylthio)-2'-O-methyl-cAMP) were injected consecutively. Therefore, a 10 mg/ml stock solution of G-1 dissolved in 100 % DMSO was prepared and G-1 was intradermally injected in a final dilution of 1, 10, 100 and 1000 ng in 2.5 µl PBS 30 min prior to the application of ESCA (1 µg/2.5 µl PBS) and the effect on the nociceptive flexion reflex was evaluated 30 min after ESCA application. To test if the

order of injections is important for the observed effect both substances were also applied in the reverse order (1. injection: ESCA with a concentration of 1 µg/2.5 µl PBS, 2. injection: G-1 with concentrations of 1, 10, 100 and 1000 ng in 2.5 µl PBS). Additionally to G-1 and ESCA, also the effect of sequential injection of estrogen (100 ng/2.5 µl) and ESCA (6.3 µg/2.5 µl), isoproterenol (1 µg/2.5 µl) and ESCA (6.3 µg/2.5 µl) as well as ryanodine (1 µg/2.5 µl) and ESCA (6.3 µg/2.5 µl) was analyzed. The second injection was always applied 30 min after administration of the first stimulus and measurement of the nociceptive threshold was performed 30 min after the second injection. As controls, the first or the second injection of a stimulus was replaced by the injection of the respective vehicle.

To analyze the effect of an intracellular Ca^{2+} rise on PKCε-dependent mechanical hyperalgesia, the nociceptive flexion reflex was analyzed 30 min after intradermal injection of 1 µg/2.5 µl ryanodine into the hindpaw of adult male rats.

6.4.2 Testing of the mechanical nociceptive threshold in the mouse

Testing of the mechanical nociceptive threshold in mice was performed by Dominika Labuz in the group of Halina Machelska-Stein at the Charité-Universitätsmedizin Berlin, Campus Benjamin Franklin.

Adult male mice with a weight between 25 and 30 g were habituated to test cages with a wire mesh bottom daily starting 6 days prior to behavioral testing. The mechanical nociceptive threshold was tested using calibrated von Frey filaments (Stoelting). Filaments were applied to the plantar surface of the hindpaws using the up-down method. Testing began using a 3.9 mN hair (0.4 g). If the animal withdrew the paw, the weaker hair was applied. In case of no withdrawal, the next-stronger hair was applied. The maximum number of applications was 6-9, and the cut-off was 39.2 mN (4 g).

To investigate the influence of estrogen as well as G-1 on the mechanical nociceptive threshold, 1, 10, 100 and 1000 ng estrogen (in PBS) or G-1 (in DMSO) were injected subcutaneously into the plantar surface of the hindpaw and von Frey testing was performed 15, 30, 45, 60 and 120 min after injection. Additionally, the basal nociceptive threshold of each animal was determined prior to estrogen/G-1 injection. Control animals were treated alike but only vehicle instead of estrogen/G-1 was injected. Experiments were performed with at least 3 different animals for each condition.

6.5 Statistical analysis

All statistical comparisons were made with one-way anovas followed by Dunnett's test for comparisons with one control value, or the Tukey–Kramer post hoc test for multiple comparisons, respectively. $p < 0.05$ was considered statistically significant.

7 Results

In my thesis, I characterized the role of estrogen in nociception on a molecular, cellular and behavioral level. In the first part, I used a pharmacological approach to identify the estrogen receptor which mediates estrogen actions in primary nociceptive neurons (7.1). In the second part I focused on the characterization of downstream events of estrogen-induced PKCε signaling. Specifically, the role of the TRPV1-microtubule complex in estrogen-induced mechanical sensitization was analyzed by structural modeling and in biochemical, cellular and behavioral experiments (7.2). Finally, finding estrogen as well as epinephrine to converge on PKCε, I addressed in the third part of this thesis the question of signal integration in the primary sensory neuron. Thereby, a new desensitizing branch of PKCε signaling was identified which interferes with subsequent sensitizing signals (7.3).

7.1   GPR30 agonists induce mechanical hyperalgesia

A large number of endogenous substances have been shown to induce mechanical hyperalgesia in rats. Intradermal injection of the β2-adrenergic agonist isoproterenol results in the reduction of the mechanical nociceptive threshold by ~40 %. This sensitizing effect is mediated by the epsilon isoform of the protein kinase C as pretreatment with the PKCε-inhibitor peptide εV1-2 abolishes the effect completely (Fig. 6 A). Nevertheless, the molecular and cellular mechanisms underlying sensitization are mostly elusive.

Recently, I assisted in a study describing the steroid hormone estrogen to induce PKCε-dependent mechanical hyperalgesia comparable to inflammatory mediators (Fig. 6 B) (Hucho et al., 2006). Similar to epinephrine we found estrogen to act directly on the nociceptive neuron itself. Both induced the translocation of PKCε from the cytoplasm to the plasma membrane (Fig. 7). The first aim of my thesis was to identify the estrogen receptor which mediates the rapid translocation of PKCε in DRG neurons.
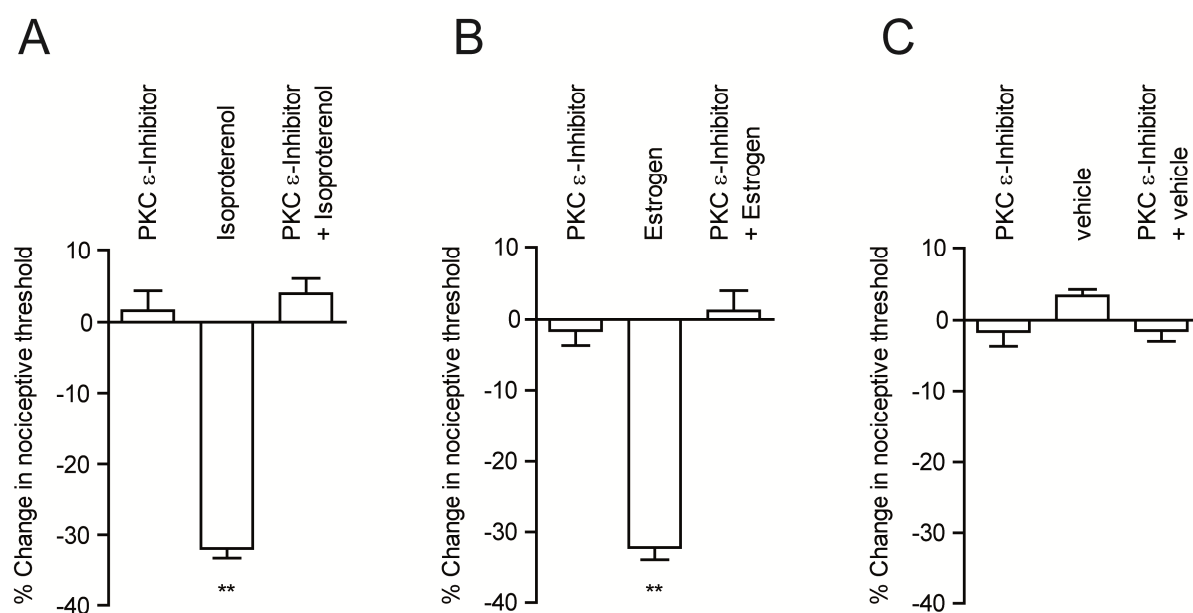
Fig. 6: The steroid hormone estrogen induces PKCε-dependent mechanical hyperalgesia similar to the inflammatory mediator isoproterenol. Injection of the β2-adrenergic receptor agonist isoproterenol (1 µg/2.5 µl) as well as injection of estrogen (100 ng/2.5 µl) in the hindpaw of male rats produced mechanical hyperalgesia in the same magnitude measured 30 min after injection (reduction of nociceptive threshold: isoproterenol 31.9 ± 1.3 % (A), estrogen 32.1 ± 1.7 % (B)). Both, estrogen as well as isoproterenol induced reduction in threshold was abolished by preinjection of the PKCε-inhibitor peptide εV1-2 (1 µg in 2.5 µl) 30 min prior to estrogen/isoproterenol application (A and B). Neither injection of the vehicle, nor injection of the PKCε inhibitor peptide εV1-2 nor the combination of both affected the mechanical nociceptive threshold (C). Measurements of the nociceptive threshold were preformed with the Randall-Selitto paw pressure device. ** $p < 0.001$ for estrogen/isoproterenol compared to estrogen/isoproterenol + PKCε inhibitor peptide, error bars represent SEM.

7.1.1 Agonists of ERα and ERβ do not lead to rapid PKCε translocation in DRG neurons

The translocation to a cell membrane is an essential step in the activation process of PKCs. In DRG neurons immunocytochemical detection of PKCε at the plasma membrane is a sensitive surrogate measurement of PKCε activation (Cesare et al., 1999; Hucho et al., 2005). Recently, Tim Hucho observed estrogen to cause PKCε translocation in about 15 % of DRG neurons. The translocation was transient peaking after 90 sec and returning to baseline levels after 5 min stimulation (Fig. 7 B). Rapid, non- transcriptional estrogen actions can be mediated by the classical estrogen receptors ERα and ERβ (Manavathi and Kumar, 2006). Both receptors have been shown to be expressed in subpopulations of DRG neurons (Papka and Storey-Workley, 2002; Taleghany et al., 1999). I tested if ERα and/or ERβ mediate estrogen-induced PKCε translocation in primary sensory neurons. Dissociated DRG neurons were treated with the ERα-specific agonist PPT as well as the ERβ-specific agonist DPN and neurons were evaluated for PKCε translocation.
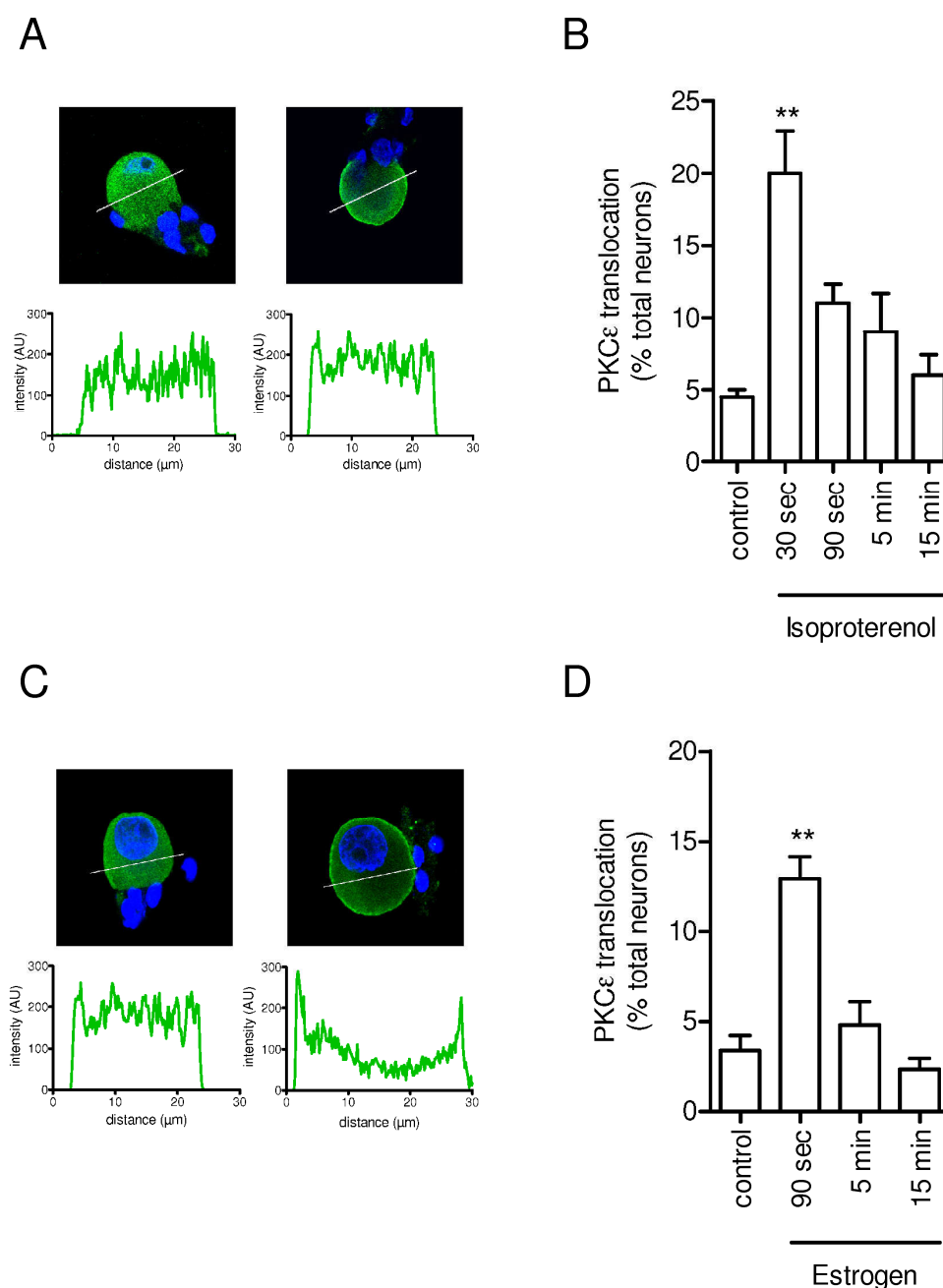
A

B

Isoproterenol

C

D

Estrogen

Fig. 7: Isoproterenol as well as estrogen induces rapid PKCε translocation in a subset of rat DRG neurons.
(A) Immunofluorescence analysis of PKCε distribution in DRG neurons. Confocal images show a cytoplasmic localization of PKCε in untreated cells (left image). In contrast, incubation with isoproterenol (1 µM, 30 sec) induced PKCε translocation to the plasma membrane in a subgroup of DRG neurons (right image). White lines indicate the position of PKCε intensity histograms shown below. White lines = 30 µm. **(B)** Quantification of neurons showing plasma membrane localization of PKCε. Isoproterenol treatment (1 µM) for 30 sec resulted in PKCε translocation to the plasma membrane in 20.0 ± 2.9 % of neurons, decreasing after 90 sec (11.0 ± 1.3 % total neurons) and 5 min of incubation (9.0 ± 2.6 % total neurons). After 15 min of isoproterenol treatment, no significant change of PKCε translocation was detected in comparison to untreated controls (15 min isoproterenol 6.0 ± 1.4 % total neurons, negative controls 4.5 ± 0.5 % total neurons). **(C)** Confocal images show membrane staining of PKCε after estrogen treatment (10 nM, 90 sec) in a subgroup of DRG neurons (right image). In contrast, no prevalent membrane staining was detected in vehicle treated controls (left image). White lines indicate the position of intensity measurements shown below. White lines = 30 µm. **(D)** Estrogen-induced PKCε translocation to the plasma membrane after 90 sec in 12.9 ± 1.2 % of all neurons. After longer exposures translocation could not be detected (5 min estrogen 4.8 ± 1.3 % total neurons, 15 min estrogen 2.3 ± 0.6 % total neurons, negative controls 3.4 ± 0.8 % total neurons). PKCε localization was analyzed by immunofluorescence microscopy (n = 6 cultures, ** $p < 0.001$ compared to vehicle controls). Error bars represent SEM.

After treatment with the ERα-specific agonist, PPT (1 nM) (Boulware et al., 2005; Jelks et al., 2007) which has a 410-fold selectivity for ERα over ERβ, no PKCε translocation was observed 30 sec to 5 min after stimulation. Also a 10-fold increase in the PPT concentration to a final concentration of 10 nM did not result in a detectable PKCε translocation (Fig. 8 A).

To test whether ERβ mediates estrogen-induced PKCε translocation, over night cultures of DRG neurons were treated with the potent ERβ agonist DPN for 30 sec to 5 min. Stimulation with 10 and 100 nM DPN (Boulware et al., 2005; Jelks et al., 2007) did not induce any detectable PKCε translocation in comparison with negative controls (Fig. 8 B).

These cellular results indicate that neither ERα nor ERβ mediate rapid estrogen-induced PKCε translocation in primary sensory neurons.
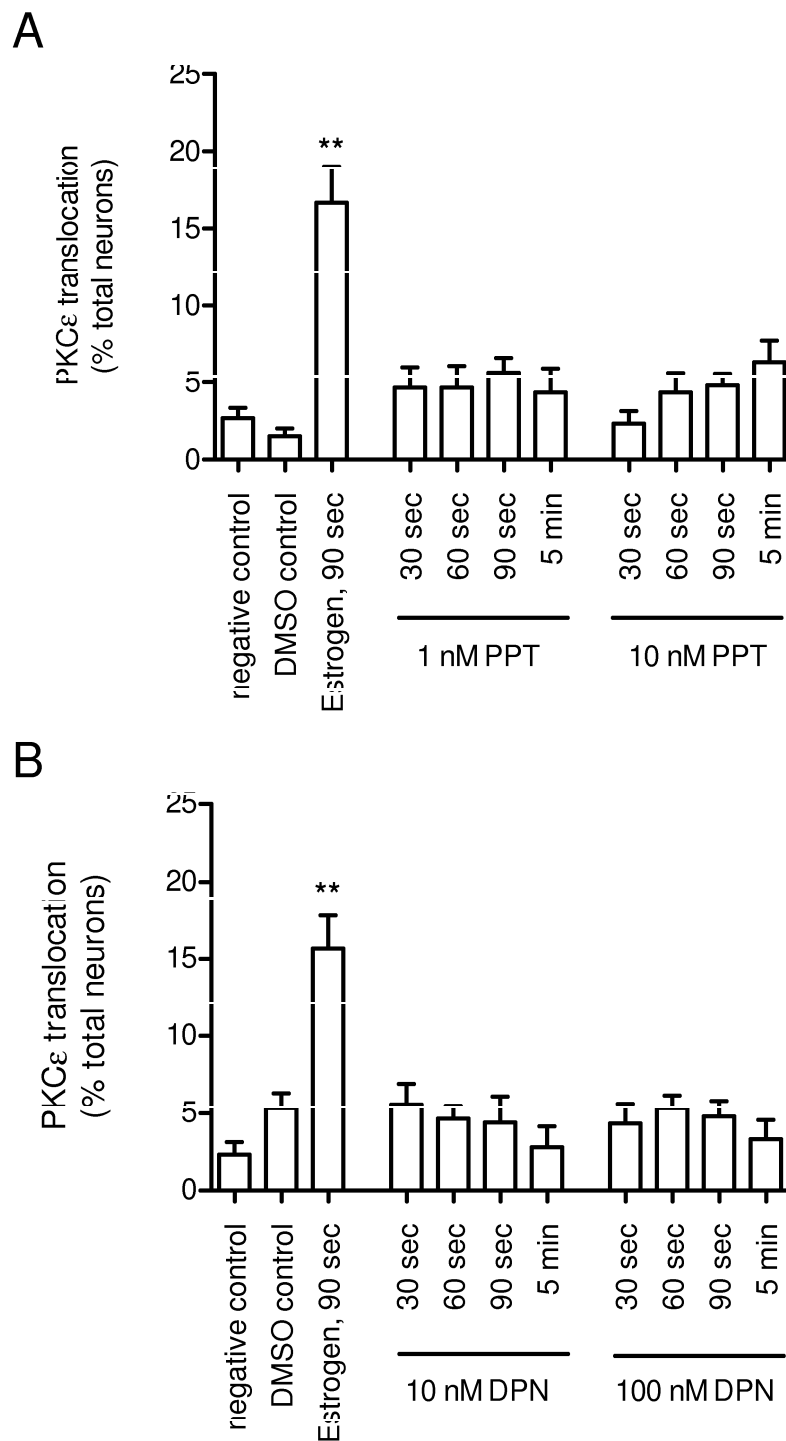
Fig. 8: Neither the ERα agonist PPT nor the ERβ agonist DPN cause rapid PKCε activation in primary sensory neurons. (A) Treatment of dissociated DRG neurons with the ERα-specific agonist PPT at concentrations of 1 nM and 10 nM for the period of 30 sec to 5 min did not induce PKCε translocation to the plasma membrane in a significant number of neurons compared to vehicle treated controls. Estrogen treated cells served as a positive control (16.6 ± 2.3 % neurons with translocation). **(B)** Incubation with 10 nM and 100 nM of the ERβ agonist DPN for time periods between 30 sec and 5 min did not affect PKCε localization in cultured DRG neurons, while estrogen-induced PKCε translocation in 15.7 ± 2.2 % of neurons within 90 sec. PKCε localization was analyzed by immunofluorescence microscopy (n = 6 cultures, ** p < 0.001 compared to vehicle controls). Error bars represent SEM.

7.1.2   Inhibition of the adenylyl cyclase blocks estrogen-induced PKCε translocation

Epinephrine/isoproterenol induces PKCε activation mediated by an αs coupled G-protein coupled receptor (GPCR). To analyze if also estrogen-induced PKCε translocation is mediated by a GPCR, DRG cultures were pre-incubated with an adenylyl cyclase (AC) inhibitor prior to estrogen treatment. Similar to isoproterenol-induced PKCε translocation, pre-incubation with the cell-permeable AC inhibitor MDL-12,330A (50 μM, 30 min) completely abolished estrogen-induced translocation of PKCε (neurons with PKCε translocation: estrogen = 12.0 ± 2.9 %, AC inhibitor and estrogen = 3.0 ± 0.4 %; Fig. 9).
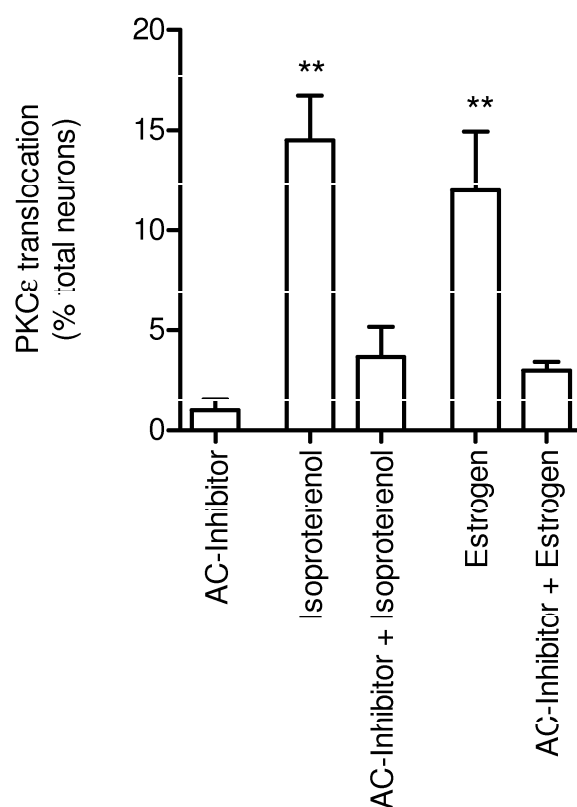
Fig. 9: Inhibition of the adenylyl cyclase blocks estrogen-induced PKCε translocation. In dissociated DRG neurons pre-incubation with the adenylyl cyclase (AC) inhibitor MDL-12,330A (50 μM, 30 min) abolished completely PKCε translocation normally observed after treatment with 10 nM estrogen for 90 sec (estrogen 12.0 ± 2.9 % total neurons, MDL-12,330A + estrogen 3.0 ± 0.4 % total neurons). The observed effect was comparable to the inhibition of isoproterenol (1 μM, 30 sec) induced PKCε translocation by MDL-12,330A (isoproterenol 14.5 ± 2.2 % total neurons, MDL-12,330A + isoproterenol 3.7 ± 1.5 % total neurons). PKCε localization was analyzed by immunofluorescence microscopy (n = 6 cultures, ** $p < 0.001$ compared to vehicle controls). Error bars represent SEM.

7.1.3 GPR30 mRNA is expressed in DRGs

In 2005, Revankar et al. published the orphan GPCR GPR30 to bind estrogen and to act as a membrane estrogen receptor. GPR30 has been reported to couple to the small G-protein αs. Finding estrogen-induced PKCε translocation not to depend on ERα/β but on adenylyl cyclase activity suggests a GPCR such as GPR30 to be the mediating estrogen receptor. First the mRNA expression of GPR30 in DRGs was examined. Performing a RT-PCR with GPR30 specific primers from total RNA preparations of adult male rat DRG showed a clear band at the expected size of 172 bp (Fig. 10). RNA from rat brain extract served as positive control (Brailoiu et al., 2007; Sakamoto et al., 2007).
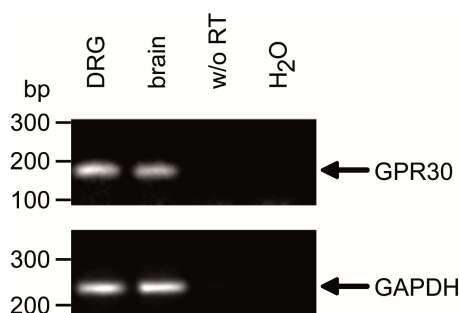
Fig. 10: GPR30 mRNA is expressed in the DRG. Analysis of GPR30 mRNA expression in DRG and brain extract derived from male rats by RT-PCR show a clear band with the expected size of 172 bp in both samples. Lane 1, DRG extract; lane 2, brain extract; lane 3, reaction without reverse transcriptase; lane 4, water control.

7.1.4 The GPR30 agonist G-1 causes rapid PKCε translocation

Bologa et al. described in 2006 the first GPR30 specific agonist, G-1 which is able to bind to and activate GPR30 while not mediating signal transduction through ERα and ERβ.

Thus, I used G-1 to investigate if GPR30 induces activation of PKCε in primary sensory neurons. DRG neurons were treated with 100 nM G-1, a concentration described to result in GPR30-specific cellular responses in other systems (Albanito et al., 2007; Bologa et al., 2006; Brailoiu et al., 2007). PKCε intensity profiles from confocal images show a clear increase in signal intensity at the plasma membrane of G-1-stimulated cells compared with negative controls (Fig. 11 A). Observable translocation peaked at 30 sec and returned to baseline levels after 60 sec (Fig. 11 B). Stimulation for 30 sec resulted in a significant increase of PKCε translocating neurons (17.3 ± 3.0 % of total neurons). This effect is comparable to PKCε translocation observed in response to estrogen (Fig. 7 D). To ensure, that the observed G-1 effect is indeed mediated by a GPCR, DRG cultures were pre-incubated with the adenylyl cyclase inhibitor MDL-12,330A prior to G-1 treatment. As expected, in presence of the adenylyl cyclase inhibitor no PKCε translocation was detected in response to G-1 (Fig. 11 C).
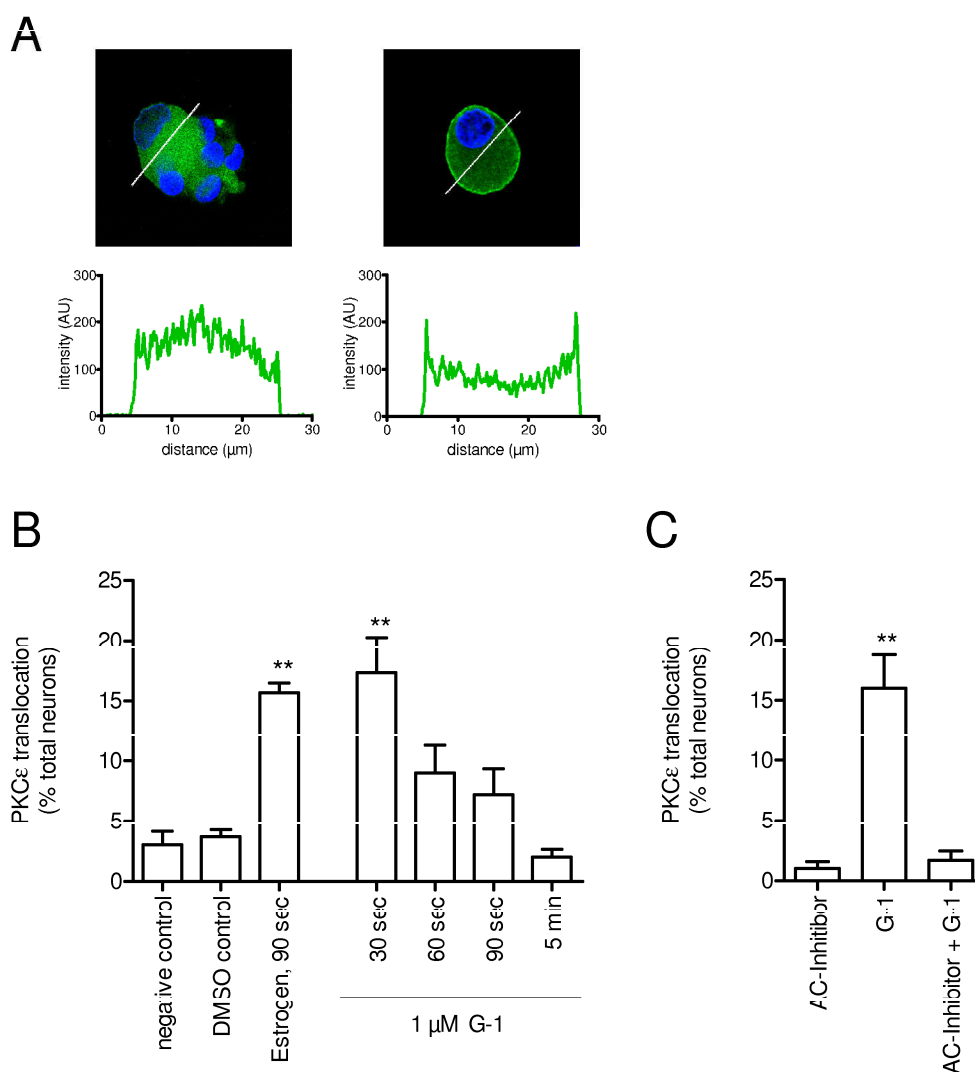
Fig. 11: The GPR30 agonist G-1 induces PKCε translocation in a subgroup of DRG neurons. (A) Confocal images of DRG neurons show PKCε translocation to the plasma membrane after treatment with the GPR30 agonist G-1 (100 nM, 30 sec, right image) compared to vehicle treated controls (left image). Intensity histograms along the white lines indicate PKCε distribution within the cell. White lines = 30 μm. **(B)** Quantification of DRG neurons showing PKCε translocation to the plasma membrane after G-1 treatment (1 μM) for the indicated time. While a plasma membrane staining of PKCε was detected in a significant number of neurons after stimulation with G-1 for 30 sec (17.3 ± 3.0 % total neurons), plasma membrane staining returned to base line levels after 90 sec of stimulation (7.2 ± 2.2 % total neurons, negative controls 3.7 ± 0.6 % total neurons). **(C)** Pre-incubation with the adenylyl cyclase inhibitor MDL-12,330A (50 μM, 30 min) blocked PKCε translocation normally induced by G-1 (100 nM, 30 sec) completely (G-1 16.0 ± 2.8 % total neurons , MDL-12,330A + G-1 1.7 ± 0.8 % total neurons), while MDL-12,330A itself did not affect PKCε localization. PKCε localization was analyzed by immunofluorescence microscopy (n = 6 cultures, ** $p < 0.001$ compared to vehicle controls). Error bars represent SEM.

7.1.5 The ERα/ERβ inhibitor ICI 182,780 induces PKCε translocation

G-1 was identified by its ability to activate GPR30 but not ERα and ERβ. If it activates GPCRs beyond GPR30, is not extensively investigated (Bologa et al., 2006). Thus, to corroborate the involvement of GRP30, a second GRP30 agonist was tested. Recently, the inhibitor of classical estrogen receptors, ICI 182,780, has been reported to activate GPR30 in concentrations between 1 μM and 10 μM (Thomas et al., 2005). Treatment with 1 μM ICI 182,780 for 30 sec resulted in PKCε activation in a significant number of neurons (13.1 ± 1.0 %). Similar to estrogen and G-1, the translocation induced by ICI 182,780 was transient and returned to baseline after 90 sec of incubation (Fig. 12).

Taken together, these results indicate that estrogen-induced translocation of PKCε in sensory neurons is not mediated by classical estrogen receptors but by a GPCR such as GPR30.
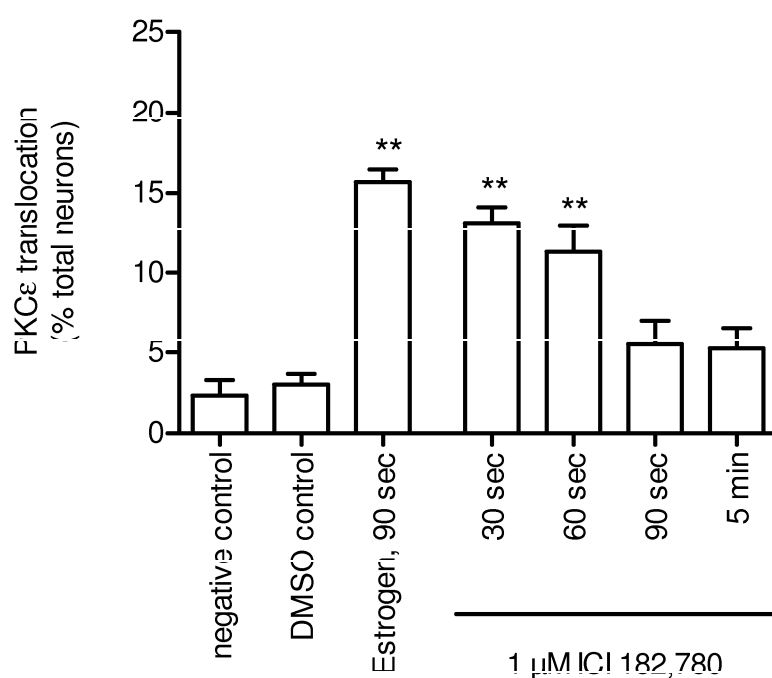
Fig. 12: The ERα/ERβ antagonist and GPR30 agonist ICI 182,780 induces PKCε translocation in sensory neurons. After incubation of cultured DRG neurons with the ERα/ERβ antagonist and GPR30 agonist ICI 182,780 (1 μM) for 30 or 60 sec PKCε translocation to the plasma membrane was detected in a significant number of neurons (30 sec ICI 182,780 13.1 ± 1.0 % total neurons, 60 sec ICI 182,780 11.3 ± 1.7 % total neurons) compared to vehicle treated controls. After longer incubation times (90 sec or 5 min), no PKCε translocation was observed (90 sec ICI 182,780 5.5 ± 1.5 % total neurons, 5 min ICI 182,780 5.3 ± 1.3 % total neurons). PKCε localization was analyzed by immunofluorescence microscopy (n = 6 cultures, ** p < 0.001 compared to vehicle controls). Error bars represent SEM.

7.1.6   PKCε translocates in IB4-positive and TRPV1-expressing DRG neurons

PKCε translocation in response to sensitizing stimuli such as epinephrine/isoproterenol or estrogen was detected in ~ 15-20 % of DRG neurons. This suggests a mechanism specific for a subpopulation of neurons. Isoproterenol was shown to activate PKCε only in the subgroup of IB4 positive neurons (Hucho et al., 2005). Therefore it was first evaluated if estrogen- as well as G-1- induced PKCε translocation also occurred in neurons binding fluorescently-labeled isolectin B4. In cultures treated with estrogen or G-1, the majority of PKCε-translocating cells showed strong IB4 staining. After estrogen treatment, 86.8 ± 4.9 % of neurons showing PKCε translocation were positive for IB4. And in 85.3 ± 2.1 % of neurons showing PKCε translocation in response to G-1 IB4 signals were detected (Fig. 13).
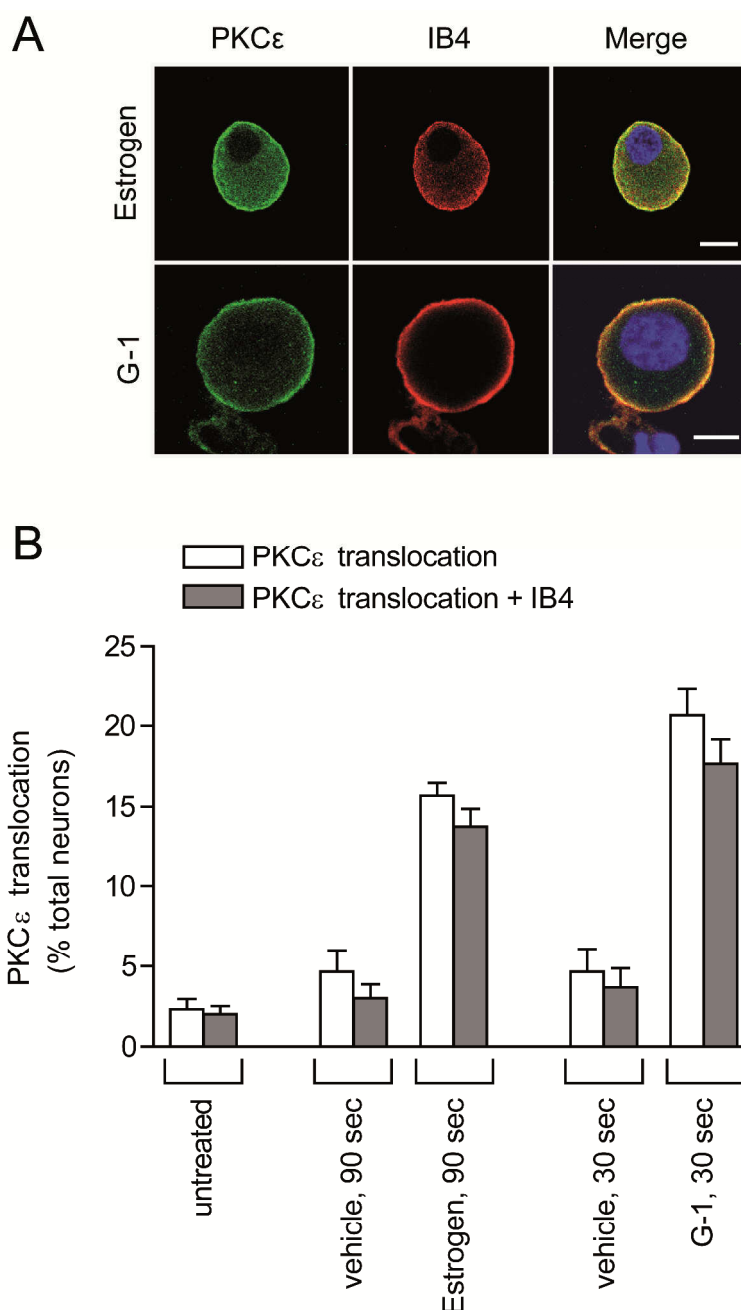
Fig. 13: PKCε activation occurs in IB4-positive DRG neurons. (A) Confocal images of dissociated DRG neurons stimulated with estrogen (10 nM, 90 sec, upper panel) or G-1 (100 nM, 30 sec, lower panel). Plasma membrane localization of PKCε was detected almost exclusively in IB4-positive neurons (green, PKCε; red, IB4). Scale bar = 10 µm. **(B)** Quantification of PKCε translocation to the plasma membrane after treatment with estrogen (10 nM, 90 sec) or G-1 (100 nM, 30 sec). PKCε translocation was detected in 15.7 ± 0.8 % (estrogen) or 20.7 ± 1.6 % (G-1) of total neurons. The majority of PKCε translocating neurons was positive for the subgroup marker IB4 (IB4 positive neurons: 86.8 ± 4.9 % (estrogen), 85.3 ± 2.1 % (G-1) of PKCε translocating neurons). PKCε localization and IB4 binding were analyzed by immunofluorescence microscopy. Error bars represent SEM.

To analyze the responding DRG neurons in more detail, the ion channel TRPV1 was used as a second marker expressed in a subpopulation of nociceptive neurons. To examine if estrogen and G-1 cause PKCε translocation in TRPV1 expressing nociceptive neurons, double staining experiments were performed using specific antibodies against PKCε and TRPV1. The analysis of

confocal images of cells showing PKCε translocation in response to estrogen (100 nM, 90 sec), G-1 (1 µM, 30 sec) or the β-adrenergic agonist isoproterenol (1 µM, 30 sec) revealed clear TRPV1 staining at the plasma membrane of PKCε translocating cells (Fig. 14 A). Indeed, the majority of neurons showing PKCε translocation were also positive for TRPV1 (after estrogen treatment 82.9 ± 1.4 %, after G-1 treatment 77.5 ± 0.9 %, after treatment with the β-adrenergic agonist isoproterenol 87.5 ± 2.1 %) (Fig. 14 B).

This result indicates that the neurons showing PKCε translocation in response to estrogen receptor agonists as well as the inflammatory mediator isoproterenol are indeed nociceptive neurons and belong to the subgroup of IB4-positive and TRPV1-expressing cells.
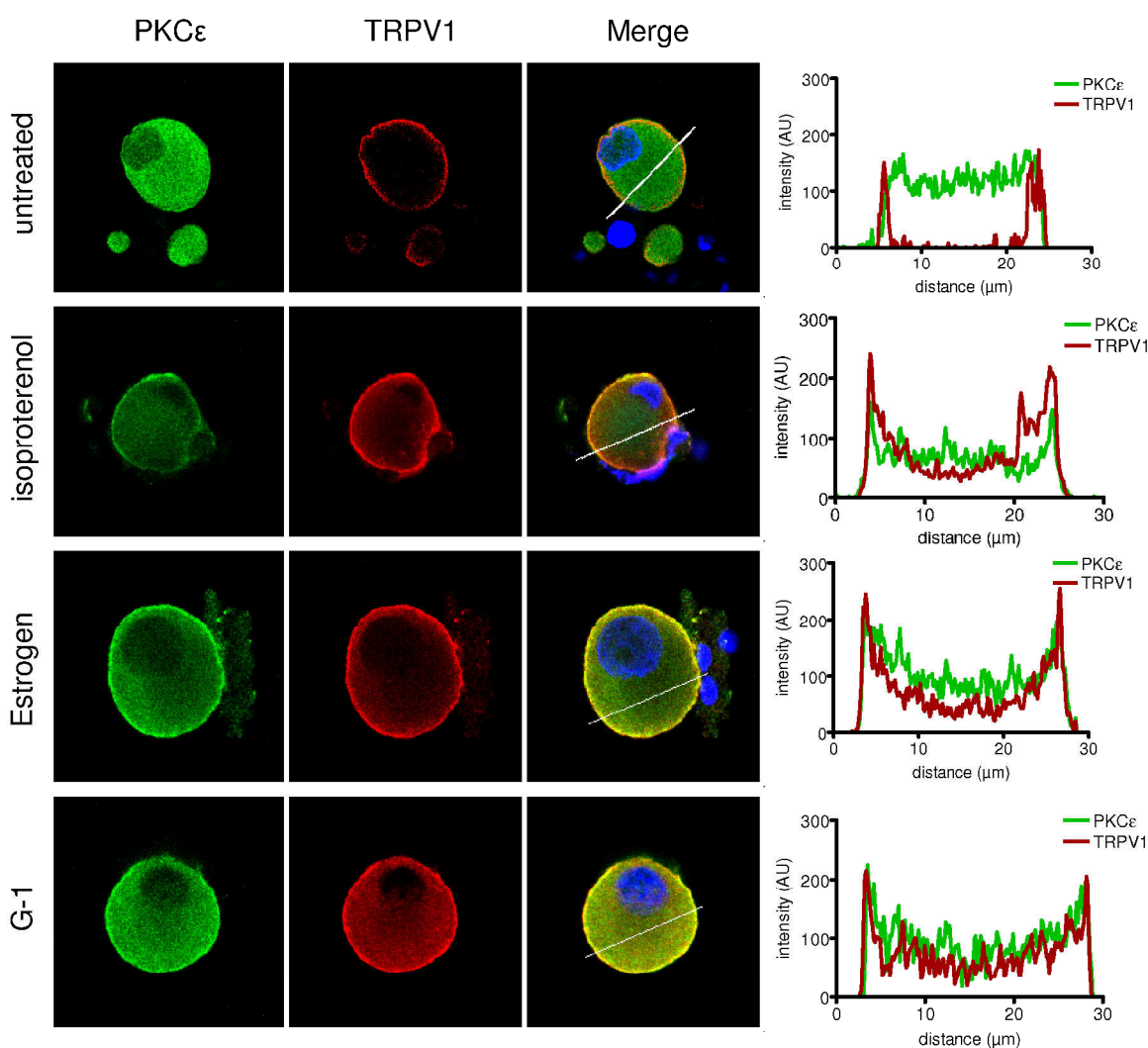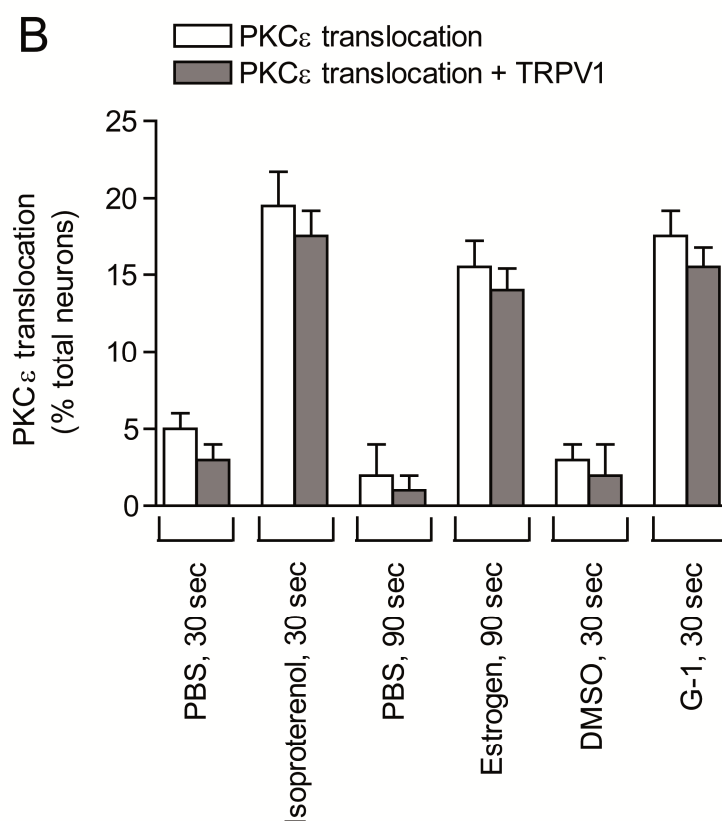
Fig. 14: PKCε is activated in TRPV1-expressing DRG neurons. (A) Confocal immunofluorescence microscopy shows PKCε translocation to the plasma membrane in response to different stimuli in TRPV1 expressing cells. In untreated controls, a cytoplasmic distribution of PKCε was observed (upper panel). Treatment with isoproterenol, estrogen or G-1 induced rapid PKCε translocation to the plasma membrane in a subpopulation of DRG neurons (lower panels). Double labeling with antibodies directed against the ion channel TRPV1 which is expressed in a subpopulation of nociceptive neurons, showed membranous antibody staining in neurons, where PKCε translocation was detected. Intensity histograms of PKCε- and TRPV1-labeling are shown in the diagrams on the right. White lines indicate the position of the of intensity diagrams. Green, PKCε; red, TRPV1; white line = 30 μm. **(B)** Correlation of TRPV1 expression and membrane localization of PKCε in response to different noxious stimuli. Neurons showing plasma membrane localization of PKCε were quantified and TRPV1 expression was analyzed in neurons showing PKCε translocation. Treatment with different noxious stimuli resulted in an increase of neurons showing membrane staining for PKCε as indicated in the white bars (isoproterenol = 19.5 ± 3.0 %, estrogen = 15.5 ± 2.3 %, G-1 = 17.0 ± 0.8 % of total neurons). In all cases, the majority of cells with PKCε translocation also showed strong membrane staining using TRPV1 specific antibodies (grey bars) (isoproterenol = 87.5 ± 2.1 %, estrogen = 82.9 ± 1.4 %, G-1 = 77.5 ± 0.9 % of neurons showing PKCε translocation). PKCε localization and TRPV1 expression were analyzed by immunofluorescence microscopy. Error bars represent SEM.

7.1.7 GPR30 agonists induce PKCε-dependent mechanical hyperalgesia in the rat

Injection of estrogen into the hindpaw of male rats rapidly induces PKCε-dependent mechanical hyperalgesia (Hucho et al., 2006). In DRG neurons, GPR30 agonists induced PKCε activation similar to estrogen. Therefore, next it was investigated if GPR30 activators mimic estrogen actions also in the behavioral experiment and induce mechanical sensitization.

In collaboration with Olayinka Dina of Jon D. Levine's laboratory, the nociceptive flexion reflex was quantified using the Randall-Selitto paw pressure device. Increasing pressure to the dorsum of the hindpaw is applied and the pressure, when the rat retracts its paw, is taken as threshold for mechanical pain. Injection of the GPR30 agonists G-1 as well as ICI 182,780 intradermally into the hindpaw of adult male rats evoked mechanical hyperalgesia in a concentration dependent manner (1 to 1000 ng/2.5 µl vehicle). Injection of 1 ng G-1 or ICI 182,780 did not cause a significant lowering of the mechanical nociceptive threshold. In contrast, injection of 100 ng G-1 or ICI 182,780 resulted in a near-maximal reduction of the nociceptive threshold by 35.6 ± 0.7 % (G-1) and 35.3 ± 2.2 % (ICI 182,780) (Fig. 15 A). The observed lowering of the nociceptive threshold induced by G-1 and ICI 182,780 is comparable to the effect observed in response to estrogen (Fig. 15 A). As ICI 182,780 is an antagonist of ERα and ERβ, the involvement of classical ERs can be excluded also in the behavioral experiment. Neither spontaneous pain nor redness or swelling was observed.

In previous studies it was shown that estrogen-induced sensitization is dependent on PKCε (Hucho et al., 2006) (Fig. 6). To test whether PKCε is involved in G-1 and ICI 182,780 induced mechanical hyperalgesia, we blocked PKCε by intradermal injection of the PKCε-inhibitor peptide εV1-2 (Johnson et al., 1996) 30 min prior to G-1 or ICI 182,780 injection. Application of the inhibitor itself did not affect the nociceptive threshold. However, mechanical hyperalgesia induced by G-1 or ICI 182,780 was completely abolished by pretreatment with the PKCε inhibitor peptide (Fig. 15 B).
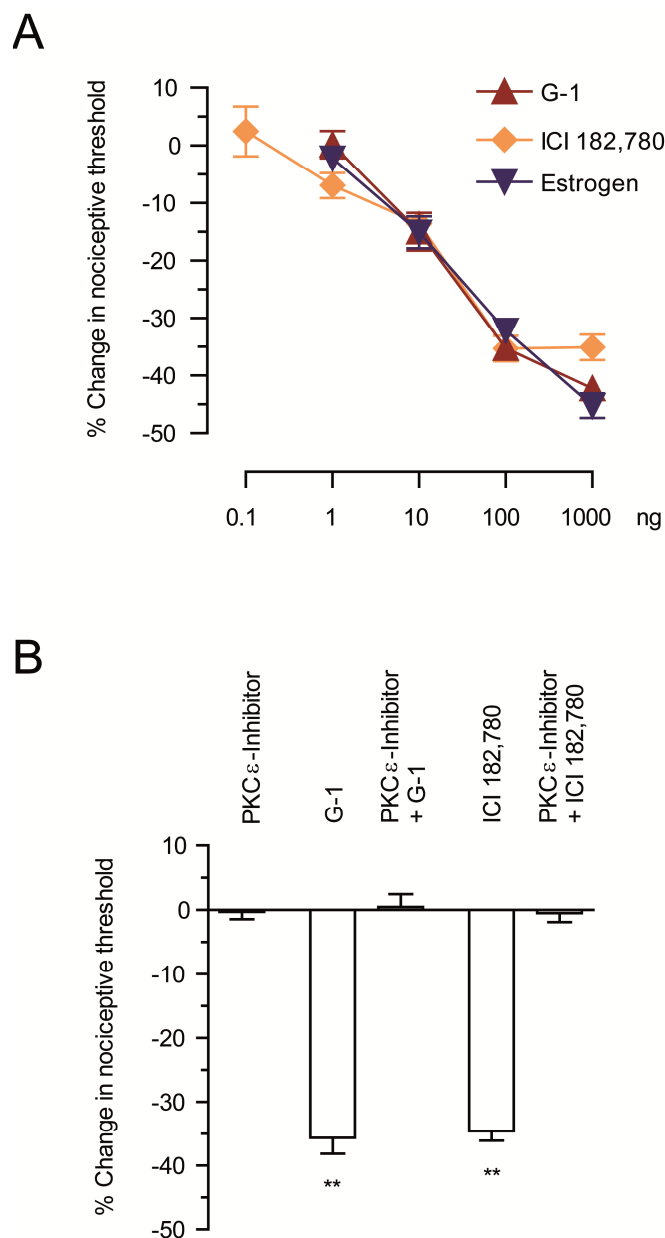
A

B

Fig. 15: GPR30 activators induce PKCε-dependent mechanical hyperalgesia in rats. **(A)** Injection of the GPR30 activators G-1 (final concentration 1 to 1000 ng/2.5 µl) or ICI 182,780 (final concentration 0.1 to 1000 ng/2.5 µl) into the hindpaw of male rats induced concentration dependent mechanical hyperalgesia similar to estrogen (final concentration 1 to 1000 ng), with a maximal decrease in nociceptive threshold of 41.0 ± 1.2 % (G-1), 35.3 ± 2.2 % (ICI 182,780) and 45.2 ± 2.2 % (estrogen). **(B)** Blocking of PKCε by intradermal injection of 1 µg of the PKCε inhibitor peptide εV1-2 prevented mechanical hyperalgesia normally induced by the subsequent injection of G-1 (100 ng/2.5 µl) or ICI 182,780 (1 µg/2.5 µl) completely. The inhibitor peptide εV1-2 itself did not affect the nociceptive threshold. Measurements of the nociceptive threshold were preformed with the Randall-Selitto paw pressure device. ** $p < 0.001$ for agonists compared to agonist + PKCε inhibitor peptide, error bars represent SEM.

7.1.8   G-1 induces mechanical hyperalgesia in the mouse

To substantiate the result of the rat behavioral experiments, the G-1 effect on the mechanical nociceptive threshold was tested also in a sensitization experiment in mice (collaboration Dominika Labuz and Halina Machelska-Stein). There, the mechanical nociceptive threshold was determined using calibrated von Frey filaments which were applied to the plantar surface of the hindpaws.

Comparable to the effect observed in rats (Fig. 15), the GPR30 agonist G-1 induced a concentration dependent reduction of the nociceptive threshold 30 min after G-1 injection into the hindpaw. While injection of 1 ng G-1 resulted in a decrease of the nociceptive threshold by 53.7 ± 2.9 %, injection of 100 ng G-1 caused a near-maximal reduction of the nociceptive threshold by 93.1 ± 2.6 % in comparison with baseline thresholds (Fig. 16 A). Comparable to the estrogen and G-1 effects in rat behavioral experiments, G-1 also mimicked the lowering of the mechanical nociceptive threshold induced by estrogen in mice (Fig. 16).
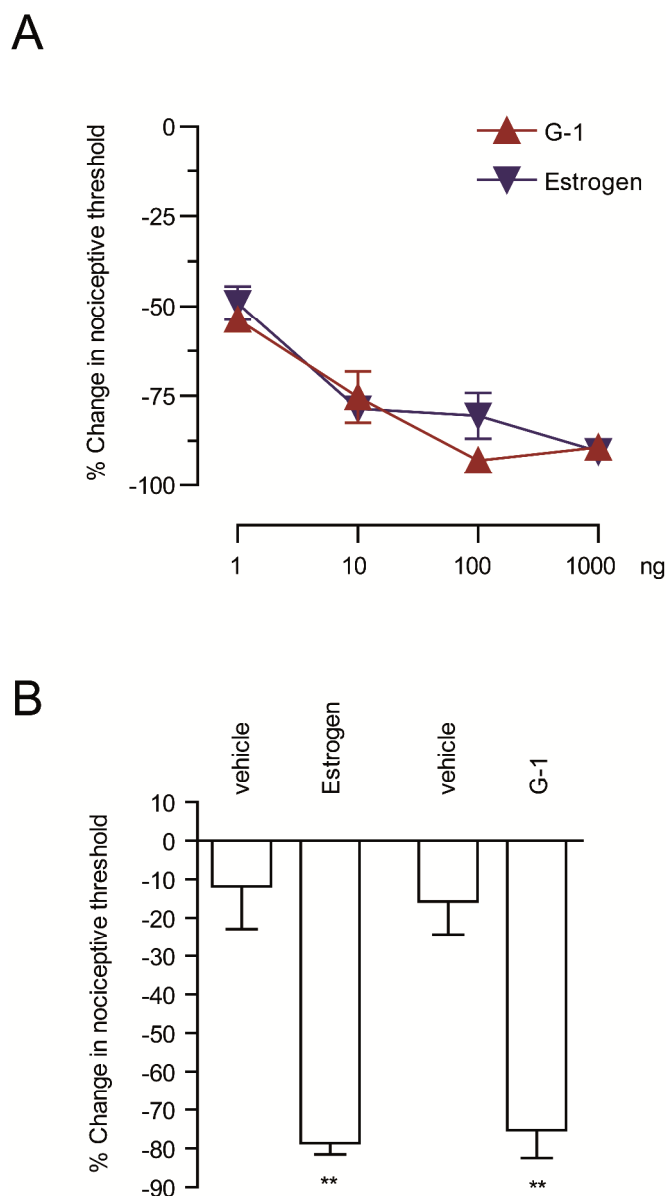
Fig. 16: The GPR30 agonist G-1 mimics estrogen-induced mechanical sensitization in mice. (A) Injection of 1 to 1000 ng estrogen or G-1 into the hindpaw of male mice resulted in the development of concentration dependent mechanical sensitization 30 min after injection. Maximal decrease in nociceptive thresholds were observed after injection of 1000 ng estrogen (reduction by 90.4 ± 3.1 %) or 100 ng G-1 (reduction by 93.1 ± 2.6 %). **(B)** Injection of 10 ng estrogen or G-1 already induced a significant reduction in nociceptive threshold 30 min after application compared to vehicle controls (reduction of nociceptive threshold compared to baseline thresholds: estrogen 78.6 ± 2.9 %, vehicle estrogen 11.7 ± 11.1 %, G-1 75.3 ± 7.1 %, vehicle G-1 15.7 ± 8.6 %). The mechanical nociceptive threshold was tested using calibrated von Frey filaments. ** $p < 0.001$ for estrogen/G-1 compared to the respective vehicle controls, error bars represent SEM.

7.1.9   Summary part I

I showed that agonists of the novel estrogen receptor GPR30 mimic estrogen actions on nociceptive neurons. Estrogen as well as GPR30 agonists caused rapid PKCε translocation to the plasma membrane similar to the inflammatory mediator epinephrine/isoproterenol. In contrast, agonists of the classical estrogen receptors ERα and ERβ induced no translocation. Corroborating

an involvement of GPR30 as mediating receptor, PKCε translocation was dependent on adenylyl cyclase activity. I further identified estrogen to act only on a subgroup of sensory neurons which is labeled by the lectin IB4 and expresses the ion channel TRPV1. I thereby identified a novel estrogen responsive specific subgroup of nociceptive neurons and crucial parts of the signaling pathway toward PKCε activation. In behavioral experiments performed in rats and mice, GPR30 agonists as well as estrogen induced robust mechanical sensitization. This effect was comparable to sensitization induced by established inflammatory mediators, indicating the high potential of estrogen to modulate nociceptive signaling. The effect of GPR30 agonists suggested thereby a first biological role for the novel estrogen receptor GPR30.

7.2 Characterization of TRPV1 as a downstream mediator of estrogen signaling in nociceptive neurons

In the first part I characterized estrogen signaling in nociceptive neurons towards the activation of PKCε. But so far, nothing is known about the transmission of estrogen signals in nociceptive neurons downstream of PKCε activation.

One way to investigate signaling events of protein kinases is the identification of their substrates. The best described PKCε substrate involved in nociception is the vanilloid receptor TRPV1. Recently, tubulin as well as microtubules has been shown to bind to the TRPV1-C terminus in close vicinity to its PKCε-specific phosphorylation site at serine 800 (Goswami et al., 2007b; Mandadi et al., 2006). As the microtubule cytoskeleton contributes specifically to PKCε-dependent mechanical hyperalgesia (Dina et al., 2003), I analyzed in this part of my thesis the estrogen-induced regulation of the TRPV1-microtubule complex and its contribution to mechanical sensitization.

7.2.1 Structural modeling indicates interference of PKCε-mediated phosphorylation and binding of the TRPV1-C terminus to tubulin

Biochemical experiments have been shown that tubulin as well as microtubules directly bind to the ion channel TRPV1 (Goswami et al., 2004). One binding site (aa 771 and aa 797) is localized in close vicinity to the PKCε-specific phosphorylation site at TRPV1-serine 800 (Fig. 5). Therefore it was explored if PKCε-mediated phosphorylation interferes with tubulin binding to the TRPV1-C terminus (TRPV1-Ct) (Goswami et al., 2007b).

In 2008, Gregorio Fernández-Ballester and Antonio Ferrer-Montiel postulated a three-dimensional structure of TRPV1 by computational modeling (Fernandez-Ballester and Ferrer-Montiel, 2008). In collaboration with them this model was used to investigate how tubulin or microtubules can interact with the TRPV1-Ct and if PKCε-mediated phosphorylation at serine 800 influences such an interaction.

Essential for an interaction of two proteins is that the surface area of both interaction partners allows binding. The tubulin binding region of the TRPV1-Ct identified by deletion mapping belongs to the globular region of TRPV1-Ct with a calculated surface area of 81.7 nm^2. As conventional mammalian microtubules are composed of 13 protofilaments with a surface area of 490 nm^2, it is very unlikely that whole microtubule filaments fit properly on the surface of the globular region. On the other hand, each tubulin dimer has a size of 4.6 nm x 8.0 nm x 6.5 nm (width, height and depth, respectively) (Nogales et al., 1998). Thus, only soluble tubulin dimers and/or tubulin dimers present at the tip of single protofilaments can fit into the groove formed by the TRPV1-Ct surface.

In a random trial of possible tubulin-TRPV1 interactions obtained at GRAMM-X protein docking web server (http://vakser.bioinformatics.ku.edu/resources/gramm/grammx) with default optional parameters (Tovchigrechko and Vakser, 2006), 155 out of 200 possibilities showed an interaction of tubulin dimers with TRPV1-Ct, indicating a high probability for a direct interaction between tubulin and the globular region of TRPV1-Ct.

In absence of tubulin, the serine 800 (S800) residue of TRPV1 is solvent exposed and therefore fully accessible to phosphorylation by PKCε (Fig. 17). Interestingly, many of the observed interactions between tubulin and TRPV1 are centered on the PKCε phosphorylation site at S800 of TRPV1. Figure 17 shows an exemplary binding conformation where the tubulin dimer directly interacts with S800 through the formation of several hydrogen bonds: S800 and R802 with D163 (β-tubulin), R797 with H406 (main chain, α-tubulin), and R802 with E97 (main chain, α-tubulin). Thereby tubulin binding to TRPV1 renders the otherwise easily accessible PKCε phosphorylation site at S800 inaccessible.

The space between S800 and TRPV1-bound tubulin is very limited. Thus, the presence of a phosphate group at the S800 position should disrupt the tubulin interaction with TRPV1. The negatively charged phosphate group strongly clashes both sterically as well as charge wise with D163 of β-tubulin and simultaneously repels the negatively charged E411 of α-tubulin.

Thus, these modeling data suggest a direct binding of tubulin dimers or tips of microtubule protofilaments to the globular region of the TRPV1-Ct, while whole microtubule filaments are too big to fit into the groove of the TRPV1-C terminal region. Furthermore, the computational modeling indicates that PKCε-mediated phosphorylation of TRPV1-S800 interferes with the TRPV1-tubulin interaction.
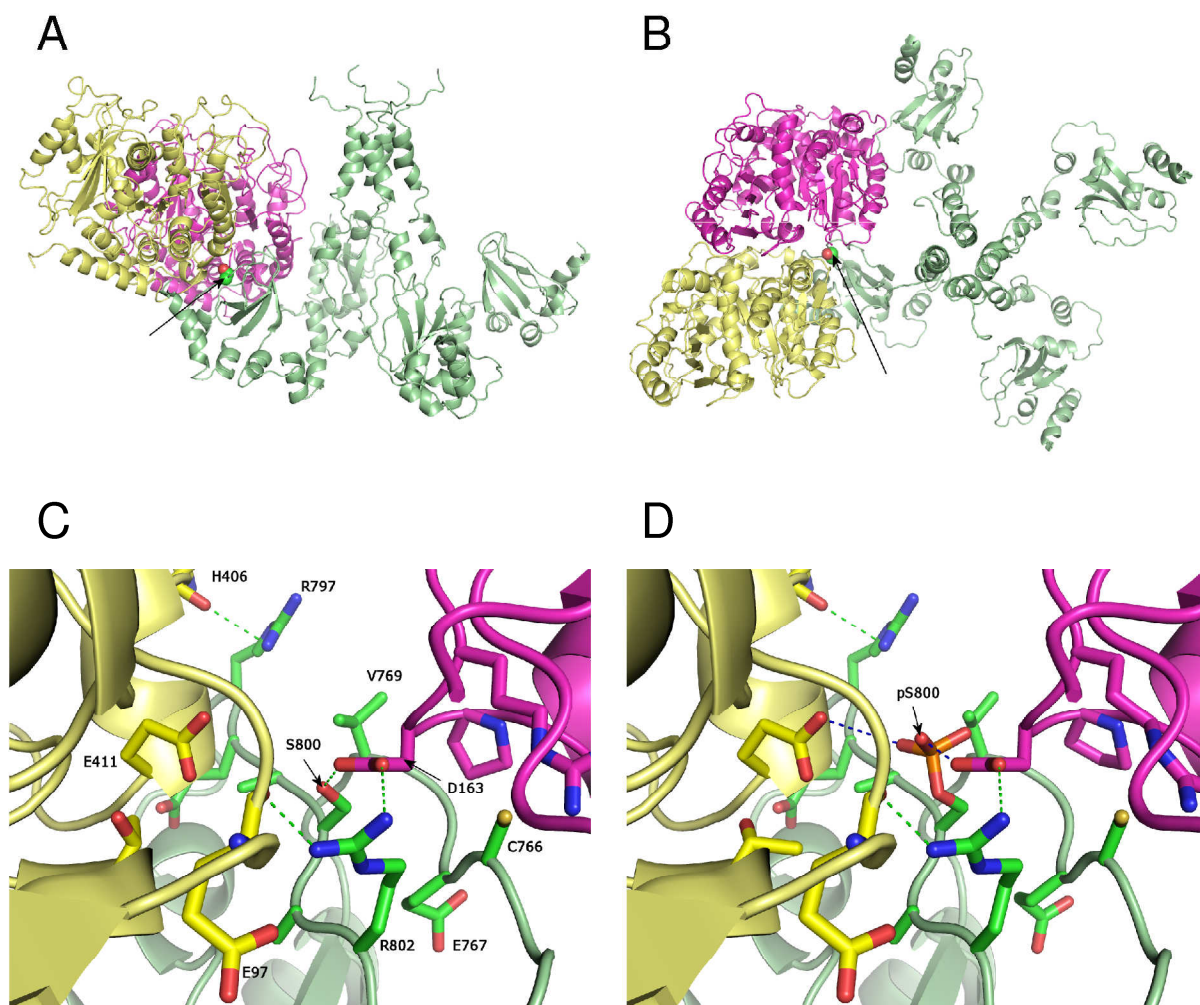
Fig. 17: Computational modeling indicates the interference of tubulin binding to TRPV1 and PKCε-mediated phosphorylation of TRPV1 serine 800. (A) and (B) Side view (A) and top (membrane) view (B) of the interaction of soluble α-tubulin (yellow) and β-tubulin (magenta) dimers with the tetrameric-TRPV1-C-terminus (green). Position of S800 is indicated by arrows. Most of the computed interactions between tubulin and TRPV1 are centered similarly around S800 and involve both the α- and β-tubulin interface. **(C) and (D)** enlarged view of the tubulin-TRPV1 interaction at S800 in the non-phosphorylated (C) and phosphorylated (D) state. In C, the interaction is stabilized among others by R802 hydrogen bonds to D163 from β-tubulin and E97 from α-tubulin and R797 hydrogen bonds to the backbone of H406 from α-tubulin) as well as by a hydrogen bond between S800 to D163. In contrast, phosphorylation of S800 by PKCε clashes sterically with E411 as well as repelling its negative charge. Hydrogen bonds are represented in dotted green lines; atom clashes are represented in dotted blue lines.

7.2.2 Biochemical evidence for competition between PKCε-phosphorylation and tubulin binding at the TRPV1-Ct

Based on the structural modeling data, next in a biochemical experiment performed by Chandan Goswami it was explored if 1) tubulin binding to TRPV1-Ct reduces PKCε-mediated phosphorylation and 2) if phosphorylation of TRPV1-S800 results in a reduction of tubulin binding.

The PKCε phosphorylation of TRPV1-Ct fused to the maltose binding protein (MBP-TRPV1-Ct) was analyzed in presence or absence of tubulin. Purified tubulin was incubated with purified MBP-TRPV1-Ct to allow the formation of a tubulin-TRPV1 complex before phosphorylation with activated PKCε was attempted. Tubulin binding to MBP-TRPV1-Ct resulted in reduced PKCε-mediated phosphorylation of TRPV1 compared with tubulin-free controls (Fig. 18 A). This result supports the computational prediction that tubulin association with TRPV1 hinders PKCε to access and phosphorylate TRPV1.

Structural modeling also predicted that a phosphate group at the S800 residue of TRPV1 interferes with tubulin binding. To test this biochemically, first MBP-TRPV1-Ct was incubated with active PKCε before tubulin was added. Comparing tubulin binding to PKCε-phosphorylated versus non-phosphorylated TRPV1-Ct less tubulin was detected in pull down samples of phosphorylated TRPV1 (Fig. 18 B).
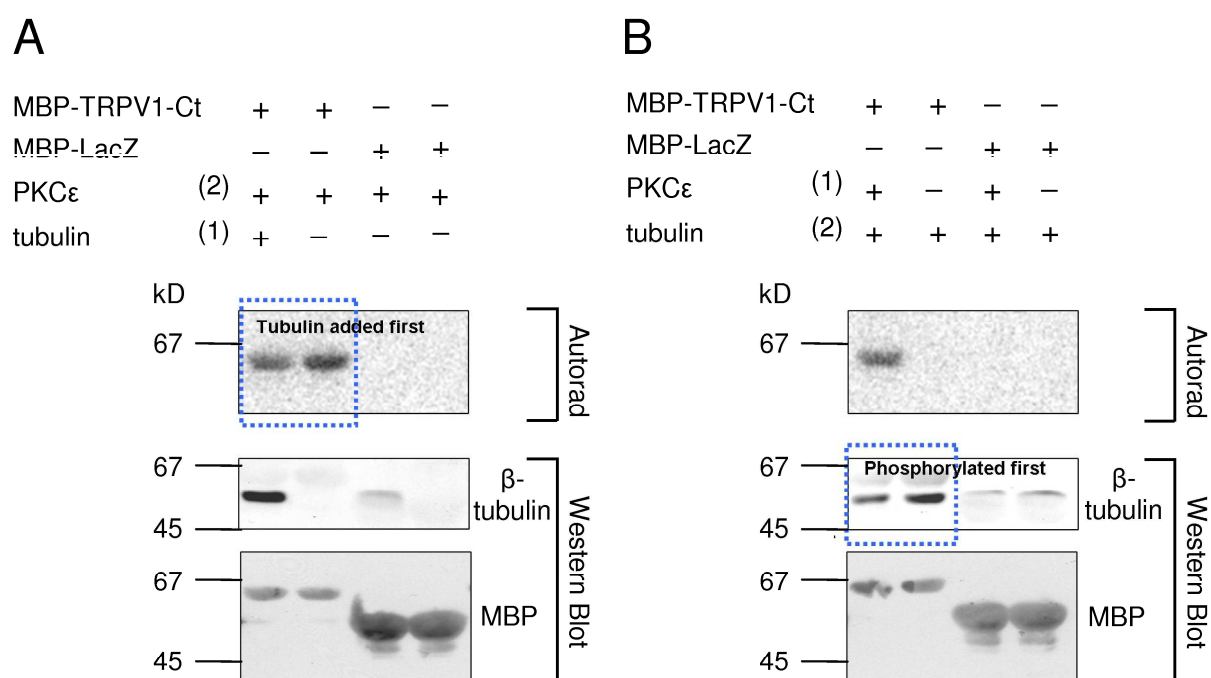

Fig. 18: Competition between PKCε-mediated phosphorylation and tubulin binding to the TRPV1-Ct. (A) Competition between tubulin binding and PKCε-mediated phosphorylation of TRPV1-Ct. Purified tubulin was incubated with MBP-TRPV1-Ct before PKCε was allowed to phosphorylate TRPV1-Ct in a kinase assay. Pre-incubation with tubulin resulted in decreased PKCε-mediated phosphorylation of TRPV1-Ct on an autoradiogram compared to tubulin-free controls. **(B)** PKCε-mediated phosphorylation of MBP-TRPV1-Ct resulted in less tubulin binding compared to non-phosphorylated controls.

7.2.3 mRNA of classical estrogen receptors and GPR30 is expressed in F-11 cells

Computational as well as biochemical experiments indicate that PKCε-mediated phosphorylation of TRPV1 alters the interaction between the microtubule cytoskeleton and TRPV1. TRPV1 has been shown to stabilize as well as destabilize microtubules. In order to understand the consequences of PKCε-induced alteration of the TRPV1-tubulin interaction on microtubule stability, the effect of estrogen-induced PKCε activation onto microtubule structures was analyzed on a cellular level. As primary DRG neurons are a complex, heterogeneous cellular system, DRG neuron-derived F-11 cells are often used to study signaling events of primary sensory neurons. To examine if F-11 cells are also suitable to study intracellular signaling pathways induced by estrogen, the expression of estrogen receptors was analyzed. Performing a RT-PCR analysis from RNA preparations of F-11 cell lysates with specific primers for ERα, ERβ and GPR30 clear bands with the expected sizes for all three estrogen receptors were detected (Fig. 19). Thus, F-11 cells can be used to study estrogen signaling mediated by classical ERs as well as signaling pathways upon GPR30 activation.
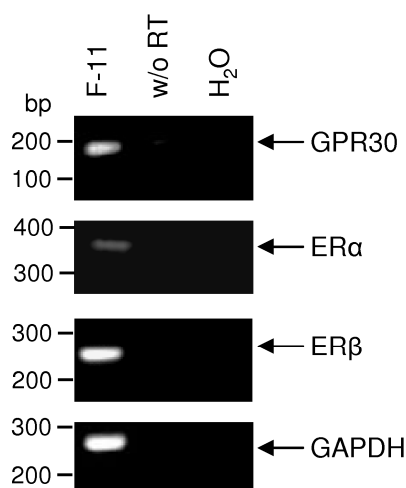

Fig. 19: mRNA of classical estrogen receptors as well as GPR30 is expressed in F-11 cells. RT-PCR analysis of F-11 cell lysates shows the mRNA expression rat ERα, ERβ and GPR30. Clear bands with the expected size were detected for ERα (345 bp), ERβ (262 bp), GPR30 (172 bp). Lane 1, F-11 extract; lane 2, reaction without reverse transcriptase; lane 3, water control.

7.2.4 Estrogen induces morphological changes in TRPV1 expressing F-11 cells

Cytoskeletal alterations often result in morphological changes. I first analyzed if estrogen treatment leads to morphological changes in TRPV1-expressing cells. As F-11 cells do not express TRPV1 endogenously they were transfected with TRPV1 fused to the green fluorescent protein (TRPV1-GFP).

In live cell imaging experiments, rapid morphological changes were observed in response to estrogen (1 nM) in F-11 cells expressing TRPV1-GFP and tubulin-cherry. Morphological changes included cell retraction, growth cone retraction and varicosity formation within 1 to 10 min after estrogen application (Fig. 20 A).

To investigate if the observed effects were indeed dependent on TRPV1, live cell imaging experiments were performed with F-11 cells only transfected with tubulin-cherry but lacking expression of TRPV1. No similar morphological changes were observed (Fig. 20 B). Thus, estrogen-induced morphological alterations are dependent on TRPV1.
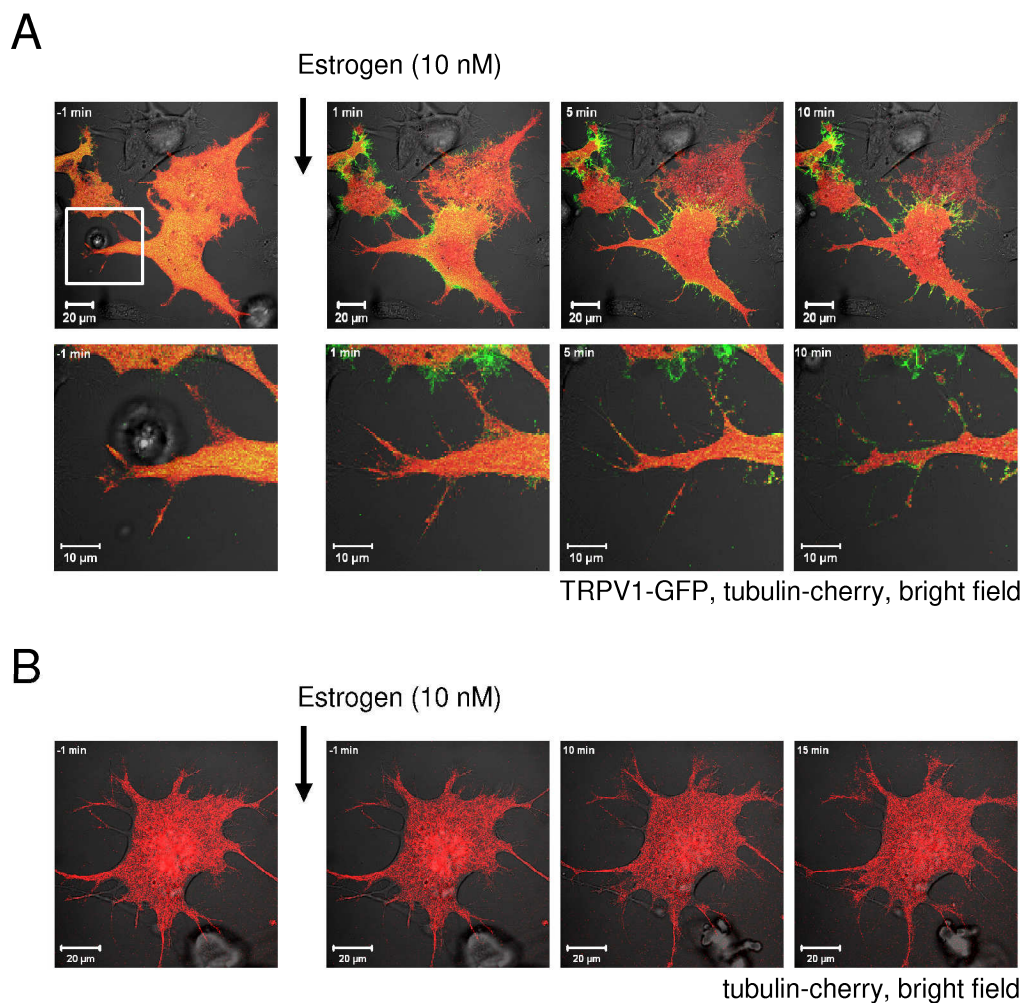
Fig. 20: Estrogen induces morphological changes in a TRPV1-dependent manner. (A) A combination of fluorescence and bright field live cell imaging of tubulin-cherry and TRPV1-GFP expressing F-11 cells showed rapid morphological changes including cell retraction, growth cone retraction and varicosity formation in response to estrogen (10 nM) within 5 to 10 min (upper panel). Enlarged area of the TRPV1-GFP and tubulin-cherry expressing cell shown in the upper panel. Rapid growth cone retraction and varicosity formation is clearly visible in response to estrogen. **(B)** In contrast to TRPV1-GFP expressing cells, no similar changes were detected in F-11 cells expressing only tubulin-cherry.

7.2.5   Microtubules are destabilized by estrogen treatment in a TRPV1-dependent manner

Morphological changes can be induced by alterations of microtubules but also by other cytoskeletal components. Therefore it was tested if estrogen treatment results indeed in an alteration of microtubule filaments as expected from the computational consideration. The microtubule structure of estrogen-treated F-11 cells was analyzed using confocal immunofluorescence microscopy. To separate soluble tubulin from filamentous microtubules, cells were extracted with a digitonin-containing isotonic buffer before fixation. Digitonin permeabilizes the cell membrane without changing the cellular morphology. Thereby, soluble cytoplasmic components such as soluble tubulin can be removed leaving behind the intact polymeric cytoskeletal network and its associated proteins (Goswami et al., 2006; Lieuvin et al., 1994). Microtubule structures were detected using anti-tubulin antibodies (YL1-2).

In unstimulated F-11 cells, a rich filamentous microtubule network was observed independent of TRPV1 expression. In contrast, application of estrogen (10 nM, 1 min) resulted in a rapid destabilization of microtubules only in TRPV1-expressing cells. In these cells, microtubules no longer appeared as smooth filaments. The remaining immunofluorescence signal was restricted to the vicinity of the microtubule-organizing center. Similar to the live cell imaging experiments the rapid effect of estrogen was dependent on expression of TRPV1. Non-transfected and therefore TRPV1 negative cells were not affected by estrogen exposure and intact microtubule filaments were observed all over the cells (Fig. 21 A).
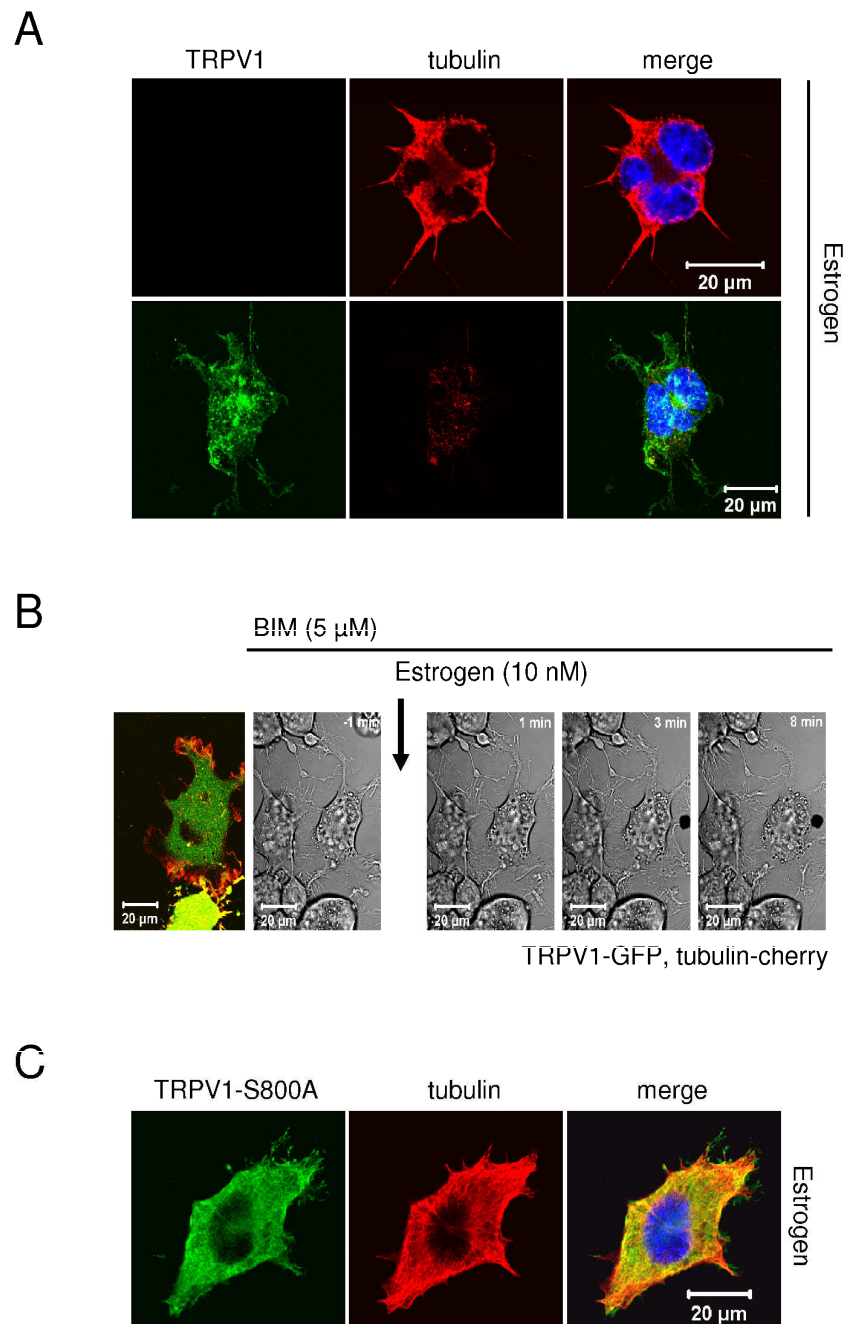
Fig. 21: The PKCε-phosphorylation site at S800 of TRPV1 is essential for estrogen-induced microtubule destabilization. (A) Estrogen-induced microtubule destabilization in TRPV1 expressing F-11 cells. After treatment with 10 nM estrogen for 1 min cells were extracted with a digitonin containing buffer removing soluble cytoplasmic components. Microtubule structure was analyzed with confocal immunofluorescence microscopy using anti-tubulin antibodies, TRPV1 expression was visualized with anti-TRPV1 antibodies. In TRPV1 expressing cells, no filamentous microtubules were detected after estrogen treatment, while TRPV1 negative cells showed normal microtubule network. **(B)** The PKC inhibitor Bisindolylmaleimde I hydrochloride (BIM) blocks estrogen-induced microtubule destabilization in TRPV1-expressing F-11 cells. In live cell imaging experiments incubation with BIM (5 μM) 12 min prior to estrogen application (1 nM) inhibited morphological changes normally observed in response to estrogen. Due to the strong autofluorescence of BIM, fluorescence image of TRPV1-GFP and tubulin-cherry expressing cells was taken before BIM application and imaging was continued in the bright field channel for at least 20 min (1 frame/min). **(C)** In cells expressing TRPV1-S800A-GFP, a mutant lacking the PKCε phosphorylation site, no microtubule destabilization was observed in response to estrogen. Analysis of TRPV1-S800A-GFP expressing cells after estrogen treatment (10 nM, 1 min) and digitonin-extraction showed complete microtubule filaments after staining with anti-tubulin and anti-TRPV1 antibodies using fluorescence confocal microscopy.

7.2.6 The PKCε phosphorylation site S800 is essential for estrogen-induced rapid microtubule destabilization

The results presented above indicated that estrogen can activate PKCε in DRG neurons (s. 7.1). To investigate if also in F-11 cells the effect of estrogen is mediated by PKCε, cells were incubated with the general PKC-inhibitor BIM prior to estrogen application. BIM blocks all classical PKC isoforms as well as novel PKCs including PKCε.

Pre-incubation with BIM (5 µM) alone for 12 min did not change the morphology of TRPV1-GFP expressing F-11 cells (Fig. 21 A). But BIM abolished completely estrogen (1 nM) induced morphological alterations in TRPV1 expressing F-11 cells indicating that PKCs are involved in this process (Fig. 21 B).

F-11 cells express different PKC isoforms (Goswami, *unpublished data*). In absence of a PKCε-specific cell-permeable inhibitor TRPV1-S800A mutant was used to test if PKCε is responsible for estrogen-induced microtubule destabilization. The TRPV1-S800A mutant lacks the PKCε specific phosphorylation site at serine 800, but still integrates into cellular membranes and forms functional channels (Mandadi et al., 2006). In contrast to cells expressing wild type TRPV1-GFP, estrogen did not lead to microtubule destabilization in TRPV1-S800A-GFP expressing cells. Confocal immunofluorescence analysis of tubulin staining showed clear microtubule networks after estrogen treatment and digitonin extraction (Fig. 21 C).

7.2.7 Microtubule destabilization is independent of the TRPV1 channel function

Opening of the ion channel TRPV1 using the TRPV1 agonists capsaicin or RTX results in rapid disassembly of the microtubule cytoskeleton (Goswami et al., 2006). Thus, I explored if estrogen-induced microtubule disassembly is also due to TRPV1 channel opening. TRPV1-GFP transfected F-11 cells were incubated with the TRPV1 channel inhibitor 5'I-RTX prior to estrogen treatment. After digitonin-extraction the microtubule structure was analyzed by confocal immuno-fluorescence microscopy using antibodies against tubulin. Treatment with 1 µM 5'I-RTX for 30 min alone did not alter microtubule stability in TRPV1 expressing cells. Surprisingly, estrogen caused rapid disassembly of microtubules also in cells pretreated with 5'I-RTX (Fig. 22 A).

To corroborate that estrogen-induced microtubule destabilization is indeed independent of the TRPV1 channel function, we expressed a TRPV1 fragment that lacks the entire N-terminal cytoplasmic domain (TRPV1-ΔN). This truncated fragment was reported to localize to the plasma membrane but it lacks capsaicin-induced channel activity (Jung et al., 2002). TRPV1-ΔN expressing cells also showed microtubule disassembly in response to estrogen comparable to the microtubule disassembly observed in cells expressing full length TRPV1 after estrogen treatment (Fig. 22 B). Taken together, these data suggest that estrogen-induced microtubule disassembly is TRPV1-dependent. The data are also a first evidence of a channel-independent function of TRPV1.
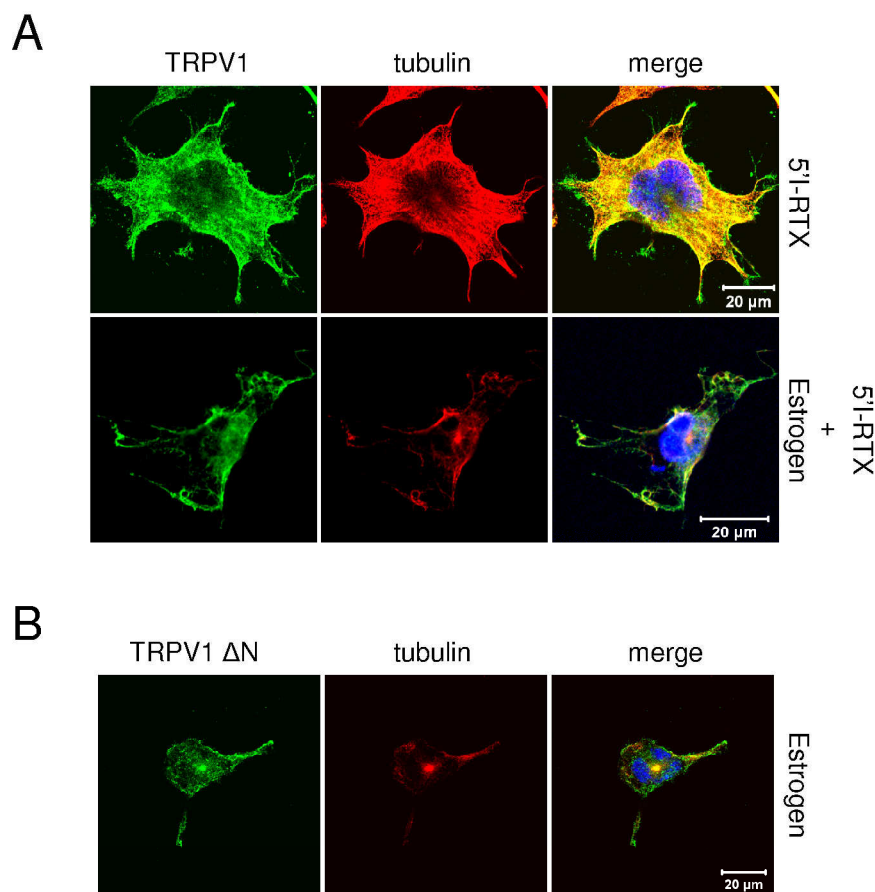
Fig. 22: Estrogen-induced microtubule destabilization is independent of the TRPV1 channel function. (A) Microtubule destabilization could not be blocked with the TRPV1 antagonist 5'I-RTX. Pretreatment of F-11 cells with 1 μM 5'I-RTX for 30 min did not inhibit microtubule destabilization induced by estrogen application (10 nM, 1 min). After digitonin extraction loss of the microtubule network was detected using confocal immunofluorescence microscopy in TRPV1 expressing cells, while no similar effects were observed in TRPV1-negative cells. **(B)** Expression of the not channel forming N-terminal deletion mutant of TRPV1 (TRPV1-ΔN) is sufficient to mediate estrogen-induced microtubule destabilization. F-11 cells expressing TRPV1-ΔN showed similar loss of microtubule filaments after estrogen treatment (10 nM, 1 min) followed by digitonin-extraction. Microtubule structure and TRPV1-ΔN expression was analyzed by confocal immunofluorescence microscopy using specific antibodies against tyrosinated tubulin and the C-terminal region of TRPV1.

7.2.8 The GPR30 agonist G-1 mimics estrogen effects in TRPV1 expressing F-11 cells

In the first part of this thesis I showed that agonists of the novel estrogen receptor GPR30 but not of the classical estrogen receptors ERα and ERβ result in PKCε translocation. Thus, next it was examined if similar to estrogen also the GPR30 agonist G-1 induces TRPV1-dependent destabilization of the microtubule cytoskeleton.

The influence of the GPR30 agonist G-1 on the cellular morphology in cells co-expressing tubulin-cherry and TRPV1-GFP was monitored in live cell imaging experiments. Comparable to estrogen also in response to G-1 (100 nM) morphological changes including cell retraction, growth cone retraction and varicosity formation were observed 2 to 10 min after application. F-11

cells lacking TRPV1 expression showed no morphological changes (Fig. 23 A). And, G-1 actions were not blocked by the TRPV1 channel inhibitor 5'I-RTX (Fig. 23 B).
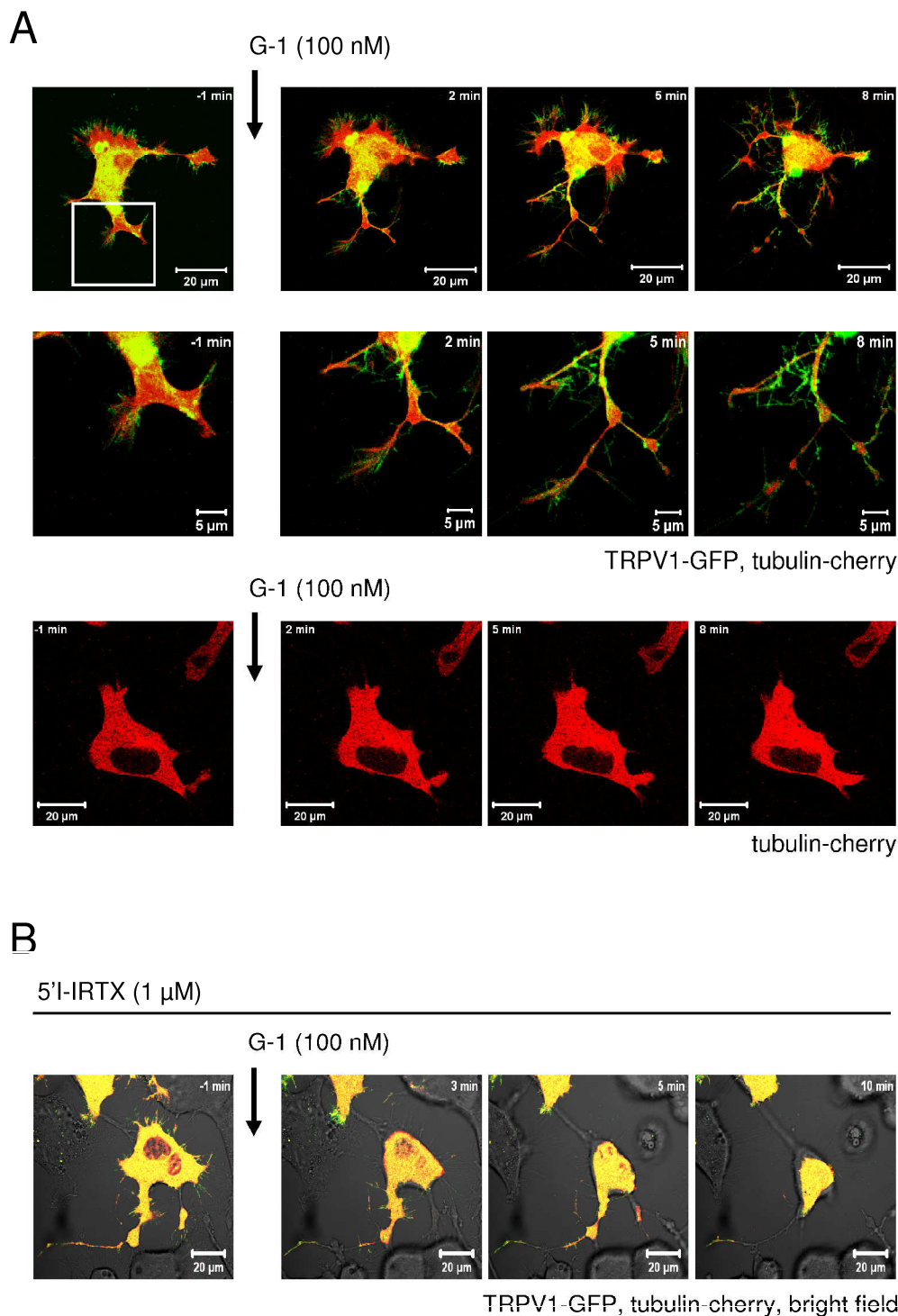

Fig. 23: The GPR30 agonist G-1 mimics estrogen-induced morphological changes in TRPV1-expressing F-11 cells. (A) In live cell imaging experiments using fluorescence confocal microscopy the GPR30 agonist G-1 (100 nM) induced rapid morphological changes (cell retraction, growth cone retraction, varicosity formation) within 2 to 10 min in TRPV1-GFP/tubulin cherry expressing cells (upper panel), while no similar alterations were detected in only tubulin cherry expressing cells (lower panel). **(B)** Morphological alterations described in (A) could not be blocked by pre-incubation with the TRPV1 antagonist 5'I-RTX (1 µM, 30 min).

As estrogen caused rapid destabilization of microtubules, microtubule structure was analyzed by immunofluorescence microscopy after G-1 treatment (100 nM, 1 min) followed by digitonin extraction. Again, G-1 treatment resulted in destabilized microtubules only in TRPV1-GFP expressing cells, while no comparable destabilization was observed in TRPV1-negative controls (Fig. 24).
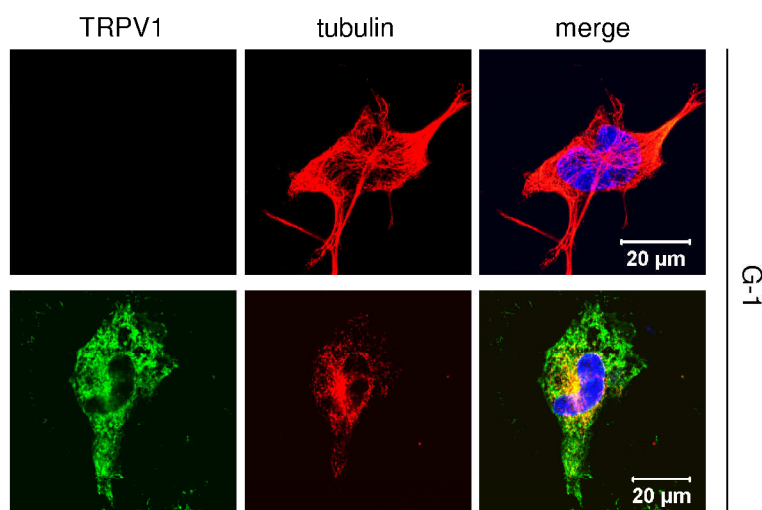

Fig. 24: G-1 induces destabilization of the microtubule cytoskeleton similar to estrogen. Immunofluorescence analysis indicated a loss of microtubule filaments in response to G-1 in TRPV1-GFP expressing cells, while no similar changes were detected in TRPV1 negative cells. Cells were treated with 100 nM G-1 for 1 min followed by a digitonin extraction. Tubulin was visualized using specific antibodies against tyrosinated tubulin (YL1-2).

To examine the involvement of PKCε, the TRPV1-S800A-GFP mutant was expressed. Comparable to estrogen effects, also G-1-induced microtubule destabilization was blocked by ablation of the PKCε phosphorylation site at TRPV1-serine 800. Immunofluorescence analysis of the tubulin cytoskeleton showed complete microtubule networks after G-1 treatment (10 nM, 1 min) and digitonin extraction (Fig. 25 A). Also in live cell imaging experiments of TRPV1-S800A-GFP expressing cells, no rapid varicosity formation was observed in response to G-1, indicating no rapid microtubule disassembly in these cells (Fig. 25 B). However, even in TRPV1-S800A-GFP expressing cells, where prior G-1 application did not alter the microtubule cyto-skeleton, rapid varicosity formation was induced by the TRPV1 channel opener RTX indicating that the channel is still functional and that the microtubules are in a state responsive to strong destabilizing stimuli (Fig. 25 B). This observation again strengthens the argument that G-1-induced varicosity formation is independent of the TRPV1 channel function.

Taken together, these data indicate that the GPR30 agonist G-1 mimics estrogen effects on the microtubule cytoskeleton via a signaling pathway involving PKCε and TRPV1.
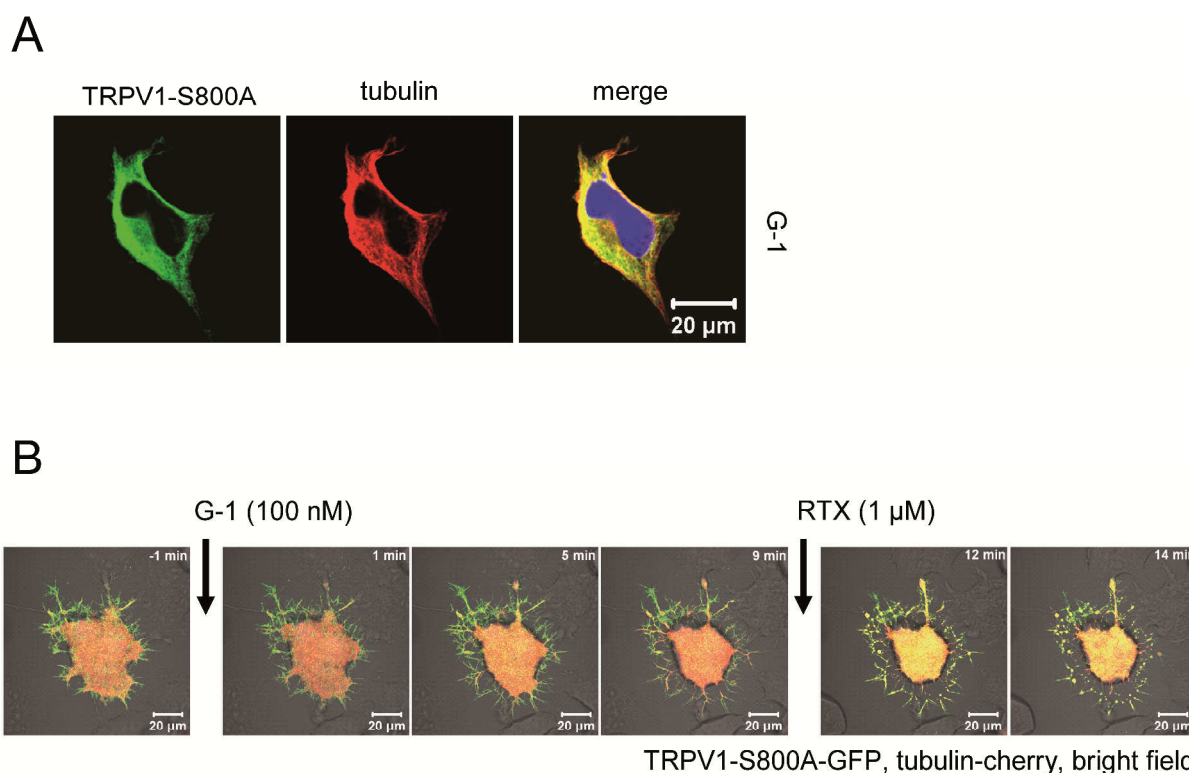
Fig. 25: G-1-induced microtubule destabilization depends on serine 800 of TRPV1. (A) In cells expressing a TRPV1 mutant lacking the PKCε phosphorylation site (TRPV1-S800A-GFP) no microtubule destabilization was observed in response to G-1. Analysis of TRPV1-S800A-GFP expressing cells after treatment with G-1 (100 nM, 1 min) followed by a digitonin extraction showed complete microtubule filaments after staining with anti-tubulin antibodies using fluorescence confocal microscopy. **(B)** Fluorescence live cell imaging of F-11 cells expressing TRPV1-S800A-GFP and tubulin-cherry did not show varicosity formation within 10 min after G-1 application (100 nM). In contrast, additional application of the TRPV1 agonist RTX (1 µM) induced varicosity formation within 4 min.

7.2.9 Estrogen as well as G-1 causes rapid microtubule disassembly in a subset of DRG neurons

To confirm the relevance of the described signaling pathway for nociceptive neurons, it was examined if PKCε activation by estrogen as well as G-1 can influence the microtubule cytoskeleton of DRG neurons. Primary DRG neurons were prepared from adult male rats and cultured until an extensive neurite network was established. Live cell imaging showed varicosity formation after stimulation with 10 nM estrogen or 100 nM G-1 within 5 to 15 min, indicating the disassembly of microtubule filaments (Fig. 26). However, not all neurons responded to this treatment. As DRG neurons represent a highly heterogeneous system, responding neurons may reflect a distinct subpopulation such as the TRPV1 expressing subpopulation of nociceptors.
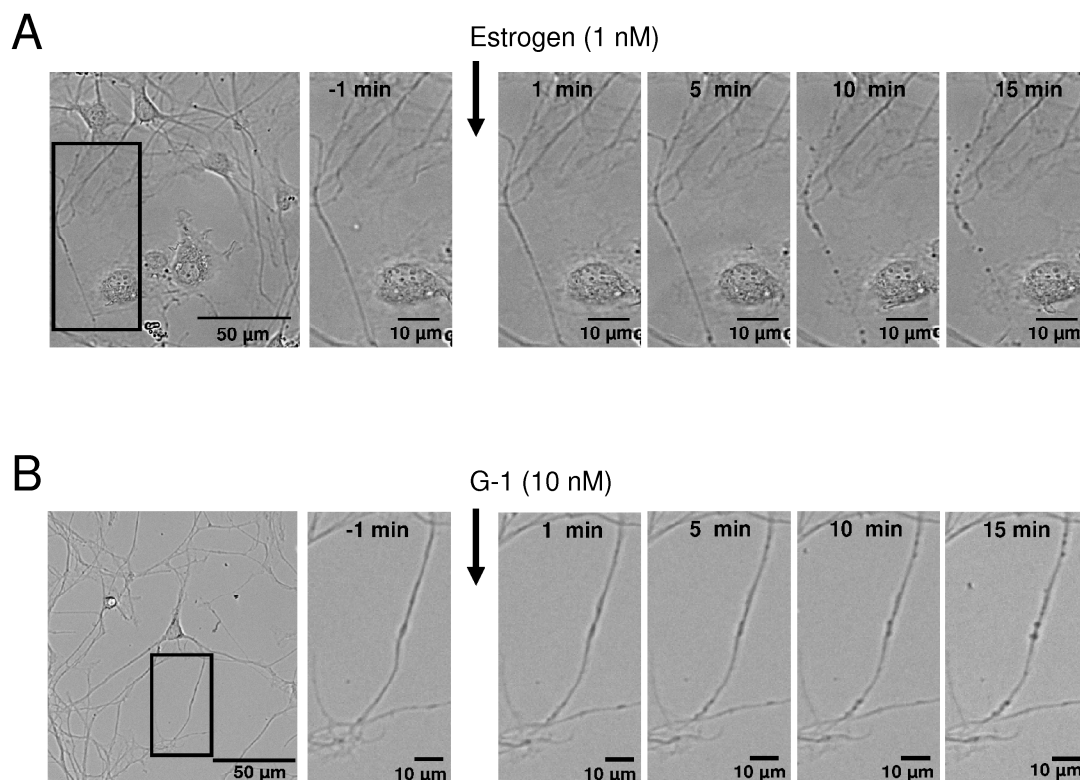
Fig. 26: Estrogen as well as G-1 induces rapid varicosity formation in a subset of DRG neurons. (A) Live cell imaging of 4-5 day cultured rat DRG neurons showed rapid varicosity formation in response to estrogen (10 nM) within 5 to 15 min occurring only in a subset of neurons. First image show an overview; the following images show the enlarged region (black rectangle). (B) Similar to estrogen, treatment with the GPR30 agonist G-1 (100 nM) induced varicosity formation within 5 to 15 min in a subset of DRG neurons. First images represent an overview; the following images show the enlarged region (black rectangle).

7.2.10 The microtubule cytoskeleton contributes to G-1-induced mechanical hyperalgesia in the rat

The microtubule network has been shown to be important for epinephrine-induced PKCε-dependent sensitization in rat behavioral experiments (Dina et al., 2003). Nocodazole-induced microtubule destabilization resulted in abrogation of epinephrine-induced mechanical hyperalgesia. The cellular analysis presented above now indicates that the cytoskeleton serves as a downstream target of PKCε signaling in nociceptive neurons. Based on these findings, it was addressed if cytoskeleton-dependence is a more general property of PKCε-dependent sensitization beyond epinephrine-induced sensitization. Therefore it was tested if also estrogen/G-1-induced sensitization is affected by modulators of the microtubule cytoskeleton.

The effect of microtubule active drugs on G-1-induced mechanical hyperalgesia was examined in collaboration with Olayinka Dina. Injection of G-1 intradermally into the hindpaw of adult male rats evoked PKCε-dependent mechanical hyperalgesia (Fig. 27 A, see also Fig. 15) (Kuhn et al., 2008). Intradermal injection of the microtubule destabilizing agent nocodazole on the dorsum of

rat hindpaws 30 min before G-1 injection abolished mechanical hyperalgesia completely. In contrast, injection of the microtubule stabilizing agent Taxol 30 min prior to the G-1 injection showed rather the tendency to increase G-1-induced sensitization against mechanical stimuli (Fig. 27 A). Thus, indeed, the microtubule cytoskeleton contributes to G-1-induced sensitization in a similar manner as observed in a model of epinephrine-induced hyperalgesia (Dina et al., 2003). This suggests that the involvement of the microtubule cytoskeleton in PKCε-dependent sensitization is a more general phenomenon and not a specific effect of a single nociceptive stimulus.

Injection of nocodazole or Taxol alone did not affect the nociceptive threshold measured 30 min after injection (Fig. 27 B). This observation indicates that neither the state (i.e. intact filament versus disassembled dimer) nor the dynamics of the microtubule cytoskeleton is responsible for the development of mechanical hyperalgesia by their own. Moreover, it suggests that not microtubule disassembly as such mediates the sensitizing signal, but that the microtubule cytoskeleton plays a central role only in the context of PKCε-dependent signaling.
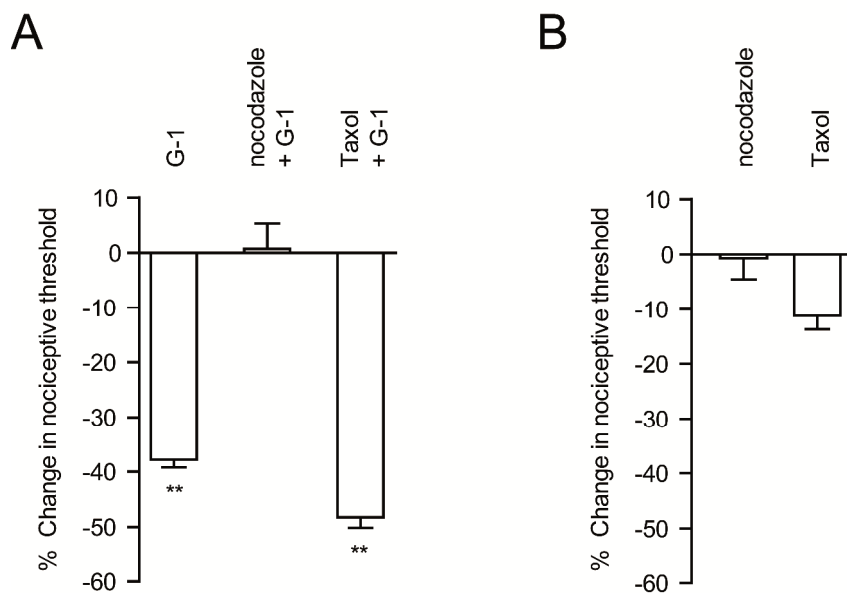

Fig. 27: Alteration of the microtubule cytoskeleton influences G-1-induced mechanical sensitization. (A) G-1 injection (1 µg/2.5 µl) into the hindpaw of rats induced mechanical hyperalgesia 30 min after application (change of nociceptive threshold -37.9 ± 1.4 %). Application of the microtubule disrupting drug nocodazole (NDZ, 1 µg in 2.5 µl PBS) 30 min prior to G-1 injection, abolished G-1-induced hyperalgesia completely (change of nociceptive threshold 0.2 ± 4.6 %), while Taxol injection (1 µg/ 2.5 µl) had no effect of G-1-induced reduction of the nociceptive threshold (change of nociceptive threshold -48.3 ± 1.9 %). (B) Nocodazole (1 µg/2.5 µl) as well as Taxol (1 µg/2.5 µl) injection itself does not change the mechanical nociceptive threshold 30 min after application (change of nociceptive threshold: nocodazole -0.2 ± 3.9 %, Taxol -10.8 ± 5.1 %). Measurements of the nociceptive threshold in rats were preformed with the Randall-Selitto paw pressure device. ** p < 0.001 for G-1 or nocodazole/Taxol + G-1 treatment compared to vehicle controls; error bars represent SEM.

7.2.11 TRPV1 defines the influence of microtubule alternating drugs onto PKCε-dependent mechanical hyperalgesia

In the cellular system PKCε signaling modulated the microtubule cytoskeleton in a TRPV1-dependent manner. Therefore it was addressed if TRPV1 is also involved in PKCε- and microtubule-dependent pain sensitization in the animal.

To examine the influence of TRPV1, the effect of the microtubule alternating drugs nocodazole and Taxol on PKCε-dependent sensitization was tested after downregulation of TRPV1. In collaboration with Olayinka A. Dina, antisense oligodeoxynucleotides (ODN) against mRNA of TRPV1 which have been shown to down regulate TRPV1 (Christoph et al., 2006), were intrathecally injected into adult male rats daily for a period of three days. Indeed, while in wild type animals G-1-induced sensitization was increased by pretreatment with Taxol, in TRPV1-knock down animals Taxol abolished G-1-induced sensitization. Similarly, also the effect of nocodazole on sensitization was inverted in absence of TRPV1. While G-1-induced sensitization was abolished by nocodazole in normal male rats, nocodazole had no effect on mechanical sensitization in TRPV1 knock down animals (Fig. 28 A).

Confirming results from TRPV1 knock out animals, downregulation per se did not change the induction of mechanical hyperalgesia: G-1 caused a reduction of the mechanical nociceptive threshold by 37.8 ± 1.4 % in naïve rats, by 33.8 ± 1.3 % in animals treated with mismatch ODN and by 35.0 ± 1.3 % in rats treated with antisense ODNs against TRPV1 under normal cytoskeletal conditions (Fig. 28 B). These results suggest that TRPV1 is not an essential component of a linear signaling pathway toward sensitization. Instead, these findings indicate that the dynamic TRPV1-microtubule interaction is a part of the sensitization process, an aspect observable by pharmacologically constraining the microtubule dynamics.
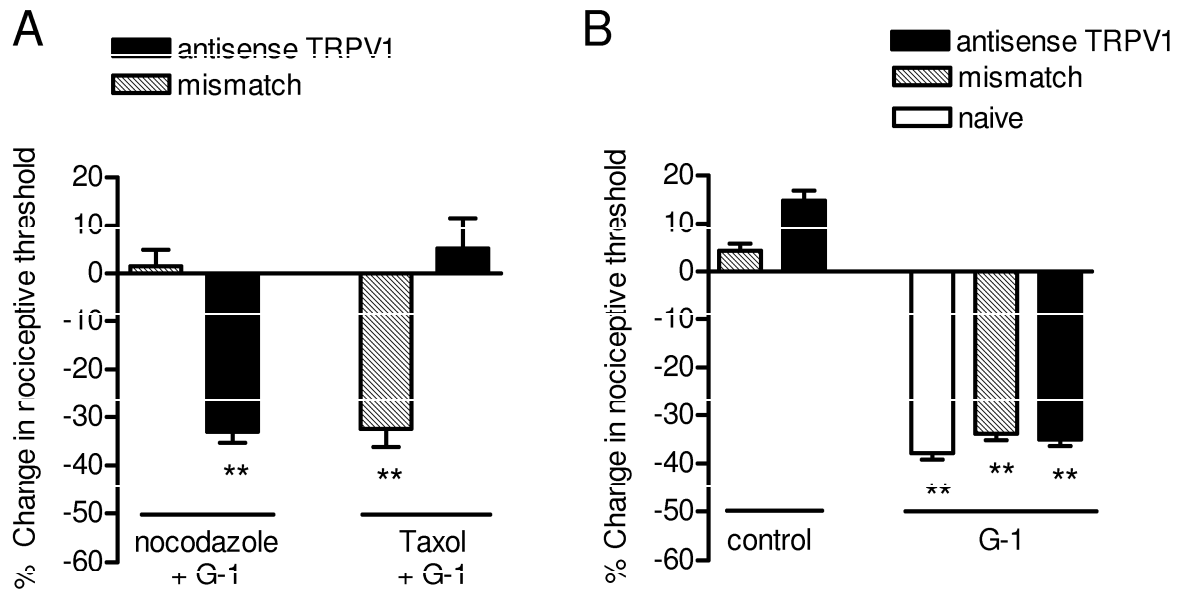
Fig. 28: TRPV1 defines the influence of microtubule alternating drugs onto PKCε-dependent mechanical hyperalgesia. (A) Downregulation of TRPV1 reversed the effect of microtubule alternating drugs on G-1 induced hyperalgesia. Application of nocodazole (1 µg/2.5 µl) did not affect G-1-induced sensitization (application of 1 µg/2.5 µl) in TRPV1 antisense treated rats, while in rats treated with mismatch ODNs hyperalgesia was abolished similar to naïve animals (change of nociceptive threshold: antisense TRPV1 -33.1 ± 2.3 %, mismatch 1.5 ± 3.3 %, naïve 0.2 ± 4.6 % (s. graph B)). In contrast, pre-treatment with Taxol (1 µg/2.5 µl) did not change the nociceptive threshold after G-1 application in naïve as well as mismatch ODN treated animals, while it abolished G-1-induced sensitization in antisense TRPV1 ODN treated rats (change of nociceptive threshold: antisense TRPV1 5.2 ± 6.4 %, mismatch -32.4 ± 3.8 %, naïve -48.27 ± 1.91 (s. graph B)). **(B)** Downregulation of TRPV1 using antisense oligodeoxynucleotides (ODN) as well as application of mismatch ODNs (40 µg in a volume of 20 µl once daily for 3 days, intrathecally) did not change the induction of mechanical hyperalgesia by G-1 compared to naïve rats (change of threshold: antisense TRPV1 -35.0 ± 1.3 %, mismatch -33.8 ± 1.3 %, naïve -37.8 ± 1.4 %). Measurements of the nociceptive threshold in rats were preformed with the Randall-Selitto paw pressure device. ** $p < 0.001$ for nocodazole/Taxol + G-1 treatment compared to corresponding negative controls (A) or G-1 treatment compared to corresponding negative controls (B); error bars represent SEM.

7.2.12 Summary part II

Structural modeling and biochemical experiments indicated that PKCε-mediated phosphorylation of TRPV1 serine 800 interferes with tubulin binding to the TRPV1-C terminus. In DRG neuron derived F-11 cells, treatment with estrogen or the GPR30 agonist G-1 resulted in PKCε- and TRPV1-dependent microtubule destabilization and induced morphological changes including cell retraction, growth cone retraction and varicosity formation. The observed alterations were independent of the TRPV1 channel function, as microtubule disassembly also occurred in the presence of the potent TRPV1 channel blocker 5'I-RTX as well as in cells expressing an N-terminal deletion mutant of TRPV1 which does not form a functional channel. While independent of the channel function, a point mutation of the PKCε-specific phosphorylation site at serine 800 (TRPV1-S800A) attenuated destabilization of microtubule filaments. In pain behavioral experiments, G-1-induced PKCε-dependent mechanical hyperalgesia was abolished by the microtubule destabilizer nocodazole while the microtubule stabilizing agent Taxol had no effect. In the absence of TRPV1 the effects of Taxol and nocodazole were inverted: Taxol abolished PKCε-dependent mechanical hyperalgesia while nocodazole had no effect.

These results support the suggestion that PKCε controls signaling in nociceptive neurons by regulating the relationship between TRPV1 and the tubulin cytoskeleton upon activation. Thus, TRPV1 serves as a signaling intermediate in estrogen-induced mechanical hyperalgesia, a property unrelated to its ion channel function.

7.3 The dual role of estrogen: Identification of a Ca^{2+}-dependent analgesic signaling branch

In part I and II I characterized a linear signaling pathway in nociceptive neurons. I collected data supporting the involvement of the novel estrogen receptor GPR30, identified estrogen to activate the G-protein αs upstream of PKCε, and described the interaction of TRPV1 with tubulin as a novel downstream target of PKCε in estrogen-induced mechanical sensitization. In part III I will now leap from the linear pathway to signaling events involved in a cellular signal-computation mechanism, dealing with the integration of multiple signals. Under painful or sensitizing conditions, i.e. during inflammation, many different inflammatory mediators are released from the surrounding tissue. Thus, neurons are exposed simultaneously as well as successively to a broad variety of signaling mediators. To understand how primary neurons process multiple signals, signaling events induced by repeated activation of the PKCε signaling pathway were analyzed in behavioral experiments and on the cellular level.

In an experimental series performed in Tim Hucho's laboratory it was shown, that a sensitizing signaling pathway could not be activated a second time as observed by lack of translocation of PKCε in response to a second treatment of DRG cultures. The observed block of PKCε

translocation was rapid (<30 sec) and long lasting (>20 h). Further experiments indicated the branching of the signaling cascade into a PKCε-dependent sensitizing and an IP3-dependent desensitizing pathway. In behavioral experiments, injection of a second normally sensitizing stimulus did not result in additional sensitization. Instead, sequential administration of two sensitizing stimuli reversed already established mechanical hyperalgesia (Fig. 29).

In the following part of my thesis I investigated the cellular mechanism underlying the desensitizing/analgesic effect of estrogen. Thereby I focused on the role of Ca^{2+} as a second messenger in the inhibitory branch of estrogen signaling in nociceptive neurons.
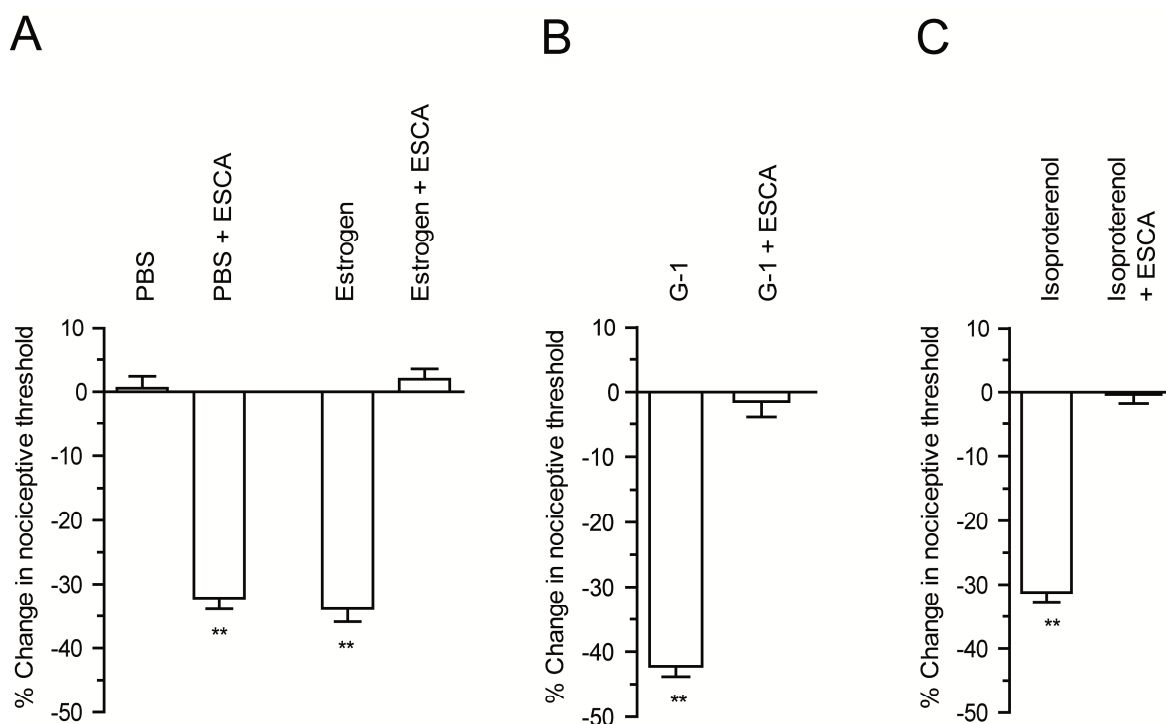

Fig. 29: A second sensitizing stimulus reverses PKCε-dependent mechanical sensitization. (A) Injection of estrogen as well as the Epac-activator ESCA (6.3 µg/2.5 µl) or estrogen (100 ng/2.5 µl) intradermally into the hindpaw of rats results after 30 min in robust mechanical hyperalgesia (reduction of nociceptive threshold compared to vehicle controls: ESCA = 32.1 ± 1.7 %, Estrogen = 33.9 ± 2.0 %). Stimulation with the pronociceptive Epac-activator ESCA 30 min after preceding estrogen stimulation reverses the established hyperalgesia completely. (B) Mechanical sensitization induced by intradermal injection of the GPR30 agonist G-1 (1 µg/2.5 µl) into the hindpaws of male rats is completely abolished after injection of the Epac-activator ESCA (6.3 µg/2.5 µl) (reduction of nociceptive threshold compared to vehicle controls: G-1 = 42.2 ± 1.6 %, G-1 + ESCA = 1.4 ± 2.4 %). (C) Similar to estrogen- and G-1-induced mechanical hyperalgesia, also mechanical sensitization induced by the intradermal injection of the β-adrenergic agonist isoproterenol (1 µg/2.5 µl) into the hindpaw of male rats is abolished by a subsequent injection of the Epac-activator ESCA (6.3 µg/2.5 µl) which normally induces PKCε-dependent mechanical sensitization if applied alone. Error bars indicate SEM.

7.3.1 Estrogen induces Ca^{2+} influx in a subset of DRG neurons

In vitro, nociceptive neurons can be switched from a sensitization responsive to a non-responsive state. Further experiments indicate the branching of the PKCε activating signaling cascade. One branch, including PKCε, leads to mechanical sensitization. The other branch, including IP3, interferes with successive signaling events and has the potential to reverse mechanical hyperalgesia. The involvement of IP3 indicated that Ca^{2+} plays a role in the inhibitory branch of the signaling cascade. If estrogen induces Ca^{2+} signaling in nociceptive neurons, is unknown.

Therefore, I examined if estrogen treatment leads to a rise of intracellular Ca^{2+} levels in DRG neurons. In live cell calcium imaging experiments using Fura-2 AM a rapid increase of intra-cellular Ca^{2+} concentration was observed in a subset of DRG neurons. At the end of the recordings, responding and non-responding neurons were tested for viability by a depolarizing KCl pulse. 15.1 % of all viable DRG neurons showed an increase in Ca^{2+} concentration in response to estrogen (Fig. 30) (16 out of 106 neurons). This percentage is very similar to the number of neurons showing PKCε activation after estrogen treatment (Fig. 7 B).
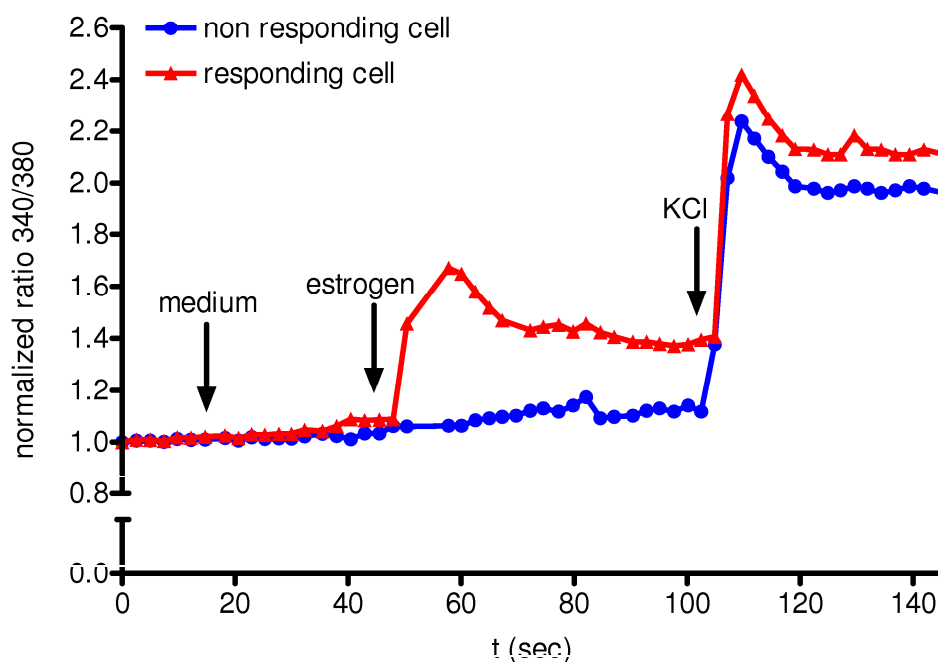

Fig. 30: Estrogen induces calcium influx in rat DRG neurons. Fura-2 based ratiometric calcium imaging indicates calcium influx in response to estrogen (10 nM) in a subgroup of DRG neurons. Representative traces of responsive (red) and non-responsive (blue) DRG neurons are shown for cultures treated with estrogen. Ratiometric images were taken ~2 sec. Black errors indicate the time point of the test pulse (medium), the stimulus and the control stimulus KCl.

7.3.2 PKCε translocation occurs in neurons showing intracellular Ca²⁺ rise in response to estrogen

PKCε translocation as well as intracellular Ca²⁺ rise occurs only in a subgroup of DRG neurons. Experiments from our group suggested that the intracellular Ca²⁺ signal is involved in the block of subsequent PKCε translocation and the reversal of mechanical sensitization. Therefore, I investigated if the Ca²⁺ rise occurs in the very same cells which translocate PKCε in response to a sensitizing stimulus. To analyze the subcellular localization of PKCε in neurons showing Ca²⁺ rise, live cell imaging has to be combined with immunofluorescence analysis of fixed neurons. To overcome the challenge to find the same cells monitored in calcium recordings again for evaluation of PKCε translocation, a combined assay was established on an automated high content immunofluorescence microscope. There, the identification of the absolute coordinates of each cell allowed us to perform both evaluations in the very same neuron.

Over night DRG cultures derived from adult male rats were loaded with Fura-2 AM and changes in intracellular Ca²⁺ concentrations were monitored by taking paired images excited at 340 and 380 nm about every 2 sec until the end of the live cell imaging protocol. As DRG cultures are a heterogeneous cell system including various mechanosensitive neurons, a vehicle pulse was applied after 15 sec baseline scan and cells sensitive to this low level mechanical stimulation were excluded from further analysis. Images were taken for another 30 sec before the PKCε-translocation inducing stimulus was applied. Cells were fixed 40 sec after estrogen application and PKCε translocation was analyzed by immunofluorescence microscopy. Using this combinatory approach PKCε translocation was observed in neurons also responding to estrogen with an increase of intracellular Ca²⁺ levels (Fig. 31). This suggests that, indeed, both signaling events take place in the same cells.
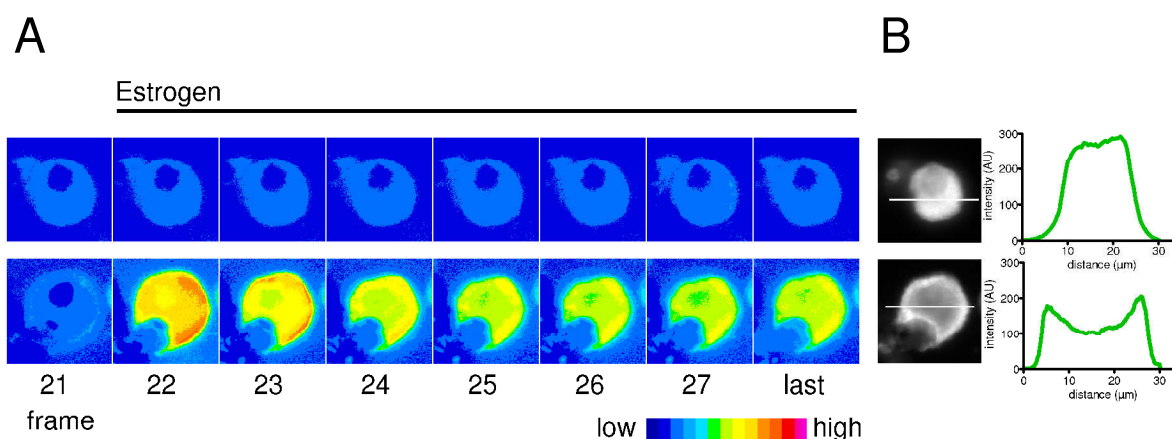

Fig. 31: PKCε translocation occurs in neurons showing calcium influx in response to estrogen. (A) Representative images of Fura2-loaded cells treated with estrogen (10 nM). One responding and one non-responding cells is shown. The 340/380 nm ratio has been converted into false colors. Images were taken about every 2 sec (numbers underneath indicate the respective frame). The treatment started with the second presented frame. **(B)** After fixation and immunofluorescence labeling, PKCε translocation to the plasma membrane was detected in neurons with calcium influx (epifluorescent images, 20 x objective). Intensity histograms along the white lines are represented on the right.

7.3.3   PKCε-activating substances initiate Ca^{2+} signaling in DRG neurons

So far, all estrogen effects were mimicked by the estrogen receptor GPR30 agonist G-1 in cellular and behavioral experiments. Thus, it was analyzed if also rise of intracellular Ca^{2+} is initiated by G-1. Performing Ca^{2+} imaging experiments, a rapid increase of the intracellular Ca^{2+} levels was observed in ~19 % of DRG neurons (18 out of 95 neurons, total number of viable neurons defined by a KCl response) after application of 10 nM G-1 (Fig. 32 A). Similar to estrogen treated cells, neurons responding with an increase of intracellular Ca^{2+} to G-1 treatment also showed PKCε translocation (Fig. 33).
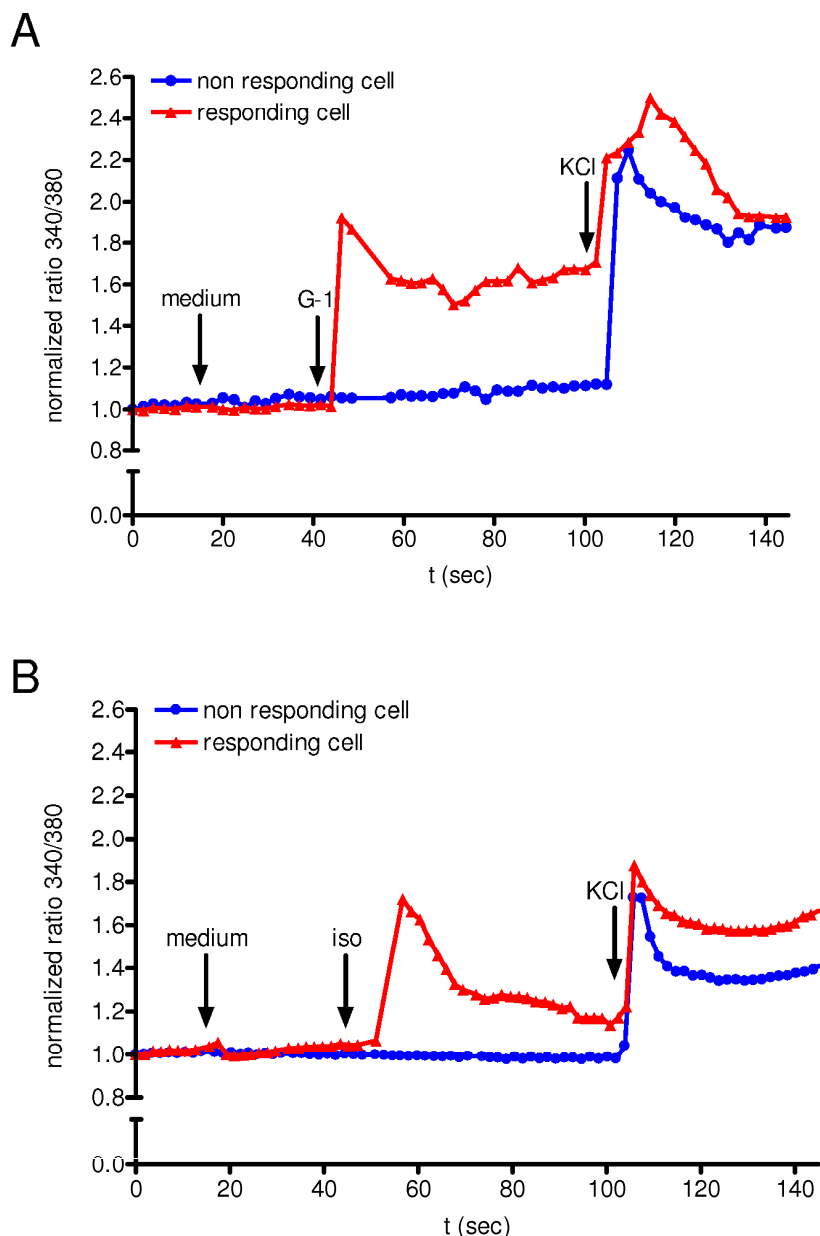

Fig. 32: The PKCε-activating stimuli G-1 and isoproterenol mimic estrogen-induced calcium influx. Fura-2 based ratiometric calcium imaging shows calcium influx in response to the GPR30 agonist G-1 (10 nM) as well as the β-adrenergic agonist isoproterenol in a subgroup of DRG neurons. Representative traces of responsive (red) and non-responsive (blue) DRG neurons are shown for cultures treated with G-1 (A) or isoproterenol (B). Ratiometric images were taken ~2 sec. Black errors indicate the time point of the test pulse (medium), the stimulus and the control stimulus KCl.

To generalize these results and to assure a signaling mechanism not only specific for estrogen and estrogen receptor agonists, it was next examined if treatment with the β-adrenergic agonist isoproterenol also induces a Ca^{2+} rise in DRG neurons. Calcium imaging experiments using the protocol described above showed a rapid increase of intracellular Ca^{2+} levels in a subgroup of DRG neurons. The effect was comparable to changes observed in response to estrogen or G-1 Fig. 32 B, Fig. 33) (16.7 % neurons responding, 18 out of 100 neurons, total number of viable neurons defined by KCl response). And again, in neurons showing Ca^{2+} rise, also PKCε translocation to the plasma membrane was observed (Fig. 33).
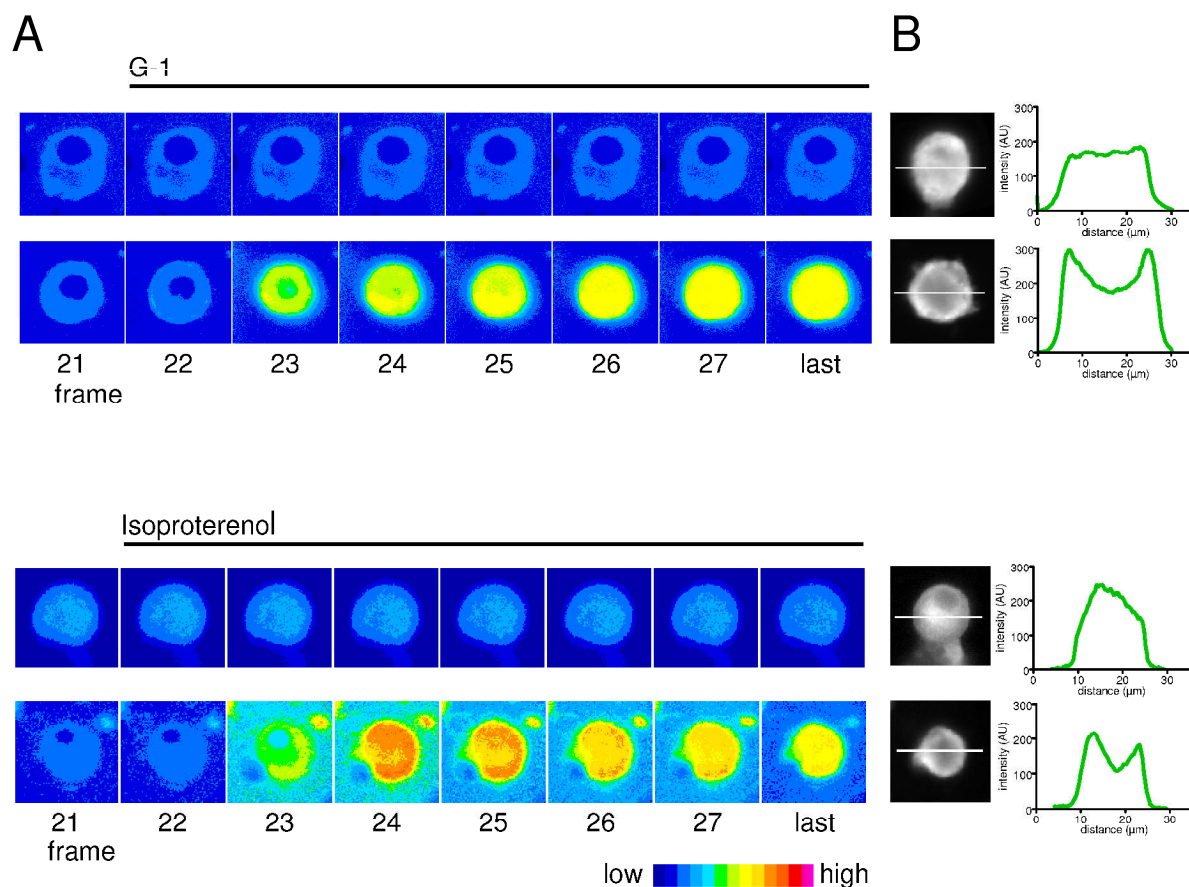

Fig. 33: G-1 and isoproterenol induce calcium influx and PKCε translocation in the same neurons. (A) Representative images of G-1- (10 nM, first pair of rows) or isoproterenol-treated (1 μM, second pair of rows) rat DRG neurons loaded with Fura-2 AM. One responding and one non-responding cells is shown for every treatment. The 340/380 nm ratio has been converted into false colors. Images were taken about every 2 sec (numbers underneath indicate the respective frame). The treatment started with the second presented frame. **(B)** After fixation and immunofluorescence labeling, PKCε translocation to the plasma membrane was detected in neurons with calcium influx (epifluorescent images, 20 x objective). Intensity histograms along the white lines are represented on the right.

7.3.4 Intracellular Ca^{2+} rise itself does not induce mechanical sensitization

Cellular data indicated a branching of the signaling cascade in a PKCε-dependent sensitizing signal and a Ca^{2+}-dependent signal controlling the signal transduction of following stimuli. To verify that intracellular Ca^{2+} rise is indeed a signaling branch independent of the mechanical sensitization event, it was examined if direct stimulation of Ca^{2+} release through ryanodine induces mechanical sensitization. Injection of ryanodine (1 µg/2.5 µl) into the hindpaw of adult male rats did not influence the mechanical nociceptive threshold (Fig. 34).

7.3.5 Ryanodine-induced Ca^{2+} release reversed PKCε-dependent mechanical sensitization *in vivo*

Cellular experiments performed in Tim Hucho's laboratory showed that the inhibitory branch of the signaling cascade can be activated independently of a sensitizing stimulus by inducing Ca^{2+} release from intracellular stores. Therefore it was investigated if ryanodine administration reverses mechanical hyperalgesia in sensitized rats, even though ryanodine itself did not affect the mechanical nociceptive threshold. In behavioral experiments performed in Jon D. Levine's laboratory, rats were sensitized by injection of the Epac activator ESCA in a concentration known to induce mechanical hyperalgesia (6.3 µg/2.5 µl). After 30 min, when robust hyperalgesia was detectable, ryanodine (1 µg/2.5 µl) was injected into the hindpaw of sensitized rats. Indeed, no mechanical hyperalgesia was detectable 30 min after ryanodine administration, indicating that the inhibitory effect is indeed independent of the sensitization event (Fig. 34).

As an elevation of intracellular Ca^{2+} levels was able to reverse already established hyperalgesia, it was also examined if ryanodine injection inhibits following sensitizing signals and therefore prevents the development of mechanical hyperalgesia. After injection of ryanodine (1 µg/2.5 µl) 30 min prior to ESCA administration (6.3 µg/2.5 µl) into the hindpaw of adult male rats no mechanical sensitization was detectable measured 30 min after ESCA injection (Fig. 34).

These results strengthen the hypothesis, that the inhibitory effect observed after sequential administration of sensitizing/nociceptive substances in behavioral experiments is mediated by a second branch of the signaling cascade which can be activated independent of the sensitizing event.
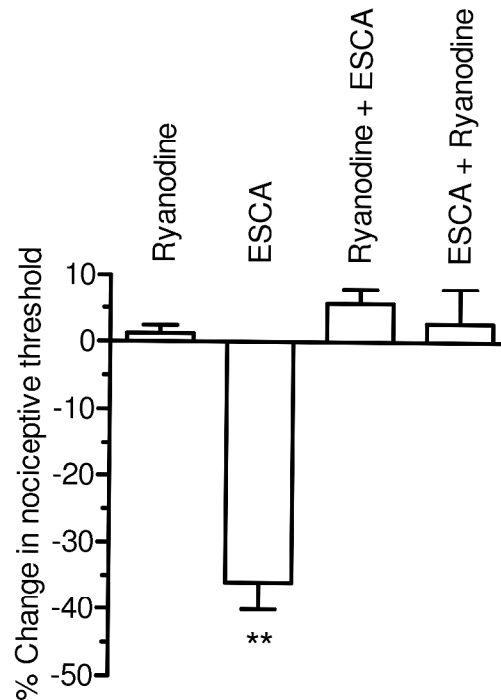
Fig. 34: Ryanodine abolishes PKCε-dependent mechanical sensitization. Stimulation of calcium release by ryanodine injection (1 µg/2.5 µl) into the hindpaw of adult male rats does not induce mechanical sensitization. On the other hand, ryanodine injection (1 µg/2.5 µl) reverses mechanical hyperalgesia induced by the Epac-activator ESCA (6.3 µg/2.5 µl) in adult male rats independent of the order of application (change of nociceptive threshold: ESCA = -35.9 ± 4.1 %, ryanodine + ESCA = 5.8 ± 2.2 %, ESCA + ryanodine = 2.8 ± 5.3 %). ** $p < 0.001$, error bars represent SEM.

7.3.6 Summary part III

I showed in this part of my thesis that Ca^{2+} is a central second messenger mediating the desensitizing/analgesic effect of estrogen. Estrogen causes not only PKCε activation in nociceptive neurons; it additionally initiates Ca^{2+} signaling in the very same cells. This dual role of signaling is not an estrogen-specific phenomenon; it was also observed in response of other nociceptive stimuli such as the β-adrenergic receptor agonist isoproterenol. Pain behavioral experiments showed that Ca^{2+} signaling itself does not induce mechanical sensitization. But inducing Ca^{2+} signaling independent of a nociceptive stimulus by injection of ryanodine was sufficient to abolish PKCε-dependent sensitization completely.

Together these results suggest that estrogen and other nociceptive stimuli initiate two different processes in the primary sensory neuron: on one hand they cause PKCε-dependent mechanical sensitization if no other sensitizing stimulus is present. On the other hand, they activate a Ca^{2+}-dependent signaling process which controls the transduction of following incoming signals and thereby reverses sensitization.

8 Discussion

Pain and nociception are increasingly well characterized on a behavioral and electrophysiological level. Nevertheless, the description of the underlying molecular mechanisms is often lagging behind. Recently, we identified sex steroid hormones as a new class of stimuli to act directly on primary nociceptive neurons and to influence nociception (Hucho et al., 2006). Investigating the underlying mechanism I found estrogen signaling and signaling induced by classical inflammatory mediators and mediated by GPCRs to converge onto PKCε (Cesare et al., 1999; Hucho et al., 2005). Extending the knowledge about downstream effects of estrogen-induced PKCε activation, I identified a novel aspect of sensitizing signaling: the ion channel independent regulation of the TRPV1-microtubule interaction. And finally, investigating how multiple convergent signals onto PKCε are computed in the cell resulted in the description of a novel endogenous autoinhibitory signaling mechanism.

In the first part of the discussion I will reflect over the G-protein coupled receptor, GPR30, as an estrogen receptor in nociceptive signaling, discuss novel functions for the vanilloid receptor TRPV1, and describe a way, how the identified inhibitory module could help to explain contradictory effects of estrogen in nociception.

In the second part I will highlight new physiological functions for the "female hormone" estrogen, suggest novel perspectives for pain treatment and introduce a modular concept of signaling in nociceptive neurons.

8.1 Estrogen-induced signaling mechanisms in nociceptive neurons

8.1.1 GPR30: a mediator for estrogen actions in nociceptive neurons?

Currently there are three estrogen receptors described to mediate estrogen effects, ERα, ERβ and GPR30. Which estrogen receptor mediates estrogen-induced PKCε translocation in nociceptive neurons and mechanical sensitization is unknown. All three receptors are expressed in primary sensory neurons (Bennett et al., 2003; Fehrenbacher et al., 2009; Liverman et al., 2009; Papka and Storey-Workley, 2002; Takanami et al., ; Taleghany et al., 1999). And all three are described to mediate rapid estrogen effect.

My results indicate the involvement of GPR30 in estrogen-induced PKCε activation and hyperalgesia. Both GPR30 agonists, G-1 and ICI 182,780, the latter of which is simultaneously an antagonist of the ERα/ERβ, induce rapid PKCε activation in DRG neurons similar to estrogen. In addition, estrogen and GPR30 agonists activate PKCε in the same subset of DRG neurons which bind not only to the isolectin B4, but also express TRPV1.

Additional support for the role of GPR30 is derived from the signaling cascades involved. GPCRs are widely described as mediators for sensitizing signals in nociceptive neurons. In 2005, Hucho et al. showed that stimulation of the αs coupled β2-adrenergic receptor induces PKCε activation via cAMP signaling. Also GPR30 has been reported to be coupled to the small G-protein αs (Thomas et al., 2005) and thus to adenylyl cylclase signaling. And indeed, inhibition of the adenylyl cyclase blocked estrogen-induced PKCε activation.

But what might be the physiological relevance for rapid estrogen effects in DRG neurons, which is in our system induced by concentrations of about 10-fold above peak plasma levels detected in male rats (Cornil et al., 2006)? One possible scenario is that there are fast and/or locally restricted pulses of estrogen in painful situations, e.g. after tissue injury or during inflammation. High pulses of local estrogen would open the possibility to differentiate between ERα/ERβ mediated effects and brief GPCR mediated actions. GPR30 is described to have weaker estrogen-binding affinities than the classical estrogen receptors. Thus the normal variation of plasma estrogen levels only minimally affects GPR30. In contrast, a brief and locally restricted high estrogen pulse would rapidly activate GPR30 resulting in a fast signaling response. Indeed, there is increasing evidence for local estrogen production in neuronal tissues. The estrogen-producing enzyme aromatase is expressed in several pain-related areas of the nervous system such as the DRG and the spinal dorsal horn (Evrard and Balthazart, 2002; Evrard, 2006; Schaeffer et al., 2010). Recently, Schaeffer et al. reported local estrogen synthesis in DRG neurons in a neuropathic pain model. Sciatic nerve injury (chronic constriction injury, CCI) increased local estrogen production by DRG neurons in comparison to naïve or sham-operated rats. This observation was accompanied by decreased pain thresholds against thermal as well as mechanical stimuli in CCI animals (Schaeffer et al., 2010). Thus, estrogen can be produced in close vicinity to nociceptive neurons or even by the nociceptive neurons themselves which might result in high local estrogen levels, and is therefore likely to modulate nociception, e.g. by rapid activation of nociceptive signaling cascades. Also in humans, aromatase activity and thus estrogen production seems to be associated with nociception: So far, a number of patients with mutations in the aromatase gene have been described. Besides of other severe symptoms including osteopenia and different forms of glucose-intolerance and fertility impairment, affected patients suffer from estrogen-dependent pain symptoms (Bulun, 2000; Carani et al., 1997; Maffei et al., 2004; Zirilli et al., 2008).

But beyond the circumstantial evidence, is GPR30 really the mediating estrogen receptor? GPR30 was first described to bind to and to be activated by estrogen in 2005 (Revankar et al., 2005; Thomas et al., 2005). A first GPR30 specific agonist was developed in 2006 (Bologa et al., 2006). Therefore, information about physiological functions of GPR30 as an estrogen receptor is only emerging. In fact, our description of GPR30 agonists inducing pain sensitization *in vivo* was the first indication of a biological role for GPR30 (Kuhn et al., 2008). Recently, also Liverman et al. correlated cellular data and pain behavioral experiments, where G-1 mimics estrogen actions on both levels: In trigeminal ganglion neurons, G-1 as well as estrogen induced ERK activation and both substances increased Complete Freund's Adjuvant-induced sensitization (Liverman et al., 2009). But using pharmacological approaches, it cannot be excluded that the observed estrogen

effects are mediated by other, potentially even still unidentified, estrogen receptors. Thus, taking the effectiveness of GPR30 agonists as prove for involvement of GPR30 as a mediator for estrogen effects has to be taken with caution. Some argue even that GPR30 is not an estrogen receptor in the first place (Langer et al., 2009; Otto et al., 2009). Beyond estrogen receptor mediated actions, also the direct binding of estrogen to PKCs has been reproted leading to an alteration of PKC activity (Alzamora et al., 2007). Such direct effects are often interpreted as a side-effect of extremely high estrogen concentrations in the micromolar range used in the respective experiments (Langer et al., 2009). Nevertheless, the adenylyl cyclase dependence described here renders a direct effect of estrogen on PKCε highly unlikely. Instead it suggests that a GPCR such as GPR30 mediates the estrogen-induced PKCε translocation in nociceptive neurons.

Currently, all our results point toward GPR30 as a mediator for nociceptive signaling. Still, to verify that indeed GPR30 is the receptor mediating estrogen-induced sensitization, experiments on animals after downregulation or knock out of GPR30 in the peripheral nervous system are required. On the base of my data, a supportive result is likely. But even if such experiments would disprove GPR30 as the mediating estrogen receptor, this would open an important question: Which other receptor/GPCR mediates estrogen, G-1 and ICI 182,780 signals in nociceptive neurons in an adenylyl cyclase-dependent manner and induces PKCε-dependent sensitization?

8.1.2   TRPV1 as a downstream mediator of estrogen

I described TRPV1 to be a target of rapid, non-genomic estrogen signaling. Functional relationships between TRP channels and the steroid hormone estrogen have been reported previously. Estrogen can influence the expression of TRP channels (Tong et al., 2006) and, vice versa, the activation of TRP channels can alter the expression of estrogen receptors (Malagarie-Cazenave et al., 2009). Additionally, estrogen has been reported to modulate TRP channel activity. Xu et al. showed that estrogen-treatment inhibits specifically capsaicin-induced TRPV1 activation in DRG neurons, while proton-induced activation was not affected by estrogen. Interestingly, this effect could be mimicked among others by the ERα/ERβ antagonist/GPR30 agonist ICI 182,780. The signaling mechanism which mediates these estrogen effects, is so far unknown (Xu et al., 2009)

Signaling toward TRP channels has been nearly exclusively associated with modulation of the ion conductivity of the channel. Accordingly, the influence of intracellular modifications of TRPV1 on its ion channel function is well characterized. In contrast, not much is known about the impact of TRPV1 modifications on intracellular signaling pathways. The estrogen-induced signaling presented here resulted in TRPV1 signaling towards microtubules which was insensitive to the TRPV1-channel blocker 5'I-IRTX. TRPV1 effects that were not blocked by TRPV1 antagonists have been described previously (Creppy et al., 2000; Fujimoto and Mori, 2004; Fujimoto et al., 2006). In addition to the insensitivity to TRPV1 antagonists, the TRPV1-dependent microtubule destabilization presented here also occurred in the presence of an N-terminal deletion mutant of

TRPV1 which does not form a functional channel (Jung et al., 2002). While the number of reports about non-channel functions of voltage-gated ion channels is increasing, this indicates the first example of TRPV1 signaling that is independent of its ion channel functionality.

Estrogen-induced alteration of microtubules involves the PKCε-specific phosphorylation site S800 in the C-terminal region of TRPV1. Phosphorylation at this position has also been shown to influence the channel property: It leads to the resensitization of TRPV1 (Mandadi et al., 2006). This raises the question if the ion channel function can be regulated independent of the microtubule cytoskeleton or if the observed microtubule destabilization is necessary for the regulation of the ion channel activity.

In the signaling pathway presented here, estrogen does not act directly on TRPV1. Instead it initiates an intracellular signaling mechanism that leads to the modulation of TRPV1. Thereby a GPCR, most likely the novel estrogen receptor GPR30, is involved in the transduction of estrogen signals towards TRPV1. TRPV1 has been described as a downstream target of other GPCRs (Malin et al., 2008; Moriyama et al., 2003; Zhang et al., 2007). Zhang et al. showed that activation of the NK-1 receptor modulates TRPV1 activity, postulating a signaling mechanism that involves a GPCR, PLC and PKCε (Zhang et al., 2007). Finding different GPCRs able to modulate TRPV1, it will be interesting to examine if the activation of other GPCRs also affects the microtubule cytoskeleton in a TRPV1-dependent manner.

8.1.3   Does TRPV1 act as a microtubule plus end tracking protein?

Direct binding of tubulin as well as microtubules to TRPV1 has been reported previously (Goswami et al., 2004; Goswami et al., 2006; Goswami et al., 2007b). Computational modeling now indicated that only tubulin dimers or tubulin exposed at the tips of microtubule protofilaments fit into the binding pocket at the TRPV1-Ct. Biochemical experiments showed a higher preference for β-tubulin over α-tubulin to bind to the TRPV1-Ct (Goswami et al., 2007b). This prevalence indicates that TRPV1 binds to the plus ends of microtubules which terminate their protofilaments with β-tubulin.

One important class of microtubule binding proteins interacting with the plus ends of microtubules is the group of plus-end tracking proteins (+TIPs). +TIPs are specialized microtubule associated proteins (MAPs) that accumulate at the plus ends of growing microtubules (Honnappa et al., 2009; Schuyler and Pellman, 2001). By binding to growing microtubules, +TIPs regulate microtubule dynamics, function as intracellular signaling molecules and control cell shape and architecture. Several structurally unrelated families of +TIPs have been described, such as end binding proteins, cytoskeleton-associated protein glycine-rich proteins (CAP-Gly family) and the family of proteins containing basic or serine-rich sequences (Akhmanova and Steinmetz, 2008). The TRPV1-Ct has also several serine residues and basic amino acids in the tubulin binding regions (Goswami et al., 2007b). One further characteristic of basic/serine-rich +TIPs is their regulation via phosphorylation. As microtubules are negatively charged, phosphorylation in close vicinity to the binding region reduces the binding affinity between +TIPs and microtubules

(Akhmanova and Steinmetz, 2008). For example, phosphorylation of adenomatous polyposis coli (APC) by glycogen synthase kinase 3 β induces its dissociation from microtubules (Zumbrunn et al., 2001) and thereby controls axonal growth (Zhou et al., 2004). Again, TRPV1 shares also this dynamic property of +TIPs. I found the interaction of TRPV1 with microtubules to depend on phosphorylation of S800 of the TRPV1-Ct. And even further, like other +TIPs, also TRPV1 has been shown to regulate growth cone behavior in neuronal cells, most likely in a microtubule-dependent manner (Goswami et al., 2006; Goswami et al., 2007a; Goswami and Hucho, 2007).

Another important function of +TIPs is to attach and stabilize microtubule ends at the cell cortex. Thereby, especially members of the basic/serine-rich sequence containing family serve as microtubule-stabilizing factors (Lansbergen and Akhmanova, 2006; Lansbergen et al., 2006). Some microtubule-stabilizing +TIPs, such as APC, can bind directly to actin (Moseley et al., 2007). Others act via cortical-bound proteins like CLASPs (Lansbergen et al., 2006). Also TRPV1 binding stabilizes microtubules. Localized in the plasma membrane, TRPV1 particularly stabilizes submembranous microtubules (Goswami et al., 2006; Goswami et al., 2007a; Goswami and Hucho, 2007).

While, so far, there is no description of a transmembrane +TIP localized in the plasma membrane, it is known that +TIPs can link microtubules to intracellular membranes. The transmembrane protein stromal interaction molecule 1 (STIM1) is localized in the membranes of the endoplasmic reticulum and belongs to the family of basic/serine-rich +TIPs. In addition to its function as a Ca^{2+} sensor, STIM1 is involved in the microtubule growth-dependent remodeling of the endoplasmic reticulum (Grigoriev et al., 2008). Interestingly, STIM1 is also associated with TRP channels; it interacts with TRPC1 and regulates its channel function in a microtubule-dependent manner (Pani et al., 2009; Zhang et al., 2009).

In conclusion, binding to the plus ends of microtubules and sharing many additional characteristics of +TIPs, TRPV1 might be the first candidate for a +TIP localized in the plasma membrane. To what extend TRPV1 is involved also in other aspects of +TIPs such as the tracking of growing microtubules, has to be investigated in more detail. In addition to TRPV1, other members of the TRP superfamily of ion channels have been shown to interact with tubulin (Bollimuntha et al., 2005; Goel et al., 2005) or microtubule binding proteins (Alessandri-Haber et al., 2004). Further investigation is necessary to clarify if these channels can be considered as +TIPs and if this is a new, more general signaling mechanism of TRP channels.

8.1.4   TRPV1 in mechanical sensitization

While the role of TRPV1 in heat hyperalgesia is well established, the contribution of TRPV1 to mechanical sensitization is still controversial. Several studies show that mechanical hyperalgesia can be induced in TRPV1 –/– mice using formalin, Complete Freud's Adjuvant, carrageenan or partial nerve lesion (Bolcskei et al., 2005; Caterina et al., 2000; Jin and Gereau, 2006; Kanai et al., 2007). Nevertheless, some groups indicate an involvement of TRPV1 in mechanical sensitization: Tender et al. reported that mechanical sensitization in a neuropathic pain model depends on

TRPV1. RTX-induced TRPV1-ablation reduced mechanical hyperalgesia after sciatic nerve injury. And TRPV1-ablation prior to the injury prevented the development of mechanical sensitization (Tender et al., 2008). Based on experiments with TRPV1 –/– mice, Jones and colleagues suggest that TRPV1 functions as a mechanosensor in colon afferent fibers mediating visceral nociceptive behavior in mice during inflammation (Jones et al., 2005).

How can TRPV1 be involved and also not involved in mechanical hyperalgesia? This so far unexplained conundrum is also reflected in this work: On one hand, mechanical hyperalgesia can be induced in the absence of TRPV1, indicating that TRPV1 is not an essential component for the development of mechanical sensitization. On the other hand, modulation of the microtubule cytoskeleton showed a clear TRPV1-dependent effect on mechanical hyperalgesia. In our experiments the difference was made by the presence of microtubule modulating drugs. Thus, one might suggest that there is a cytoskeleton-dependent mechanical hyperalgesia and a cytoskeleton-independent mechanical hyperalgesia and only the former is TRPV1-dependent while the latter is not. Indeed, Dina et al. found a first indication of this dichotomy (Dina et al., 2003). The differentiation of cytoskeleton-dependent versus cytoskeleton-independent hyperalgesia would lead to novel mechanism-based therapeutic approaches. For example, one is therefore tempted to speculate that capsaicin treatment which results in the downregulation/internalization of TRPV1, might lead to an alleviation of cytoskeleton-dependent mechanical hyperalgesia.

The novel role for TRPV1 in PKCε- and cytoskeleton-dependent mechanical hyperalgesia is indicated in a mechanistic model in Figure 35. There, TRPV1 does not act as a starting- or endpoint of the sensitizing signaling pathway. Instead, TRPV1 functions as an intracellular signaling scaffold: Building a complex with PLC, PKCε and microtubules, TRPV1 regulates the downstream signaling towards mechanical sensitization, while microtubules control the locally restricted signaling of PKCε. To what extent this is a signaling event common to all signaling pathways resulting in PKCε-dependent sensitization has to be investigated.
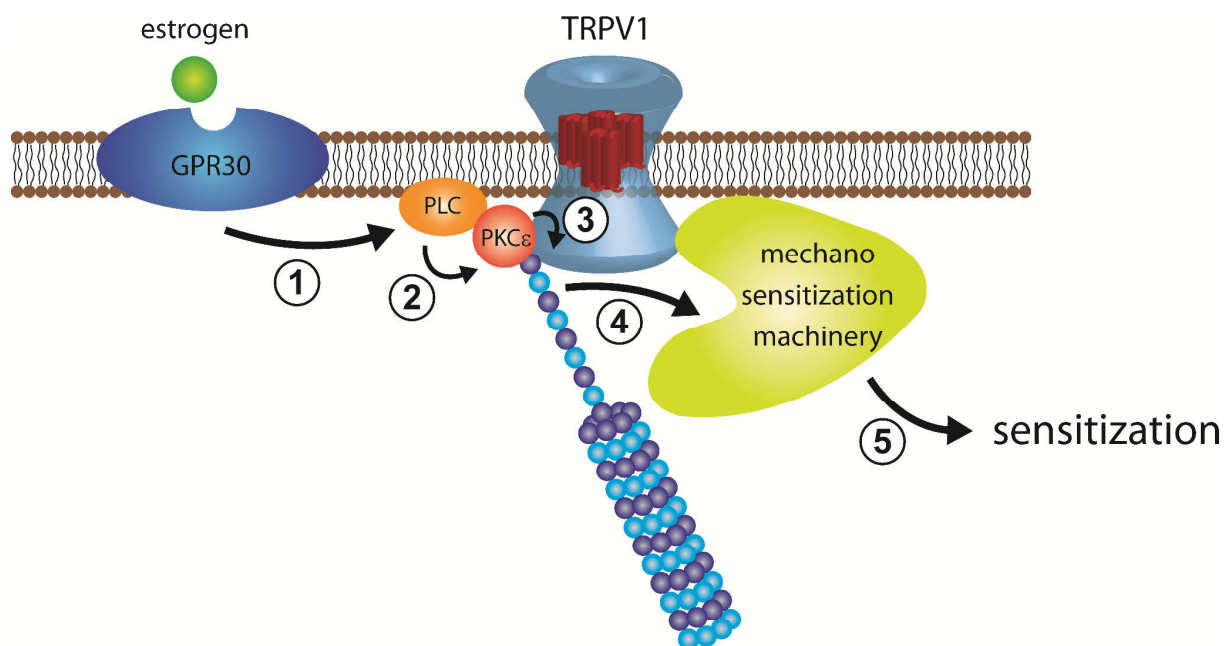
Fig. 35: Mechanistic model of the TRPV1-microtubule complex in PKCε-dependent mechanical sensitization. (1) Activation of a GPCR, i.e. of GPR30, by estrogen or G-1 induces activation of PLC. (2) PLC phosphorylates and thereby activates PKCε, binding to TRPV1 and the microtubule tip. This activation of PKCε initiates the reorganization of the TRPV1-signaling complex. (3) Phosphorylation of the TRPV1-S800 position by PKCε results in the release of the microtubule with bound PKCε from the TRPV1 scaffold. (4) Unbound microtubules allow restricted movement thereby placing PKCε in close vicinity to the so far unknown mechano-sensitization machinery resulting in mechanical hyperalgesia (5).

8.1.5   The dual role of estrogen

In this work, I presented two different effects of estrogen. On one hand, estrogen initiates a PKCε-dependent signaling pathway leading to sensitization. On the other hand, estrogen activates an inhibitory/desensitizing signaling pathway that interferes with successive sensitization signals. Studies in our group identified PKCε as one of the key components in the signal transduction towards sensitization. On the other hand, PKCε activating PLC also induced elevation of intracellular Ca^{2+} levels which seemed to be the central event to mediate an inhibitory signal (Fig. 36). While the sensitizing branch levels off rapidly, activation of the inhibitory branch alters the signaling properties of the cell for more than 20 hours. The inhibitory branch first of all blocks future activation of the PKCε-sensitization branch. Thereby, the signaling history of a cell controls the following signaling by shifting the balance from sensitizing signaling toward the desensitizing signaling branch. This unexpected context-dependence can explain the opposing effects of estrogen detected by us. Acute exposure to estrogen results in PKCε-dependent hyperalgesia. And in longer exposures to estrogen only the inhibitory Ca^{2+} signal remains.

Indeed, behavioral studies corroborate this notion. The β-adrenergic agonist epinephrine induces PKCε-dependent sensitization only in male and not in female rats (Dina et al., 2001b; Hucho et al., 2006). Ablation of estrogen from female rats or supplementation of estrogen to cultured male neurons switches the phenotypes between males and females. According to the model, the

continuous long term presence of estrogen in female rats is on the long run only able to activate the inhibitory branch without activating the PKCε sensitization branch any more and thereby ablating PKCε from isoproterenol-induced sensitization.

In behavioral experiments estrogen influences not only PKCε-, but also PKA signaling (Dina et al., 2001b) . In absence of estrogen, epinephrine-induced sensitization is mediated by PKCε, PKA and ERK. In presence of estrogen, only ERK contributes to epinephrine-induced hyperalgesia, while PKCε and PKA are not involved (Dina et al., 2001b). Two scenarios are possible to explain this observation: First, the described inhibitory pathway not only controls future PKCε signaling but also inhibits PKA-dependent signaling, indicating a cross talk between PKCε and PKA signaling in nociceptive neurons. Second, estrogen could activate an independent signaling event that in turn specifically controls following PKA signaling. Which signaling mechanism is indeed responsible for this effect, has to be analyzed in future.
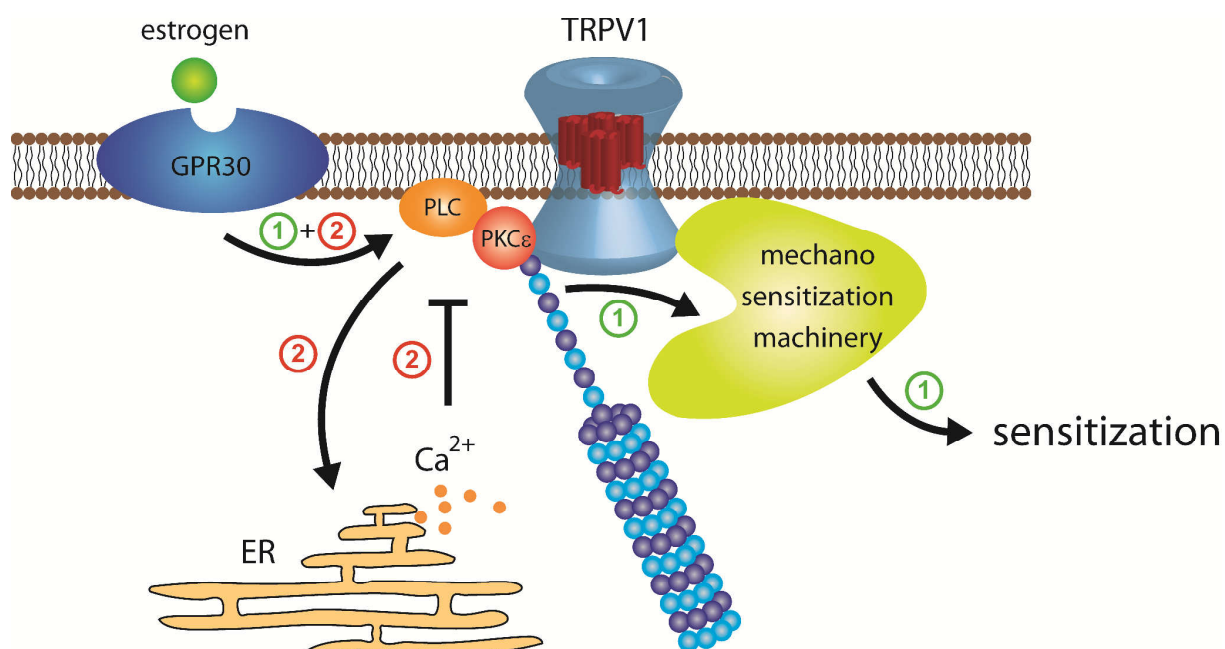

Fig. 36: Estrogen induces sensitizing as well as desensitizing signaling in nociceptive neurons. Estrogen has two opposing effects on nociceptive signaling: (1) Estrogen induces mechanical sensitization by rapidly activating a PKCε-TRPV1-microtubule-signaling pathway. (2) Estrogen inhibits PKCε-mediated sensitization in a Ca^{2+}-dependent manner. The sensitizing signaling is a short-term effect induced by high estrogen levels, while activation of the inhibitory signaling pathway inhibits long-lastingly PKCε signaling in nociceptive neurons.

8.2 Novel perspectives

8.2.1 Estrogen beyond gender: The peripheral nervous system as a target for estrogen

Estrogen is the prototypic female sex hormone. Nevertheless, there is now increasing evidence for the involvement of estrogen into multiple cellular processes far beyond its classical function as a female specific transcription-initiating sex hormone. Much of the conceptual change is driven by novel insight into the role of estrogen on neurons in the central nervous system of males and females. Several models show neuroprotective effects of estrogen in the brain and in the spinal cord (Chaovipoch et al., 2006; Dominguez et al., 2009; Yi and Simpkins, 2008; Zhang et al., 2008). Estrogen was found to be involved in memory functions (Rodgers et al., 2010; Smith et al., 2009), to modulate synaptic structures, and to influence neuronal development (Hojo et al., 2008; McCarthy et al., 2008; Schwarz et al., 2008; Srivastava et al., 2008). Classical ERs as well as membrane ERs including GPR30 mediate these estrogen functions. Finding now that estrogen rapidly initiates signaling in primary sensory neurons establishes the PNS similar to the CNS as a target of "non-classical" estrogen signaling cascades. To what extend estrogen is, similar to the CNS, involved in neuroprotection or synaptic remodeling in the PNS, has therefore to be examined.

PKCs among others contribute to the transduction of estrogen signals (Dewing et al., 2008; Jung et al., 2005; Setalo et al., 2005). Inspiring is a report from Sétáló et al. who in neocoritcal explants described estrogen-induced translocation of PKCε to the plasma membrane which in turn results in ERK phosphorylation. My results show a similar estrogen-induced PKCε translocation also in peripheral nociceptive neurons. Thus, estrogen signaling involves, at least in part, the same second messenger in the CNS and in the PNS. If also PKCε-dependent ERK phosphorylation can be found in peripheral nociceptive neurons, will have to be investigated. This would be of considerable interest, as also ERK is a known second messenger involved in peripheral nociceptor sensitization.

8.2.2 Estrogen: an inflammatory mediator in the peripheral nervous system?

In my paradigm, sudden local increases of estrogen concentration were assumed. What is a potential physiological correlate of this? Estrogen levels around 10-fold above basal plasma estrogen concentrations are described to induce mechanical sensitization similar to inflammatory mediators such as epinephrine or PGE2 (Hucho et al., 2006), while basal estrogen levels did not effect pain thresholds. The identified signaling mechanism resembles signaling induced by the β-adrenergic agonist epinephrine which is investigated in the context of inflammatory pain sensitization. Recently, Schaffer et al. reported the increase of estrogen production in DRG neurons during inflammation accompanied by a reduction of pain thresholds (Schaeffer et al.,

2010). Also in other pain models estrogen mimicked the effects of inflammation. Flake et al. showed that estrogen increased the excitability of TMJ neurons similar to Complete Freud's Adjuvant by decreasing the action potential threshold and increasing spontaneous activity (Flake et al., 2005), indicating that estrogen indeed mediates inflammatory signals in nociceptive neurons. These findings suggest that locally produced estrogen could act as a novel mediator for inflammation mediating the sensitizing effect by activating a common nociceptive signaling mechanism in primary sensory neurons.

To understand the complex system of estrogen actions on nociceptive signaling, it is necessary to analyze both functions in more detail; its role as a female sex hormone which modulates signaling pathways already at basal plasma concentrations, and its function as a nociceptive stimulus during inflammation.

8.2.3   Clinical implications

Showing a signaling mechanism by which estrogen and GPR30 agonists induce mechanical sensitization is of therapeutic interest. Anti-estrogens and GPR30 agonists such as tamoxifen or fulvestrant (ICI 182,780) are commonly used as chemotherapeutic drugs in breast cancer therapy. One severe side effect in ~20 % of fulvestrant-treated patients is long-lasting pain (Vergote and Abram, 2006). The identification that GPR30 agonists induce mechanical sensitization and that this signaling pathway involves TRPV1 and the microtubule cytoskeleton opens new perspectives for a therapeutic approach. Based on these findings it would be interesting to examine if fulvestrant-induced pain is dependent on TRPV1. If so, TRPV1 would potentially allow nociceptor subgroup-specific treatment. Low level capsaicin exposure followed by TRPV1 downregulation would be one approach suggested by my results. Alternatively, recently the transfer of analgesics through the ion channel pore of TRPV1 has been described for the lidocaine derivative QX-314 (Binshtok et al., 2007). Moreover, it would be interesting to further characterize the role of microtubules in fulvestrant-induced sensitization. Is the microtubule destabilization indeed responsible for sensitization during fulvestrant therapy? And if so, would an interruption of the TRPV1-microtubule complex prevent fulvestrant-induced peripheral neuropathies as suggested by the behavioral results shown here?

Besides GPR30 agonists such as fulvestrant, also the microtubule stabilizer Taxol and Taxol-derivates are widely used for the treatment of cancer patients. But their therapeutic benefit is limited greatly again by the induction of long-lasting mechanical sensitization (Canta et al., 2009). In behavioral experiments shown in the results section, the disruption of the TRPV1-mcirotubule interaction by downregulation of TRPV1 abolished mechanical sensitization in presence of Taxol. Therefore, an ablation of TRPV1 or the disruption of the TRPV1-microtubule complex, i.e. by inhibitory peptides or small molecules, may prevent the development of mechanical hyperalgesia in patients undergoing Taxol-based chemotherapy.

Beyond therapy-induced pain, the identification of an endogenous inhibitory/desensitizing mechanism as presented here opens new perspectives for the development of conceptual novel

analgesics. So far, analgesics mostly act by reducing inflammatory mediators (COX-inhibitors) or through the reduction of intracellular cAMP (opioids). The inhibitory signaling pathway described here is located in the periphery and its activation blocks PKCε-dependent nociceptive signaling for more than 20 h. Therefore activation of this inhibitory/desensitizing pathway could be a novel strategy for therapeutic intervention.

8.2.4   A modular concept for signal transduction in nociceptive neurons

A large variety of signaling mediators act on primary sensory neurons and activate multiple intracellular signaling pathways resulting in sensitization. As indicated in the introduction, the activated intracellular signaling pathways are still not investigated in depth. Mostly, only single signaling components instead of full signaling cascades are known. Nevertheless, there is a general mechanistic question to be answered: Do these signaling pathways act in parallel and result in the modification of distinct effector molecules that mediate sensitization? Or is (are) there one or multiple convergence point(s) for these signaling pathways leading to the activation of key sensitizing module (Hucho and Levine, 2007)? The latter would ask for the concept of signaling modules which can be added to various inputs such as activation of different membrane receptors. The existence of nociceptive modules would be of tremendous therapeutic interest. As a drug target such a module would be suitable in a range of different pain phenotypes. And indeed, this work provides considerable support for the notion of "nociceptive modules".

My data present evidence for convergent signaling pathways leading to PKCε-dependent mechanical sensitization. The comparison of signaling events underlying estrogen- and isoproterenol-induced sensitization indicates a convergence point downstream of the receptor. Estrogen and isoproterenol activate, most likely, different G-protein coupled receptors which in turn lead to the activation of adenylyl cyclase. In both cases, this activation causes the translocation of PKCε to the plasma membrane and results in PKCε-dependent mechanical hyperalgesia. Thus, these signaling components establish one such "nociceptive module" (Fig. 37). To what extend this module can be activated also by other stimuli than estrogen and isoproterenol has to be investigated.

Beyond signaling leading to the activation of PKCε are there also downstream components belonging to this nociceptive module? I found that estrogen- and isoproterenol-induced mechanical sensitization involve the microtubule cytoskeleton (Dina et al., 2003) potentially through PKCε-mediated changes of the TRPV1-microtubule interaction. This is highly suggestive to enlarge the nociceptive module by two more components, TRPV1 and the microtubule cytoskeleton. But if these two novel components are essential for PKCε-dependent sensitization, has to be investigated.

The recent results from Tim Hucho's laboratory including the one presented in this work indicate the existence not only of sensitizing but also of desensitizing nociceptive modules. Also in the desensitizing signaling pathway described here, convergence of estrogen and isoproterenol is apparent as both substances result in the increase of intracellular Ca^{2+} levels. Interestingly, this

inhibitory signaling module could be separated from the sensitizing signaling cascade. The stimulation of intracellular Ca^{2+} release also by other means such as ATP-receptor activation and/or pharmacological activation of intracellular calcium channels (data not shown) activated the inhibitory/desensitizing signaling pathway without inducing sensitization. What further components belong to this module and under which conditions it is activated endogenously or exogenously, will be investigated in the near future.

Thus, the data presented here suggest a modular signaling structure in primary sensory neurons controlling mechanical sensitization. The activation of nociceptive/sensitizing and inhibitory/desensitizing modules by different extracellular and intracellular mediators thereby determines the physiological effect. If indeed all sensitizing signaling pathways converge in the activation of a key sensitizing module or if sensitization is mediated by different sensitizing modules, has to be analyzed in future. The concept of common signaling modules opens a new perspective onto signaling mechanisms in nociceptive neurons. Thereby it might help to understand more complex pain models, where multiple extracellular and intracellular mediators act simultaneously and successively on a nociceptive neuron.
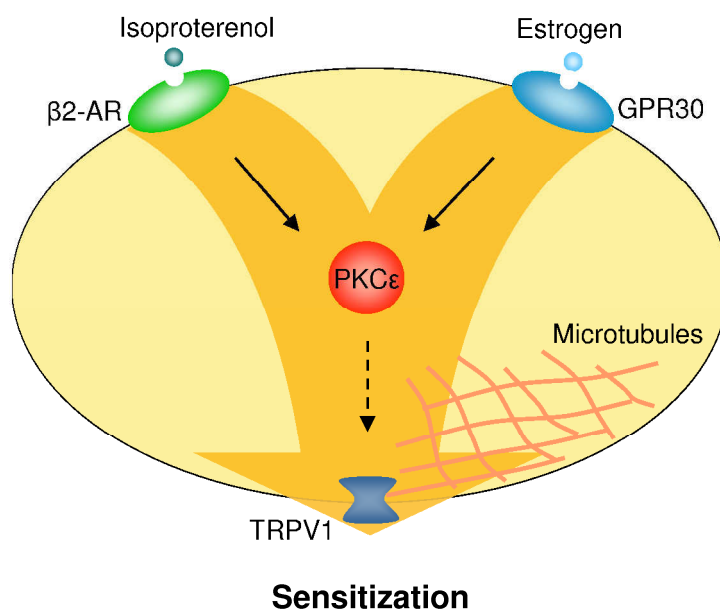

Sensitization

Fig. 37: Convergent signaling towards PKCε-dependent sensitization. The β-adrenergic agonist isoproterenol as well as the steroid hormone estrogen activate GPCR signaling in nociceptive neurons. Both signaling pathways lead to the activation of PKCε in nociceptive neurons and result in PKCε- and microtubule-dependent mechanical sensitization. This convergent signaling suggests a common nociceptive module mediating mechanical sensitization.

8.2.5 Conclusion

In this thesis I showed that the steroid hormone estrogen acts directly on the primary nociceptive neuron. Characterization of estrogen signaling led to the description of a novel signaling pathway in primary nociceptive neurons. Thereby the TRPV1-microtubule complex was identified as a new downstream target of PKCε signaling in PKCε-dependent mechanical sensitization. The identified inhibitory/desensitizing module shows a new grade of complexity for signaling mechanisms underlying pain sensitization as it indicates the integration of multiple signaling inputs already in the primary nociceptive neuron.

These findings open novel aspects for pain therapy, for gender differences in pain disorders as well as for the treatment of cancer therapy-induced pain. It highlights the importance of short term production of estrogen during inflammation and the influence of estrogen on other sensitizing inflammatory mediators. It will be interesting to analyze local estrogen production during inflammation to further understand the function of estrogen in inflammation and its influence on inflammatory pain.

9 References

Acconica, F., Barnes, C. J. and Kumar, R. (2006) Estrogen and Tamoxifen Induce Cytoskeletal Remodeling and Migration in Endometrial Cancer Cells. *Endocrinology* **147,** 1203-1212.

Akhmanova, A. and Steinmetz, M. O. (2008) Tracking the ends: a dynamic protein network controls the fate of microtubule tips. *Nature Reviews* **9**.

Akopian, A. N., Souslova, V., England, S., Okuse, K., Ogata, N., Ure, J., Smith, A., Kerr, B. J., McMahon, S. B., Boyce, S., Hill, R., Stanfa, L. C., Dickenson, A. H. and Wood, J. N. (1999) The tetrodotoxin-resistant sodium channel SNS has a specialized function in pain pathways. *Nat Neurosci* **2,** 541-8.

Albanito, L., Madeo, A., Lappano, R., Vivacqua, A., Rago, V., Carpino, A., Oprea, T. I., Prossnitz, E. R., Musti, A. M., Ando, S. and Maggiolini, M. (2007) G protein-coupled receptor 30 (GPR30) mediates gene expression changes and growth response to 17 beta-estradiol and selective GPR30 ligand G-1 in ovarian cancer cells. *Cancer Research* **67,** 1859-1866.

Alessandri-Haber, N., Yeh, J. J., Boyd, A. E., Parada, C. A., Chen, X. J., Reichling, D. B. and Levine, J. D. (2003) Hypotonicity induces TRPV4-mediated nociception in rat. *Neuron* **39,** 497-511.

Alessandri-Haber, N., Dina, O. A., Yeh, J. J., Parada, C. A., Reichling, D. B. and Levine, J. D. (2004) Transient receptor potential vanilloid 4 is essential in chemotherapy-induced neuropathic pain in the rat (pg 4444, vol 24, 2004). *Journal of Neuroscience* **24,** 5457-5457.

Aley, K. O., McCarter, G. and Levine, J. D. (1998) Nitric oxide signaling in pain and nociceptor sensitization in the rat. *Journal of Neuroscience* **18,** 7008-7014.

Aley, K. O. and Levine, J. D. (1999) Role of protein kinase A in the maintenance of inflammatory pain. *Journal of Neuroscience* **19,** 2181-2186.

Aley, K. O., Messing, R. O., Mochly-Rosen, D. and Levine, J. D. (2000) Chronic hypersensitivity for inflammatory nociceptor sensitization mediated by the epsilon isozyme of protein kinase C. *Journal of Neuroscience* **20,** 4680-4685.

Aloisi, A. M., Pari, G., Ceccarelli, I., Vecchi, I., Ietta, F., Lodi, L. and Paulesu, L. (2005) Gender-related effects of chronic non-malignant pain and opioid therapy on plasma levels of macrophage migration inhibitory factor (MIF). *Pain* **115,** 142-51.

Aloisi, A. M., Bachiocco, V., Costantino, A., Stefani, R., Ceccarelli, I., Bertaccini, A. and Meriggiola, M. C. (2007) Cross-sex hormone administration changes pain in transsexual women and men. *Pain* **132,** 60-67.

Aloisi, A. M., Affaitati, G., Ceccarelli, I., Fiorenzani, P., Lerza, R., Rossi, C., Pace, M. C., Chiefari, M., Aurilio, C. and Giamberardino, M. A. (2009) Estradiol and testosterone differently affect visceral pain-related behavioural responses in male and female rats. *Eur J Pain*.

Alzamora, R., Brown, L. R. and Harvey, B. J. (2007) Direct Binding and Activation of Protein Kinase C Isoforms by Aldosterone and 17{beta}-Estradiol. *Mol Endocrinol*.

Amadesi, S., Nie, J., Vergnolle, N., Cottrell, G. S., Grady, E. F., Trevisani, M., Manni, C., Geppetti, P., McRoberts, J. A., Ennes, H., Davis, J. B., Mayer, E. A. and Bunnett, N. W. (2004) Protease-activated receptor 2 sensitizes the capsaicin receptor transient receptor potential vanilloid receptor 1 to induce hyperalgesia. *J Neurosci* **24,** 4300-12.

Ansonoff, M. A. and Etgen, A. M. (1998) Estradiol elevates protein kinase C catalytic activity in the preoptic area of female rats. *Endocrinology* **139,** 3050-6.

Basbaum, A. I. and Jessell, T. M. (2000) Principles of Neuroscience, (eds. E. R. Kandel, J. H. Schwartz and T. M. Jessell), pp. 472-491.

Basbaum, A. I., Bautista, D. M., Scherrer, G. and Julius, D. (2009) Cellular and Molecular Mechanisms of Pain. *Cell* **139**.

Bennett, H. L., Gustafsson, J. A. and Keast, J. R. (2003) Estrogen receptor expression in lumbosacral dorsal root ganglion cells innervating the female rat urinary bladder. *Auton Neurosci* **105,** 90-100.

Bereiter, D. A., Cioffi, J. L. and Bereiter, D. F. (2005) Oestrogen receptor-immunoreactive neurons in the trigeminal sensory system of male and cycling female rats. *Arch Oral Biol* **50,** 971-9.

Berkley, K. J. (1997) Sex differences in pain. *Behav.Brain Sci.* **20,** 371-380.

Bhave, G., Zhu, W., Wang, H., Brasier, D. J., Oxford, G. S. and Gereau, R. W. t. (2002) cAMP-dependent protein kinase regulates desensitization of the capsaicin receptor (VR1) by direct phosphorylation. *Neuron* **35,** 721-31.

Bhave, G., Hu, H. J., Glauner, K. S., Zhu, W., Wang, H., Brasier, D. J., Oxford, G. S. and Gereau, R. W. t. (2003) Protein kinase C phosphorylation sensitizes but does not activate the capsaicin receptor transient receptor potential vanilloid 1 (TRPV1). *Proc Natl Acad Sci U S A* **100,** 12480-5.

Binshtok, A. M., Bean, B. P. and Woolf, C. J. (2007) Inhibition of nociceptors by TRPV1-meidated entry of impermeant sodium channel blockers. *Nature* **449**.

Bogen, O., Dreger, M., Gillen, C., Schroder, W. and Hucho, F. (2005) Identification of versican as an isolectin B4-binding glycoprotein from mammalian spinal cord tissue. *Febs J* **272,** 1090-102.

Bolcskei, K., Helyes, Z., Szabo, A., Sandor, K., Elekes, K., Nemeth, J., Almasi, R., Pinter, E., Petho, G. and Szolcsanyi, J. (2005) Investigation of the role of TRPV1 receptors in acute and chronic nociceptive processes using gene-deficient mice. *Pain* **117,** 368-76.

Bollimuntha, S., Cornatzer, E. and Singh, B. B. (2005) Plasma membrane localization and function of TRPC1 is dependent on its interaction with beta-tubulin in retinal epithelium cells. *Vis Neurosci* **22,** 163-70.

Bologa, C. G., Revankar, C. M., Young, S. M., Edwards, B. S., Arterburn, J. B., Kiselyov, A. S., Parker, M. A., Tkachenko, S. E., Savchuck, N. P., Sklar, L. A., Oprea, T. I. and Prossnitz, E. R. (2006) Virtual and biomolecular screening converge on a selective agonist for GPR30. *Nature Chemical Biology* **2,** 207-212.

Boulware, M. I., Weick, J. P., Becklund, B. R., Kuo, S. P., Groth, R. D. and Mermelstein, P. G. (2005) Estradiol activates group I and II metabotropic glutamate receptor signaling, leading to opposing influences on cAMP response element-binding protein. *J Neurosci* **25,** 5066-78.

Brailoiu, E., Dun, S. L., Brailoiu, G. C., Mizuo, K., Sklar, L. A., Oprea, T. I., Prossnitz, E. R. and Dun, N. J. (2007) Distribution and characterization of estrogen receptor G protein-coupled receptor 30 in the rat central nervous system. *Journal of Endocrinology* **193,** 311-321.

Bulun, S. E. (2000) Aromatase deficiency and estrogen resistance: from molecular genetics to clinic. *Semin Reprod Med* **18,** 31-9.

Burgess, G. M., Mullaney, I., McNeill, M., Coote, P. R., Minhas, A. and Wood, J. N. (1989a) Activation of guanylate cyclase by bradykinin in rat sensory neurones is mediated by calcium influx: possible role of the increase in cyclic GMP. *J Neurochem* **53,** 1212-8.

Burgess, G. M., Mullaney, I., McNeill, M., Dunn, P. M. and Rang, H. P. (1989b) Second messengers involved in the mechanism of action of bradykinin in sensory neurons in culture. *J Neurosci* **9,** 3314-25.

Canta, A., Chiorazzi, A. and Cavaletti, G. (2009) Tubulin: a target for antineoplastic drugs into the cancer cells but also in the peripheral nervous system. *Curr Med Chem* **16,** 1315-24.

Carani, C., Qin, K., Simoni, M., Faustini-Fustini, M., Serpente, S., Boyd, J., Korach, K. S. and Simpson, E. R. (1997) Effect of testosterone and estradiol in a man with aromatase deficiency. *N Engl J Med* **337,** 91-5.

Carmeci, C., Thompson, D. A., Ring, H. Z., Francke, U. and Weigel, R. J. (1997) Identification of a gene (GPR30) with homology to the G-protein-coupled receptor superfamily associated with estrogen receptor expression in breast cancer. *Genomics* **45,** 607-17.

Castro-Rivera, E., Samudio, I. and Safe, S. (2001) Estrogen regulation of cyclin D1 gene expression in ZR-75 breast cancer cells involves multiple enhancer elements. *J Biol Chem* **276,** 30853-61.

Caterina, M. J., Schumacher, M. A., Tominaga, M., Rosen, T. A., Levine, J. D. and Julius, D. (1997) The capsaicin receptor: a heat-activated ion channel in the pain pathway. *Nature* **389,** 816-824.

Caterina, M. J., Leffler, A., Malmberg, A. B., Martin, W. J., Trafton, J., Petersen-Zeitz, K. R., Koltzenburg, M., Basbaum, A. I. and Julius, D. (2000) Impaired nociception and pain sensation in mice lacking the capsaicin receptor. *Science* **288,** 306-313.

Cesare, P., Dekker, L. V., Sardini, A., Parker, P. J. and McNaughton, P. A. (1999) Specific involvement of PKC-epsilon in sensitization of the neuronal response to painful heat. *Neuron* **23,** 617-24.

Chaban, V. V. and Micevych, P. E. (2005) Estrogen receptor-alpha mediates estradiol attenuation of ATP-induced Ca2+ signaling in mouse dorsal root ganglion neurons. *J Neurosci Res* **81,** 31-7.

Chaovipoch, P., Jelks, K. A., Gerhold, L. M., West, E. J., Chongthammakun, S. and Floyd, C. L. (2006) 17beta-estradiol is protective in spinal cord injury in post- and pre-menopausal rats. *J Neurotrauma* **23,** 830-52.

Chen, X. and Levine, J. D. (1999) NOS inhibitor antagonism of PGE2-induced mechanical sensitization of cutaneous C-fiber nociceptors in the rat. *J Neurophysiol* **81,** 963-6.

Chen, Y., Lai, M., Maeno-Hikichi, Y. and Zhang, J. F. (2006) Essential role of the LIM domain in the formation of the PKCepsilon-ENH-N-type Ca2+ channel complex. *Cell Signal* **18,** 215-24.

Chesterton, L. S., Barlas, P., Foster, N. E., Baxter, G. D. and Wright, C. C. (2003) Gender differences in pressure pain threshold in healthy humans. *Pain* **101,** 259-66.

Christoph, T., Grunweller, A., Mika, J., Schafer, M. K., Wade, E. J., Weihe, E., Erdmann, V. A., Frank, R., Gillen, C. and Kurreck, J. (2006) Silencing of vanilloid receptor TRPV1 by RNAi reduces neuropathic and visceral pain in vivo. *Biochem Biophys Res Commun* **350,** 238-43.

Chuang, H. H., Prescott, E. D., Kong, H., Shields, S., Jordt, S. E., Basbaum, A. I., Chao, M. V. and Julius, D. (2001) Bradykinin and nerve growth factor release the capsaicin receptor from PtdIns(4,5)P2-mediated inhibition. *Nature* **411,** 957-962.

Clapham, D. E. (2003) TRP channels as cellular sensors. *Nature* **426,** 517-24.

Cornil, C. A., Ball, G. F. and Balthazart, J. (2006) Functional significance of the rapid regulation of brain estrogen action: Where do the estrogens come from? *Brain Research* **1126**.

Coyle, D. E., Sehlhorst, C. S. and Behbehani, M. M. (1996) Intact female rats are more susceptible to the development of tactile allodynia than ovariectomized female rats following partial sciatic nerve ligation (PSNL). *Neurosci Lett* **203,** 37-40.

Craft, R. M., Mogil, J. S. and Aloisi, A. M. (2004) Sex differences in pain and analgesia: the role of gonadal hormones. *European Journal of Pain* **8,** 397-411.

Craft, R. M. (2007) Modulation of pain by estrogens. *Pain* **132 Suppl 1,** S3-12.

Creppy, E. E., Richeux, F., Carratu, M. R., Cuomo, V., Cochereau, C., Ennamany, R. and Saboureau, D. (2000) Cytotoxicity of capsaicin in monkey kidney cells: lack of antagonistic effects of capsazepine and Ruthenium red. *Arch Toxicol* **74,** 40-7.

Damann, N., Voets, T. and Nilius, B. (2008) TRPs in our senses. *Curr Biol* **18,** R880-9.

Dewing, P., Christensen, A., Bondar, G. and Micevych, P. (2008) Protein kinase C signaling in the hypothalamic arcuate nucleus regulates sexual receptivity in female rats. *Endocrinology* **149,** 5934-42.

Dina, O. A., Barletta, J., Chen, X., Mutero, A., Martin, A., Messing, R. O. and Levine, J. D. (2000) Key role for the epsilon isoform of protein kinase C in painful alcoholic neuropathy in the rat. *J Neurosci* **20,** 8614-9.

Dina, O. A., Chen, X., Reichling, D. and Levine, J. D. (2001a) Role of protein kinase C epsilon and protein kinase A in a model of paclitaxel-induced painful peripheral neuropathy in the rat. *Neuroscience* **108,** 507-515.

Dina, O. A., Aley, K. O., Isenberg, W., Messing, R. O. and Levine, J. D. (2001b) Sex hormones regulate the contribution of PKC epsilon and PKA signalling in inflammatory pain in the rat. *European Journal of Neuroscience* **13,** 2227-2233.

Dina, O. A., McCarter, G. C., de Coupade, C. and Levine, J. D. (2003) Role of the sensory neuron cytoskeleton in second messenger signaling for inflammatory pain. *Neuron* **39,** 613-624.

Dina, O. A., Parada, C. A., Yeh, J., Chen, X. J., McCarter, G. C. and Levine, J. D. (2004) Integrin signaling in inflammatory and neuropathic pain in the rat. *European Journal of Neuroscience* **19,** 634-642.

Dina, O. A., Hucho, T., Yeh, J., Malik-Hall, M., Reichling, D. B. and Levine, J. D. (2005) Primary afferent second messenger cascades interact with specific integrin subunits in producing inflammatory hyperalgesia. *Pain* **115,** 191-203.

Dominguez, R., Hu, E., Zhou, M. and Baudry, M. (2009) 17beta-estradiol-mediated neuroprotection and ERK activation require a pertussis toxin-sensitive mechanism involving GRK2 and beta-arrestin-1. *J Neurosci* **29,** 4228-38.

Edwards, D. P. (2005) Regulation of signal transduction pathways by estrogen and progesterone. *Annu Rev Physiol* **67,** 335-76.

Evrard, H. C. and Balthazart, J. (2002) Localization of Oestrogen Receptors in the Sensory and Motor Areas of the Spinal Cord in Japanese Quail (Coturnix japonica). *J Neuroendocrinol* **14,** 894-903.

Evrard, H. C. and Balthazart, J. (2004) Rapid Regulation of Pain by Estrogens Synthesized in Spinal Dorsal Horn Neurons. *The Journal of Neuroscience* **24,** 7225-7229.

Evrard, H. C. (2006) Estrogen synthesis in the spinal dorsal horn: a new central mechanism for the hormonal regulation of pain. *Am J Physiol Regul Integr Comp Physiol* **291,** R291-9.

Fehrenbacher, J. C., Loverme, J., Clarke, W., Hargreaves, K. M., Piomelli, D. and Taylor, B. K. (2009) Rapid pain modulation with nuclear receptor ligands. *Brain Res Rev* **60,** 114-24.

Feng, Y. and Gregor, P. (1997) Cloning of a novel member of the G protein-coupled receptor family related to peptide receptors. *Biochem Biophys Res Commun* **231,** 651-4.

Fernandez-Ballester, G. and Ferrer-Montiel, A. (2008) Molecular modeling of the full-length human TRPV1 channel in closed and desensitized states. *Journal of Membrane Biology* **223,** 161-172.

Ferreira, S. H., Lorenzetti, B. B. and De Campos, D. I. (1990) Induction, blockade and restoration of a persistent hypersensitive state. *Pain* **42,** 365-71.

Filardo, E. J., Quinn, J. A., Bland, K. I. and Frackelton, A. R. (2000) Estrogen-induced activation of Erk-1 and Erk-2 requires the G protein-coupled receptor homolog, GPR30, and occurs via trans-activation of the epidermal growth factor receptor through release of HB-EGF. *Molecular Endocrinology* **14,** 1649-1660.

Filardo, E. J. (2002) Epidermal growth factor receptor (EGFR) transactivation by estrogen via the G-protein-coupled receptor, GPR30: a novel signaling pathway with potential significance for breast cancer. *Journal of Steroid Biochemistry and Molecular Biology* **80,** 231-238.

Filardo, E. J., Quinn, J. A., Frackelton, A. R. and Bland, K. I. (2002) Estrogen action via the G protein-coupled receptor, GPR30: Stimulation of adenylyl cyclase and cAMP-mediated attenuation of the epidermal growth factor receptor-to-MAPK signaling axis. *Molecular Endocrinology* **16,** 70-84.

Fillingim, R. B. and Ness, T. J. (2000) Sex-related hormonal influences on pain and analgesic responses. *Neurosci.Biobehav.Rev.* **24,** 485-501.

Fitzgerald, E. M., Okuse, K., Wood, J. N., Dolphin, A. C. and Moss, S. J. (1999) cAMP-dependent phosphorylation of the tetrodotoxin-resistant voltage-dependent sodium channel SNS. *J Physiol* **516 (Pt 2),** 433-46.

Flake, N. M., Bonebreak, D. B. and Gold, M. S. (2005) Estrogen and inflammation increase the excitability of rat temporomandibular joint afferent neurons. *J Neurophysiol* **93,** 1585-97.

Frot, M., Feine, J. S. and Bushnell, M. C. (2004) Sex differences in pain perception and anxiety. A psychophysical study with topical capsaicin. *Pain* **108,** 230-6.

Fujimoto, S. and Mori, M. (2004) Characterization of capsaicin-induced, capsazepine-insensitive relaxation of ileal smooth muscle of rats. *Eur J Pharmacol* **487,** 175-82.

Fujimoto, S., Mori, M., Tsushima, H. and Kunimatsu, M. (2006) Capsaicin-induced, capsazepine-insensitive relaxation of the guinea-pig ileum. *Eur J Pharmacol* **530,** 144-51.

Gaub, M. P., Bellard, M., Scheuer, I., Chambon, P. and Sassone-Corsi, P. (1990) Activation of the ovalbumin gene by the estrogen receptor involves the fos-jun complex. *Cell* **63,** 1267-76.

Gether, U. (2000) Uncovering molecular mechanisms involved in activation of G protein-coupled receptors. *Endocr Rev* **21,** 90-113.

Goel, M., Sinkins, W., Keightley, A., Kinter, M. and Schilling, W. P. (2005) Proteomic analysis of TRPC5- and TRPC6-binding partners reveals interaction with the plasmalemmal Na(+)/K(+)-ATPase. *Pflugers Arch* **451,** 87-98.

Gold, M. S., Levine, J. D. and Correa, A. M. (1998) Modulation of TTX-R INa by PKC and PKA and their role in PGE2-induced sensitization of rat sensory neurons in vitro. *J Neurosci* **18,** 10345-55.

Goswami, C., Dreger, M., Jahnel, R., Bogen, O., Gillen, C. and Hucho, F. (2004) Identification and characterization of a Ca2+-sensitive interaction of the vanilloid receptor TRPV1 with tubulin. *Journal of Neurochemistry* **91,** 1092-1103.

Goswami, C., Dreger, M., Otto, H., Schwappach, B. and Hucho, F. (2006) Rapid disassembly of dynamic microtubules upon activation of the capsaicin receptor TRPV1. *Journal of Neurochemistry* **96,** 254-266.

Goswami, C., Schmidt, H. and Hucho, F. (2007a) TRPV1 at nerve endings regulates growth cone morphology and movement through cytoskeleton reorganization. *Febs Journal* **274,** 760-772.

Goswami, C. and Hucho, T. (2007) TRPV1 expression-dependent initiation and regulation of filopodia. *Journal of Neurochemistry* **103,** 1319-1333.

Goswami, C., Hucho, T. B. and Hucho, F. (2007b) Identification and characterisation of novel tubulin-binding motifs located within the C-terminus of TRPV1. *Journal of Neurochemistry* **101,** 250-262.

Gottlicher, M., Heck, S. and Herrlich, P. (1998) Transcriptional cross-talk, the second mode of steroid hormone receptor action. *J Mol Med* **76,** 480-9.

Grigoriev, I., Gouveia, S. M., van der Vaart, B., Demmers, J., Smyth, J. T., Honnappa, S., Splinter, D., Steinmetz, M. O., Putney, J. W., Jr., Hoogenraad, C. C. and Akhmanova, A. (2008) STIM1 is a MT-plus-end-tracking protein involved in remodeling of the ER. *Curr Biol* **18,** 177-82.

Gu, Q. and Moss, R. L. (1996) 17 beta-Estradiol potentiates kainate-induced currents via activation of the cAMP cascade. *J Neurosci* **16,** 3620-9.

Gu, Q., Korach, K. S. and Moss, R. L. (1999) Rapid action of 17beta-estradiol on kainate-induced currents in hippocampal neurons lacking intracellular estrogen receptors. *Endocrinology* **140,** 660-6.

Guerois, R., Nielsen, J. E. and Serrano, L. (2002) Predicting changes in the stability of proteins and protein complexes: a study of more than 1000 mutations. *J Mol Biol* **320,** 369-87.

Guex, N. and Peitsch, M. C. (1997) SWISS-MODEL and the Swiss-PdbViewer: an environment for comparative protein modeling. *Electrophoresis* **18,** 2714-23.

Hapidou, E. G. and Rollman, G. B. (1998) Menstrual cycle modulation of tender points. *Pain* **77,** 151-61.

Hellwig, N., Albrecht, N., Harteneck, C., Schultz, G. and Schaefer, M. (2005) Homo- and heteromeric assembly of TRPV channel subunits. *J Cell Sci* **118,** 917-28.

Ho, K. J. and Liao, J. K. (2002a) Non-nuclear actions of estrogen: new targets for prevention and treatment of cardiovascular disease. *Mol Interv* **2,** 219-28.

Ho, K. J. and Liao, J. K. (2002b) Nonnuclear actions of estrogen. *Arterioscler Thromb Vasc Biol* **22,** 1952-61.

Hojo, Y., Murakami, G., Mukai, H., Higo, S., Hatanaka, Y., Ogiue-Ikeda, M., Ishii, H., Kimoto, T. and Kawato, S. (2008) Estrogen synthesis in the brain--role in synaptic plasticity and memory. *Mol Cell Endocrinol* **290,** 31-43.

Honnappa, S., Gouveia, S. M., Weisbrich, A., Damberger, F. F., Bhavesh, N. S., Jawhari, H., Grigoriev, I., van Rijssel, F. J., Buey, R. M., Lawera, A., Jelesarov, I., Winkler, F. K., Wuthrich, K., Akhmanova, A. and Steinmetz, M. O. (2009) An EB1-binding motif acts as a microtubule tip localization signal. *Cell* **138,** 366-76.

Hucho, T., Dina, O. A. and Levine, J. D. (2005) Epac mediates a cAMP-to-PKC signaling in inflammatory pain: an isolectin B4(+) neuron-specific mechanism. *J Neurosci* **25,** 6119-26.

Hucho, T., Dina, O. A., Kuhn, J. and Levine, J. D. (2006) Estrogen controls PKC epsilon-dependent mechanical hyperalgesia through direct action on nociceptive neurons. *European Journal of Neuroscience* **24,** 527-534.

Hucho, T. and Levine, J. D. (2007) Signaling pathways in sensitization: Toward a nociceptor cell biology. *Neuron* **55,** 365-376.

Iwasaki, Y., Morita, A., Iwasawa, T., Kobata, K., Sekiwa, Y., Morimitsu, Y., Kubota, K. and Watanabe, T. (2006) A nonpungent component of steamed ginger--[10]-shogaol--increases adrenaline secretion via the activation of TRPV1. *Nutr Neurosci* **9,** 169-78.

Jelks, K. B., Wylie, R., Floyd, C. L., McAllister, A. K. and Wise, P. (2007) Estradiol targets synaptic proteins to induce glutamatergic synapse formation in cultured hippocampal neurons: critical role of estrogen receptor-alpha. *J Neurosci* **27,** 6903-13.

Jeske, N. A., Diogenes, A., Ruparel, N. B., Fehrenbacher, J. C., Henry, M., Akopian, A. N. and Hargreaves, K. M. (2008) A-kinase anchoring protein mediates TRPV1 thermal hyperalgesia through PKA phosphorylation of TRPV1. *Pain* **138,** 604-16.

Jeske, N. A., Patwardhan, A. M., Ruparel, N. B., Akopian, A. N., Shapiro, M. S. and Henry, M. A. (2009) A-kinase anchoring protein 150 controls protein kinase C-mediated phosphorylation and sensitization of TRPV1. *Pain* **146,** 301-7.

Ji, R. R., Samad, T. A., Jin, S. X., Schmoll, R. and Woolf, C. J. (2002) p38 MAPK activation by NGF in primary sensory neurons after inflammation increases TRPV1 levels and maintains heat hyperalgesia. *Neuron* **36,** 57-68.

Jin, X. and Gereau, R. W. (2006) Acute p38-Mediated Modulation of Tetrodotoxin-Resistant Sodium Channels in Mouse Sensory Neurons by Tumor Necrosis Factor-{alpha}. *J Neurosci* **26,** 246-255.

Johnson, J. A., Gray, M. O., Chen, C. H. and Mochly-Rosen, D. (1996) A protein kinase C translocation inhibitor as an isozyme-selective antagonist of cardiac function. *J Biol Chem* **271,** 24962-6.

Jones, R. C., 3rd, Xu, L. and Gebhart, G. F. (2005) The mechanosensitivity of mouse colon afferent fibers and their sensitization by inflammatory mediators require transient receptor potential vanilloid 1 and acid-sensing ion channel 3. *J Neurosci* **25,** 10981-9.

Jordt, S. E., Tominaga, M. and Julius, D. (2000) Acid potentiation of the capsaicin receptor determined by a key extracellular site. *Proc.Natl.Acad.Sci.U.S.A* **97,** 8134-8139.

Joseph, E. K. and Levine, J. D. (2003a) Sexual dimorphism for protein kinase C epsilon signaling in a rat model of vincristine-induced painful peripheral neuropathy. *Neuroscience* **119,** 831-838.

Joseph, E. K. and Levine, J. D. (2003b) Sexual dimorphism in the contribution of protein kinase C isoforms to nociception in the streptozotocin diabetic rat. *Neuroscience* **120,** 907-913.

Joseph, E. K., Parada, C. A. and Levine, J. D. (2003) Hyperalgesic priming in the rat demonstrates marked sexual dimorphism. *Pain* **105,** 143-150.

Joseph, E. K., Bogen, O., Alessandri-Haber, N. and Levine, J. D. (2007) PLG-beta(3) signals upstream of PKC epsilon in acute and chronic inflammatory hyperalgesia. *Pain* **132,** 67-73.

Julius, D. and Basbaum, A. I. (2001) Molecular mechanisms of nociception. *Nature* **413,** 203-210.

Jung, J., Lee, S. Y., Hwang, S. W., Cho, H., Shin, J., Kang, Y. S., Kim, S. and Oh, U. (2002) Agonist recognition sites in the cytosolic tails of vanilloid receptor 1. *J Biol Chem* **277,** 44448-54.

Jung, M. E., Watson, D. G. and Simpkins, J. W. (2005) Suppression of protein kinase Cepsilon mediates 17beta-estradiol-induced neuroprotection in an immortalized hippocampal cell line. *J Neurochem.*

Kanai, Y., Hara, T., Imai, A. and Sakakibara, A. (2007) Differential involvement of TRPV1 receptors at the central and peripheral nerves in CFA-induced mechanical and thermal hyperalgesia. *J Pharm Pharmacol* **59,** 733-8.

Kelly, M. J., Lagrange, A. H., Wagner, E. J. and Ronnekleiv, O. K. (1999) Rapid effects of estrogen to modulate G protein-coupled receptors via activation of protein kinase A and protein kinase C pathways. *Steroids* **64,** 64-75.

Khasar, S. G., Miao, F. J. and Levine, J. D. (1995) Inflammation modulates the contribution of receptor-subtypes to bradykinin-induced hyperalgesia in the rat. *Neuroscience* **69,** 685-90.

Khasar, S. G., Lin, Y. H., Martin, A., Dadgar, J., McMahon, T., Wang, D., Hundle, B., Aley, K. O., Isenberg, W., McCarter, G., Green, P. G., Hodge, C. W., Levine, J. D. and Messing, R. O. (1999a) A novel nociceptor signaling pathway revealed in protein kinase C epsilon mutant mice. *Neuron* **24,** 253-260.

Khasar, S. G., McCarter, G. and Levine, J. D. (1999b) Epinephrine produces a beta-adrenergic receptor-mediated mechanical hyperalgesia and in vitro sensitization of rat nociceptors. *Journal of Neurophysiology* **81,** 1104-1112.

Khasar, S. G., Dina, O. A., Green, P. G. and Levine, J. D. (2005) Estrogen regulates adrenal medullary function producing sexual dimorphism in nociceptive threshold and beta(2)-adrenergic receptor-mediated hyperalgesia in the rat. *European Journal of Neuroscience* **21,** 3379-3386.

Klein-Hitpass, L., Schorpp, M., Wagner, U. and Ryffel, G. U. (1986) An estrogen-responsive element derived from the 5' flanking region of the Xenopus vitellogenin A2 gene functions in transfected human cells. *Cell* **46,** 1053-61.

Kress, M., Rodl, J. and Reeh, P. W. (1996) Stable analogues of cyclic AMP but not cyclic GMP sensitize unmyelinated primary afferents in rat skin to heat stimulation but not to inflammatory mediators, in vitro. *Neuroscience* **74,** 609-17.

Kuhn, J., Dina, O. A., Goswami, C., Suckow, V., Levine, J. D. and Hucho, T. (2008) GPR30 estrogen receptor agonists induce mechanical hyperalgesia in the rat. *European Journal of Neuroscience* **27,** 1700-1709.

Kuiper, G. G., Carlsson, B., Grandien, K., Enmark, E., Haggblad, J., Nilsson, S. and Gustafsson, J. A. (1997) Comparison of the ligand binding specificity and transcript tissue distribution of estrogen receptors alpha and beta. *Endocrinology* **138,** 863-70.

Kvingedal, A. M. and Smeland, E. B. (1997) A novel putative G-protein-coupled receptor expressed in lung, heart and lymphoid tissue. *FEBS Lett* **407,** 59-62.

Langer, G., Bader, B., Meoli, L., Isensee, J., Delbeck, M., Noppinger, P. R. and Otto, C. (2009) A critical review of fundamental controversies in the field of GPR30 research. *Steroids*.

Lansbergen, G. and Akhmanova, A. (2006) Microtubule plus end: a hub of cellular activities. *Traffic* **7,** 499-507.

Lansbergen, G., Grigoriev, I., Mimori-Kiyosue, Y., Ohtsuka, T., Higa, S., Kitajima, I., Demmers, J., Galjart, N., Houtsmuller, A. B., Grosveld, F. and Akhmanova, A. (2006) CLASPs attach microtubule plus ends to the cell cortex through a complex with LL5beta. *Dev Cell* **11,** 21-32.

Lauber, M. E. and Lichtensteiger, W. (1994) Pre- and postnatal ontogeny of aromatase cytochrome P450 messenger ribonucleic acid expression in the male rat brain studied by in situ hybridization. *Endocrinology* **135,** 1661-8.

Lieuvin, A., Labbe, J. C., Doree, M. and Job, D. (1994) Intrinsic microtubule stability in interphase cells. *J Cell Biol* **124,** 985-96.

Liu, B., Ma, W., Ryu, S. and Qin, F. (2004) Inhibitory modulation of distal C-terminal on protein kinase C-dependent phospho-regulation of rat TRPV1 receptors. *J Physiol* **560,** 627-38.

Liu, N. J. and Gintzler, A. R. (2000) Prolonged ovarian sex steroid treatment of male rats produces antinociception: identification of sex-based divergent analgesic mechanisms. *Pain* **85,** 273-81.

Liverman, C. S., Brown, J. W., Sandhir, R., McCarson, K. E. and Berman, N. E. (2009) Role of the oestrogen receptors GPR30 and ERa in peripheral sensitization: relevance to trigeminal pain disorders in women. *Cephalalgia*.

Loeser, J. D. and Treede, R. D. (2008) The Kyoto protocol of IASP Basic Pain Terminology. *Pain* **137,** 473-7.

Maffei, L., Murata, Y., Rochira, V., Tubert, G., Aranda, C., Vazquez, M., Clyne, C. D., Davis, S., Simpson, E. R. and Carani, C. (2004) Dysmetabolic syndrome in a man with a novel mutation of the aromatase gene: effects of testosterone, alendronate, and estradiol treatment. *J Clin Endocrinol Metab* **89,** 61-70.

Malagarie-Cazenave, S., Olea-Herrero, N., Vara, D. and Diaz-Laviada, I. (2009) Capsaicin, a component of red peppers, induces expression of androgen receptor via PI3K and MAPK pathways in prostate LNCaP cells. *FEBS Lett* **583,** 141-7.

Malik-Hall, M., Dina, O. A. and Levine, J. D. (2005) Primary afferent nociceptor mechanisms mediating NGF-induced mechanical hyperalgesia. *European Journal of Neuroscience* **21,** 3387-3394.

Malin, S. A., Davis, B. M., Koerber, H. R., Reynolds, I. J., Albers, K. M. and Molliver, D. C. (2008) Thermal nociception and TRPV1 function are attenuated in mice lacking the nucleotide receptor P2Y2. *Pain* **138,** 484-96.

Manavathi, B. and Kumar, R. (2006) Steering estrogen signals from the plasma membrane to the nucleus: two sides of the coin. *J Cell Physiol* **207,** 594-604.

Mandadi, S., Numazaki, M., Tominaga, M., Bhat, M. B., Armati, P. J. and Roufogalis, B. D. (2004) Activation of protein kinase C reverses capsaicin-induced calcium-dependent desensitization of TRPV1 ion channels. *Cell Calcium* **35,** 471-8.

Mandadi, S., Tominaga, T., Numazaki, M., Murayama, N., Saito, N., Armati, P. J., Roufogalis, B. D. and Tominaga, M. (2006) Increased sensitivity of desensitized TRPV1 by PMA occurs through PKCepsilon-mediated phosphorylation at S800. *Pain*.

Mangelsdorf, D. J. and Evans, R. M. (1995) The RXR heterodimers and orphan receptors. *Cell* **83,** 841-50.

Mangelsdorf, D. J., Thummel, C., Beato, M., Herrlich, P., Schutz, G., Umesono, K., Blumberg, B., Kastner, P., Mark, M., Chambon, P. and Evans, R. M. (1995) The nuclear receptor superfamily: the second decade. *Cell* **83,** 835-9.

McCarthy, M. M., Auger, A. P. and Perrot-Sinal, T. S. (2002) Getting excited about GABA and sex differences in the brain. *Trends Neurosci* **25,** 307-12.

McCarthy, M. M., Schwarz, J. M., Wright, C. L. and Dean, S. L. (2008) Mechanisms mediating oestradiol modulation of the developing brain. *J Neuroendocrinol* **20,** 777-83.

McNamara, F. N., Randall, A. and Gunthorpe, M. J. (2005) Effects of piperine, the pungent component of black pepper, at the human vanilloid receptor (TRPV1). *Br J Pharmacol* **144,** 781-90.

Meyer, L., Venard, C., Schaeffer, V., Patte-Mensah, C. and Mensah-Nyagan, A. G. (2008) The biological activity of 3alpha-hydroxysteroid oxido-reductase in the spinal cord regulates thermal and mechanical pain thresholds after sciatic nerve injury. *Neurobiol Dis* **30,** 30-41.

Minke, B. (1977) Drosophila mutant with a transducer defect. *Biophys Struct Mech* **3,** 59-64.

Mochly-Rosen, D., Khaner, H. and Lopez, J. (1991) Identification of intracellular receptor proteins for activated protein kinase C. *Proc Natl Acad Sci U S A* **88,** 3997-4000.

Mogil, J. S., Richards, S. P., O'Toole, L. A., Helms, M. L., Mitchell, S. R., Kest, B. and Belknap, J. K. (1997) Identification of a sex-specific quantitative trait locus mediating nonopioid stress-induced analgesia in female mice. *J Neurosci* **17,** 7995-8002.

Mogil, J. S., Chesler, E. J., Wilson, S. G., Juraska, J. M. and Sternberg, W. F. (2000) Sex differences in thermal nociception and morphine antinociception in rodents depend on genotype. *Neurosci.Biobehav.Rev.* **24,** 375-389.

Montell, C., Jones, K., Hafen, E. and Rubin, G. (1985) Rescue of the Drosophila phototransduction mutation trp by germline transformation. *Science* **230,** 1040-3.

Moriarty, K., Kim, K. H. and Bender, J. R. (2006) Minireview: estrogen receptor-mediated rapid signaling. *Endocrinology* **147,** 5557-63.

Moriyama, T., Iida, T., Kobayashi, K., Higashi, T., Fukuoka, T., Tsumura, H., Leon, C., Suzuki, N., Inoue, K., Gachet, C., Noguchi, K. and Tominaga, M. (2003) Possible involvement of P2Y2 metabotropic receptors in ATP-induced transient receptor potential vanilloid receptor 1-mediated thermal hypersensitivity. *J Neurosci* **23,** 6058-62.

Moseley, J. B., Bartolini, F., Okada, K., Wen, Y., Gundersen, G. G. and Goode, B. L. (2007) Regulated binding of adenomatous polyposis coli protein to actin. *J Biol Chem* **282,** 12661-8.

Nadal, A., Ropero, A. B., Laribi, O., Maillet, M., Fuentes, E. and Soria, B. (2000) Nongenomic actions of estrogens and xenoestrogens by binding at a plasma membrane receptor unrelated to estrogen receptor alpha and estrogen receptor beta. *Proc Natl Acad Sci U S A* **97,** 11603-8.

Nawata, H., Tanaka, S., Tanaka, S., Takayanagi, R., Sakai, Y., Yanase, T., Ikuyama, S. and Haji, M. (1995) Aromatase in bone cell: association with osteoporosis in postmenopausal women. *J Steroid Biochem Mol Biol* **53,** 165-74.

Nogales, E., Wolf, S. G. and Downing, K. H. (1998) Structure of the alpha beta tubulin dimer by electron crystallography. *Nature* **391,** 199-203.

Numazaki, M., Tominaga, T., Toyooka, H. and Tominaga, M. (2002) Direct phosphorylation of capsaicin receptor VR1 by protein Kinase C epsilon and identification of two target serine residues. *Journal of Biological Chemistry* **277,** 13375-13378.

Numazaki, M., Tominaga, T., Takeuchi, K., Murayama, N., Toyooka, H. and Tominaga, M. (2003) Structural determinant of TRPV1 desensitization interacts with calmodulin. *Proc Natl Acad Sci U S A* **100,** 8002-6.

O'Lone, R., Frith, M. C., Karlsson, E. K. and Hansen, U. (2004) Genomic targets of nuclear estrogen receptors. *Mol Endocrinol* **18,** 1859-75.

Obata, K., Yamanaka, H., Dai, Y., Tachibana, T., Fukuoka, T., Tokunaga, A., Yoshikawa, H. and Noguchi, K. (2003) Differential activation of extracellular signal-regulated protein kinase in primary afferent neurons regulates brain-derived neurotrophic factor expression after peripheral inflammation and nerve injury. *J Neurosci* **23,** 4117-26.

Olde, B. and Lee-Lundberg, L. M. F. (2009) GPR30/GPER1: searching for a role in estrogen physiology. *Trends in Endocrinology and Metabolism*.

Otto, C., Fuchs, I., Kauselmann, G., Kern, H., Zevnik, B., Andreasen, P., Schwarz, G., Altmann, H., Klewer, M., Schoor, M., Vonk, R. and Fritzemeier, K. H. (2009) GPR30 Does Not Mediate Estrogenic Responses in Reproductive Organs in Mice. *Biology of Reproduction* **80,** 34-41.

Owman, C., Blay, P., Nilsson, C. and Lolait, S. J. (1996) Cloning of human cDNA encoding a novel heptahelix receptor expressed in Burkitt's lymphoma and widely distributed in brain and peripheral tissues. *Biochem Biophys Res Commun* **228,** 285-92.

Pani, B., Ong, H. L., Brazer, S. C., Liu, X., Rauser, K., Singh, B. B. and Ambudkar, I. S. (2009) Activation of TRPC1 by STIM1 in ER-PM microdomains involves release of the channel from its scaffold caveolin-1. *Proc Natl Acad Sci U S A* **106,** 20087-92.

Papka, R. E. and Storey-Workley, M. (2002) Estrogen receptor-alpha and -beta coexist in a subpopulation of sensory neurons of female rat dorsal root ganglia. *Neurosci Lett* **319,** 71-4.

Pappas, T. C., Gametchu, B. and Watson, C. S. (1995) Membrane estrogen receptors identified by multiple antibody labeling and impeded-ligand binding. *Faseb J* **9,** 404-10.

Parada, C. A., Yeh, J. J., Reichling, D. B. and Levine, J. D. (2003) Transient attenuation of protein kinase C epsilon can terminate a chronic hyperalgesic state in the rat. *Neuroscience* **120,** 219-226.

Patapoutian, A., Tate, S. and Woolf, C. J. (2009) Transient receptor potential channels: targeting pain at the source. *Nature Reviews Drug Discovery* **8,** 55-68.

Perl, E. R. (2007) Ideas about pain, a historical view. *Nat Rev Neurosci* **8,** 71-80.

Pietras, R. J. and Szego, C. M. (1977) Specific binding sites for oestrogen at the outer surfaces of isolated endometrial cells. *Nature* **265,** 69-72.

Plakita, D., Boulos, M. H., Biazer, L. and Fishman, M. C. (1985) Neuronal traits of clonal cell lines derived by fusion of dorsal root ganglia neurons with neuroblastoma cells. . *PNAS* **82,** 3499-3503.

Pogatzki-Zahn, E. M., Shimizu, I., Caterina, M. and Raja, S. N. (2005) Heat hyperalgesia after incision requires TRPV1 and is distinct from pure inflammatory pain. *Pain* **115,** 296-307.

Prossnitz, E. R., Sklar, L. A., Oprea, T. I. and Arterburn, J. B. (2008a) GPR30: a novel therapeutic target in estrogen-related disease. *Trends in Pharmacological Sciences* **29,** 116-123.

Prossnitz, E. R., Arterburn, J. B., Smith, H. O., Oprea, T. I., Sklar, L. A. and Hathaway, H. J. (2008b) Estrogen signaling through the transmembrane G protein-coupled receptor GrPR30. *Annual Review of Physiology* **70,** 165-190.

Qiu, J., Bosch, M. A., C., T. S., Grandy, D. K., Scanlan, T. S., Ronnekleiv, O. K. and Kelly, M. J. (2003) Rapid Signaling of Estrogen in Hypothalamic Neurons Involves a Novel G-Protein-Coupled Estrogen Receptor that Activates Protein Kinase C. *The Journal of Neuroscience* **23,** 9529-9540.

Razandi, M., Pedram, A., Greene, G. L. and Levin, E. R. (1999) Cell membrane and nuclear estrogen receptors (ERs) originate from a single transcript: studies of ERalpha and ERbeta expressed in Chinese hamster ovary cells. *Mol Endocrinol* **13,** 307-19.

Revankar, C. M., Cimino, D. F., Sklar, L. A., Arterburn, J. B. and Prossnitz, E. R. (2005) A transmembrane intracellular estrogen receptor mediates rapid cell signaling. *Science* **307,** 1625-1630.

Riley, J. L., III, Robinson, M. E., Wise, E. A. and Price, D. D. (1999) A meta-analytic review of pain perception across the menstrual cycle. *Pain* **81,** 225-235.

Rodgers, S. P., Bohacek, J. and Daniel, J. M. (2010) Transient estradiol exposure during middle age in ovariectomized rats exerts lasting effects on cognitive function and the hippocampus. *Endocrinology* **151,** 1194-203.

Ropero, A. B., Soria, B. and Nadal, A. (2002) A nonclassical estrogen membrane receptor triggers rapid differential actions in the endocrine pancreas. *Mol Endocrinol* **16,** 497-505.

Rosenbaum, T., Gordon-Shaag, A., Munari, M. and Gordon, S. E. (2004) Ca2+/calmodulin modulates TRPV1 activation by capsaicin. *J Gen Physiol* **123,** 53-62.

Saito, N., Itouji, A., Totani, Y., Osawa, I., Koide, H., Fujisawa, N., Ogita, K. and Tanaka, C. (1993) Cellular and intracellular localization of epsilon-subspecies of protein kinase C in the rat brain; presynaptic localization of the epsilon-subspecies. *Brain Res* **607,** 241-8.

Sakamoto, H., Matsuda, K. I., Hosokawa, K., Nishi, M., Morris, J. F., Prossnitz, E. R. and Kawata, M. (2007) Expression of GPR30, a G protein-Coupled Membrane Estrogen Receptor, in Oxytocin Neurons of the Rat Paraventricular and Supraoptic Nuclei. *Endocrinology*.

Sarlani, E., Farooq, N. and Greenspan, J. D. (2003) Gender and laterality differences in thermosensation throughout the perceptible range. *Pain* **106,** 9-18.

Schaeffer, V., Meyer, L., Patte-Mensah, C., Eckert, A. and Mensah-Nyagan, A. G. (2010) Sciatic nerve injury induces apoptosis of dorsal root ganglion satellite glial cells and selectively modifies neurosteroidogenesis in sensory neurons. *GLIA* **58,** 169-80.

Schechtman, D. and Mochly-Rosen, D. (2001) Adaptor proteins in protein kinase C-mediated signal transduction. *Oncogene* **20,** 6339-47.

Schnizler, K., Shutov, L. P., Van Kanegan, M. J., Merrill, M. A., Nichols, B., McKnight, G. S., Strack, S., Hell, J. W. and Usachev, Y. M. (2008) Protein kinase A anchoring via AKAP150 is essential for TRPV1 modulation by forskolin and prostaglandin E2 in mouse sensory neurons. *J Neurosci* **28,** 4904-17.

Schuyler, S. C. and Pellman, D. (2001) Microtubule "plus-end-tracking proteins": The end is just the beginning. *Cell* **105,** 421-4.

Schwarz, J. M., Liang, S. L., Thompson, S. M. and McCarthy, M. M. (2008) Estradiol induces hypothalamic dendritic spines by enhancing glutamate release: a mechanism for organizational sex differences. *Neuron* **58,** 584-98.

Schymkowitz, J., Borg, J., Stricher, F., Nys, R., Rousseau, F. and Serrano, L. (2005) The FoldX web server: an online force field. *Nucleic Acids Res* **33,** W382-8.

Sebastian, S. and Bulun, S. E. (2001) A highly complex organization of the regulatory region of the human CYP19 (aromatase) gene revealed by the Human Genome Project. *J Clin Endocrinol Metab* **86,** 4600-2.

Setalo, G., Jr., Singh, M., Nethrapalli, I. S. and Toran-Allerand, C. D. (2005) Protein Kinase C Activity is Necessary for Estrogen-Induced Erk Phosphorylation in Neocortical Explants. *Neurochem Res* **30,** 779-90.

Sherrington, C. S. (1906) The integrative action of the nervous system. *Scribner, New York*.

Shozu, M., Sebastian, S., Takayama, K., Hsu, W. T., Schultz, R. A., Neely, K., Bryant, M. and Bulun, S. E. (2003) Estrogen excess associated with novel gain-of-function mutations affecting the aromatase gene. *N Engl J Med* **348,** 1855-65.

Silverman, J. D. and Kruger, L. (1988) Lectin and neuropeptide labeling of separate populations of dorsal root ganglion neurons and associated "nociceptor" thin axons in rat testis and cornea whole-mount preparations. *Somatosens Res* **5,** 259-67.

Simoncini, T., Rabkin, E. and Liao, J. K. (2003) Molecular basis of cell membrane estrogen receptor interaction with phosphatidylinositol 3-kinase in endothelial cells. *Arterioscler Thromb Vasc Biol* **23,** 198-203.

Smith, C. C., Vedder, L. C. and McMahon, L. L. (2009) Estradiol and the relationship between dendritic spines, NR2B containing NMDA receptors, and the magnitude of long-term potentiation at hippocampal CA3-CA1 synapses. *Psychoneuroendocrinology* **34 Suppl 1,** S130-42.

Sohrabji, F., Miranda, R. C. and Toran-Allerand, C. D. (1994) Estrogen differentially regulates estrogen and nerve growth factor receptor mRNAs in adult sensory neurons. *J.Neurosci.* **14,** 459-471.

Srivastava, D. P., Woolfrey, K. M., Jones, K. A., Shum, C. Y., Lash, L. L., Swanson, G. T. and Penzes, P. (2008) Rapid enhancement of two-step wiring plasticity by estrogen and NMDA receptor activity. *Proc Natl Acad Sci U S A* **105,** 14650-5.

Sweitzer, S. M., Wong, S. M., Tjolsen, A., Allen, C. P., Mochly-Rosen, D. and Kendig, J. J. (2004a) Exaggerated nociceptive responses on morphine withdrawal: roles of protein kinase C epsilon and gamma. *Pain* **110,** 281-9.

Sweitzer, S. M., Wong, S. M., Peters, M. C., Mochly-Rosen, D., Yeomans, D. C. and Kendig, J. J. (2004b) Protein kinase C {epsilon} and {gamma}: Involvement in formalin-induced nociception in neonatal rats. *J Pharmacol Exp Ther* **309,** 616-625.

Taiwo, Y. O. and Levine, J. D. (1991) Further confirmation of the role of adenyl cyclase and of cAMP-dependent protein kinase in primary afferent hyperalgesia. *Neuroscience* **44,** 131-5.

Takada, Y., Kato, C., Kondo, S., Korenaga, R. and Ando, J. (1997) Cloning of cDNAs encoding G protein-coupled receptor expressed in human endothelial cells exposed to fluid shear stress. *Biochem Biophys Res Commun* **240,** 737-41.

Takai, Y., Kishimoto, A., Iwasa, Y., Kawahara, Y., Mori, T. and Nishizuka, Y. (1979) Calcium-dependent activation of a multifunctional protein kinase by membrane phospholipids. *J Biol Chem* **254,** 3692-5.

Takanami, K., Sakamoto, H., Matsuda, K., Hosokawa, K., Nishi, M., Prossnitz, E. R. and Kawata, M. Expression of G protein-coupled receptor 30 in the spinal somatosensory system. *Brain Res* **1310,** 17-28.

Taleghany, N., Sarajari, S., DonCarlos, L. L., Gollapudi, L. and Oblinger, M. M. (1999) Differential expression of estrogen receptor alpha and beta in rat dorsal root ganglion neurons. *J Neurosci Res* **57,** 603-15.

Tender, G. C., Li, Y. Y. and Cui, J. G. (2008) Vanilloid receptor 1-positive neurons mediate thermal hyperalgesia and tactile allodynia. *Spine J* **8,** 351-8.

Thomas, P., Pang, Y., Filardo, E. J. and Dong, J. (2005) Identity of an estrogen membrane receptor coupled to a G protein in human breast cancer cells. *Endocrinology* **146,** 624-632.

Tong, C., Conklin, D., Clyne, B. B., Stanislaus, J. D. and Eisenach, J. C. (2006) Uterine cervical afferents in thoracolumbar dorsal root ganglia express transient receptor potential vanilloid type 1 channel and calcitonin gene-related peptide, but not P2X3 receptor and somatostatin. *Anesthesiology* **104,** 651-7.

Toran-Allerand, C. D., Singh, M. and Setalo, G., Jr. (1999) Novel mechanisms of estrogen action in the brain: new players in an old story. *Front Neuroendocrinol* **20,** 97-121.

Toran-Allerand, C. D. (2004) Estrogen and the brain: beyond ER-alpha and ER-beta. *Exp Gerontol* **39,** 1579-86.

Tovchigrechko, A. and Vakser, I. A. (2006) GRAMM-X public web server for protein-protein docking. *Nucleic Acids Res* **34,** W310-4.

Trevisani, M., Smart, D., Gunthorpe, M. J., Tognetto, M., Barbieri, M., Campi, B., Amadesi, S., Gray, J., Jerman, J. C., Brough, S. J., Owen, D., Smith, G. D., Randall, A. D., Harrison, S., Bianchi, A., Davis, J. B. and Geppetti, P. (2002) Ethanol elicits and potentiates nociceptor responses via the vanilloid receptor-1. *Nat Neurosci* **5,** 546-51.

Unruh, A. M. (1996) Gender variations in clinical pain experience. *Pain* **65,** 123-167.

Van Kolen, K., Pullan, S., Neefs, J. M. and Dautzenberg, F. M. (2007) Nociceptive and behavioural sensitisation by protein kinase Cepsilon signalling in the CNS. *J Neurochem.*

Venkatachalam, K. and Montell, C. (2007) TRP channels. *Annu Rev Biochem* **76,** 387-417.

Vergote, I. and Abram, P. (2006) Fulvestrant, a new treatment option for advanced breast cancer: tolerability versus existing agents. *Ann Oncol* **17,** 200-4.

Vriend, G. (1990) Parameter relation rows: a query system for protein structure function relationships. *Protein Eng* **4,** 221-3.

Wang, S., Dai, Y., Fukuoka, T., Yamanaka, H., Kobayashi, K., Obata, K., Cui, X., Tominaga, M. and Noguchi, K. (2008) Phospholipase C and protein kinase A mediate bradykinin sensitization of TRPA1: a molecular mechanism of inflammatory pain. *Brain* **131,** 1241-51.

Watson, C. S., Campbell, C. H. and Gametchu, B. (2002) The dynamic and elusive membrane estrogen receptor-alpha. *Steroids* **67,** 429-37.

Woolf, C. J. (1996) Phenotypic modification of primary sensory neurons: the role of nerve growth factor in the production of persistent pain. *Philos Trans R Soc Lond B Biol Sci* **351,** 441-8.

Xu, H., Blair, N. T. and Clapham, D. E. (2005) Camphor activates and strongly desensitizes the transient receptor potential vanilloid subtype 1 channel in a vanilloid-independent mechanism. *J Neurosci* **25,** 8924-37.

Xu, H., Qin, S., Carrasco, G. A., Dai, Y., Filardo, E. J., Prossnitz, E. R., Battaglia, G., Doncarlos, L. L. and Muma, N. A. (2009) Extra-nuclear estrogen receptor GPR30 regulates serotonin function in rat hypothalamus. *Neuroscience* **158,** 1599-607.

Xu, S. H., Cheng, Y., Keast, J. R. and Osborne, P. B. (2008) 17 beta-Estradiol Activates Estrogen Receptor beta-Signalling and Inhibits Transient Receptor Potential Vanilloid Receptor 1 Activation by Capsaicin in Adult Rat Nociceptor Neurons. *Endocrinology* **149,** 5540-5548.

Yi, K. D. and Simpkins, J. W. (2008) Protein phosphatase 1, protein phosphatase 2A, and calcineurin play a role in estrogen-mediated neuroprotection. *Endocrinology* **149,** 5235-43.

Zhang, D. and Trudeau, V. L. (2006) Integration of membrane and nuclear estrogen receptor signaling. *Comp Biochem Physiol A Mol Integr Physiol* **144,** 306-15.

Zhang, H., Cang, C. L., Kawasaki, Y., Liang, L. L., Zhang, Y. Q., Ji, R. R. and Zhao, Z. Q. (2007) Neurokinin-1 receptor enhances TRPV1 activity in primary sensory neurons via PKCepsilon: a novel pathway for heat hyperalgesia. *J Neurosci* **27,** 12067-77.

Zhang, N., Inan, S., Cowan, A., Sun, R., Wang, J. M., Rogers, T. J., Caterina, M. and Oppenheim, J. J. (2005a) A proinflammatory chemokine, CCL3, sensitizes the heat- and capsaicin-gated ion channel TRPV1. *Proc Natl Acad Sci U S A* **102,** 4536-41.

Zhang, Q. G., Wang, R., Khan, M., Mahesh, V. and Brann, D. W. (2008) Role of Dickkopf-1, an antagonist of the Wnt/beta-catenin signaling pathway, in estrogen-induced neuroprotection and attenuation of tau phosphorylation. *J Neurosci* **28,** 8430-41.

Zhang, X., Huang, J. and McNaughton, P. A. (2005b) NGF rapidly increases membrane expression of TRPV1 heat-gated ion channels. *Embo J* **24,** 4211-23.

Zhang, Z. Y., Pan, L. J. and Zhang, Z. M. (2009) Functional interactions among STIM1, Orai1 and TRPC1 on the activation of SOCs in HL-7702 cells. *Amino Acids*.

Zhou, F. Q., Zhou, J., Dedhar, S., Wu, Y. H. and Snider, W. D. (2004) NGF-induced axon growth is mediated by localized inactivation of GSK-3beta and functions of the microtubule plus end binding protein APC. *Neuron* **42,** 897-912.

Zhu, W. and Oxford, G. S. (2007) Phosphoinositide-3-kinase and mitogen activated protein kinase signaling pathways mediate acute NGF sensitization of TRPV1. *Mol Cell Neurosci* **34,** 689-700.

Zhuang, Z. Y., Xu, H., Clapham, D. E. and Ji, R. R. (2004) Phosphatidylinositol 3-kinase activates ERK in primary sensory neurons and mediates inflammatory heat hyperalgesia through TRPV1 sensitization. *J Neurosci* **24,** 8300-9.

Zirilli, L., Rochira, V., Diazzi, C., Caffagni, G. and Carani, C. (2008) Human models of aromatase deficiency. *J Steroid Biochem Mol Biol* **109,** 212-8.

Zumbrunn, J., Kinoshita, K., Hyman, A. A. and Nathke, I. S. (2001) Binding of the adenomatous polyposis coli protein to microtubules increases microtubule stability and is regulated by GSK3 beta phosphorylation. *Curr Biol* **11,** 44-9.

Zygmunt, P. M., Petersson, J., Andersson, D. A., Chuang, H., Sorgard, M., Di, M., V, Julius, D. and Hogestatt, E. D. (1999) Vanilloid receptors on sensory nerves mediate the vasodilator action of anandamide. *Nature* **400,** 452-457.

10 Definitions

All definitions are taken from "The Kyoto protocol of IASP Basic Pain Terminology" (Loeser and Treede, 2008).

Hyperalgesia	Increased pain sensitivity
Nociceptive neuron	A central or peripheral neuron that is capable of encoding noxious stimuli
Nociceptive stimulus	An actual or potentially tissue-damaging event transduced by nociceptors
Nociception	The neural processes of encoding and processing noxious stimuli
Pain	An unpleasant sensory or emotional experience associated with actual or potential tissue damage or described in terms of such damage
Pain threshold	The minimal intensity of a stimulus that is perceived as painful
Sensitization	Increased responsiveness of neurons to their normal input or recruitment of a response to normally subthreshold inputs

11 Abbreviations

aa	amino acid
AC	adenylyl cyclase
ASIC	acid sensing ion channel
ATP	adenosine-5′-triphosphate
β2-AR	beta-2-adrenergic receptor
BIM	Bisindolylmaleimde I hydrochloride (PKC inhibitor)
bp	base pair
BSA	bovine serum albumin
CamKII	calmodulin-dependent kinase II
cAMP	cyclic adenosine 5'-monophosphate
CCI	chronic constriction injury
cGMP	cyclic guanosine 5'monoposhpate
cDNA	complementary DNA
CGRP	calcitonin-gene related peptide
CNS	central nervous system
COX	cyclooxigenase
D	aspartic acid
DAG	diacylglycerol
DAPI	4′,6-diamidino-2-phenylindol-dihydrochlorid
DNA	deoxyribonucleic acid
DMSO	dimethyl sulfoxide
dNTP	deoxynucleotide triphosphate
DPN	2,3-bis(4-hydroxyphenyl)-propionitrile (ERβ agonist)
DRG	dorsal root ganglia
E	glutamic acid
E2	estrogen, 17-β-estradiol
EPAC	exchange proteins activated directly by cAMP
epi	epinephrine
ER	estrogen receptor
ERα	estrogen receptor alpha
ERβ	estrogen receptor beta
ERE	estrogen responsive element
ERK	extracellular regulated kinase
ESCA	Epac-selective cAMP analogues
εV1-2	PKCε inhibitor peptide
FBS	fetal bovine serum
Fig.	figure

G	glutamic acid
GABA	gamma-aminobutyric acid
GAPDH	glyceraldehyde 3-phosphate dehydrogenase
GDNF	glia cell-derived neurotrophic factor
GFP	green fluorescent protein
GPCR	G-protein coupled receptor
GPR30	G-protein coupled receptor 30
GSK3	glycogen synthase kinase 3
h	hour
H	histidine
IB4	isolectin B4 from *Bandeiraea simplicifolia*
IP3	inositol 1,4,5-trisphosphate
IP3-R	inositol 1,4,5-trisphosphate receptor
iso	isoproterenol
JNK	c-jun N-terminal kinase
kDa	kilo dalton
MAP	microtubule associated protein
MAPK	mitogen activated protein kinase
MBP	maltose binding protein
MEM	minimal essential medium
min	minute
mRNA	messenger ribonucleic acid
MW	molecular weight
NCBI	National Center for Biotechnology Information
NDS	normal donkey serum
NGF	nerve growth factor
NGS	normal goat serum
NO	nitric oxide
ODN	oligodeoxynucleotide
o.n.	over night
PAGE	poly acrylamide gel electrophoresis
PBS	phosphate buffered saline
PCR	polymerase chain reaction
PGE2	prostaglandine E2
PI3K	phosphatidylinositol 3-kinase
PKA	protein kinase A
PKC	protein kinase C
PNS	peripheral nervous system
PLC	phospholipase C
PLD	phospholipase D

PPT	4,4',4''-(4-Propyl-[1H]-pyrazole-1,3,5-triyl)trisphenol (ERα agonist)
R	arginine
RACK	receptor for activated kinase
RNA	ribonucleic acid
RTK	receptor tyrosine kinase
RT	room temperature
RT-PCR	reverse transcritpase-polymerase chain reaction
RTX	reasinfera toxin
RyR	ryanodine receptor
S	serine
SDS	sodium dodecyl sulfate
sec	second
STIM1	stromal interaction molecule 1
Tab.	table
TAE	tris-acetic acid-EDTA
TEMED	N,N,N',N'-tetramethylethylenediamine
TG	trigeminal ganglia
+TIP	microtubule plus-end tracking protein
TMJ	temporomandibular joint
TNFα	tumor necrosis factor alpha
Tris	tris hydroxymethylaminoethane
trkA	transforming tyrosine kinase A
TRP	transient receptor potential
TRPA1	transient receptor potential ankyrin 1 receptor
TRPV1	transient receptor potential vanilloid subtype 1 receptor
TRPV1-Ct	TRPV1 C-terminus
TTX-R	tetrodotoxin resistant
VR1	vanilloid receptor subtype 1
v/v	volume per volume
wt	wild type
w/v	weight per volume

12   Acknowledgement

13 Publication list

Publications

Goswami*, C., <u>Kuhn, J.</u>*, Fernández-Ballester, G., Ferrer-Montiel, A., Hucho T. Estrogen destabilizes microtubules through a channel-independent TRPV1 pathway.
*authors contributed equally
submitted

Hucho, T., Suckow, V, Dina O., Chen, X., <u>Kuhn, J.</u>, Schmoranzer, J., Karst, M., Bernateck, M., Levine, J. D., Ropers, H.H. Stimulus context erases pain sensitization.
in revision

<u>Kuhn, J.</u>, Dina, O. A., Goswami, C., Suckow, V., Levine, J. D. and Hucho, T. (2008) GPR30 estrogen receptor agonists induce mechanical hyperalgesia in the rat. *European Journal of Neuroscience* **27,** 1700-1709.

Hucho, T., Dina, O. A., <u>Kuhn, J.</u> and Levine, J. D. (2006) Estrogen controls PKC epsilon-dependent mechanical hyperalgesia through direct action on nociceptive neurons. *European Journal of Neuroscience* **24,** 527-534.

Oral presentations

<u>Kuhn, J.</u>
Estrogen in pain signaling pathways.
Doktorandentagung der Studienstiftung des deutschen Volkes, **Köln**, 2008

<u>Kuhn, J.</u>
Novel functions for the ion channel TRPV1.
Doktorandentagung der Studienstiftung des deutschen Volkes, **Berlin**, 2009

<u>Kuhn, J.</u>, Goswami C., Dina, O., Levine, J. D., Hucho, T.
Estogen signaling in primary nociceptive neurons.
European Pain School „Translating Pain Science into Pain Medicine", **Siena**, 2009

Poster presentations

<u>Kuhn, J.</u>, Dina, O. A., Levine, J. D., Hucho, T.
The novel estrogen receptor GPR30 mediates estrogen-induced and PKCε-dependent mechanical hyperalgesia.
GBM Herbsttagung „Molecular Live Science" and „Molecular Pathways in Health and Desease", Neurochemistry Group, **Hamburg**, 2007

<u>Kuhn, J.</u>, Dina, O. A., Levine, J. D., Hucho, T.
The GPR30 Agonist G-1 induces PKCε-dependent mechanical hyperalgesia.
4th Symposium Sex and Gender in Medicine, **Berlin**, 2007

<u>Kuhn, J.</u>, Goswami, C., Hucho, T.
Estrogen induces TRPV1-dependent cytoskeletal rearrangement.
Berlin Neuroscience Forum, **Liebenwalde**, 2008

Kuhn, J., Goswami, C., Dina, O., Levine, J.D., Hucho, T.
Estrogen and GPR30 agonists induce fast TRPV1- and PKCε-dependent cytoskeletal rearrangements in neuronal cells.
Society for Neuroscience Annual Meeting, **Washington**, 2008

Kuhn, J., Goswami, C., Hucho, T.
Estrogen induces microtubule destabilization in primary sensory neurons.
EMBO Course on Light Microscopy in Living Cells, **Lissabon**, 2009

Kuhn, J.*, Goswami, C.*, Dina, O., Fernández-Ballester, G., Ferrer-Montiel, A., Levine, J., Hucho, T.
Alteration of the microtubule-TRPV1 complex modulates PKCε-dependent mechanical hyperalgesia.
TRP-meeting "TRP channels: From sensory signaling to human disease", **Stockholm**, 2009
*authors contributed equally

14 Curriculum Vitae

Der Lebenslauf ist in der Online-Version aus Gründen des Datenschutzes nicht enthalten.